Thermal-hydraulics simulation of a benchmark case for a typical Materials Test Reactor using FLOWNEX

Rohan Slabbert
B.Eng (Mechanical)
(20277881)

Mini-dissertation submitted in partial fulfilment of the requirements for the degree
Master of Engineering in Nuclear Engineering
at the Potchefstroom Campus of the North-West University

Supervisor: Dr. Vishnu Naicker
Co-supervisor: Prof. Pieter Rousseau

Potchefstroom

2011

Abstract

The purpose of this study was to serve as a starting point in gaining understanding and experience of simulating a typical Pool Type Research Reactor with the thermal hydraulic software code Flownex®. During the study the following evaluations of Flownex® were done:

- Assessment of the simplifying assumptions and possible shortcomings built into the software.
- Definition of the applicable modelling methodology and further simplifying assumptions that have to be made by the user.
- Evaluation of the accuracy and compatibility with the Pool Type Research Reactor.
- Comparing the results of this study with similar studies found in the open literature.

For the study the IAEA MTR 10 MW benchmark reactor (IAEA, 1992a) was used. A steady state simulation using Flownex® was done on a single fuel assembly, and this was compared with a model that was developed using the software package EES (Engineering Equation Solver). The results have shown good agreement between the different packages.

After this verification, a steady state simulation of the entire core was done to obtain the characteristics of the reactor operating under normal condition. Finally, transient simulations were done on various LOFAs (Loss of Flow Accidents). The results of the various LOFAs were compared with studies that were previously done on the IAEA MTR 10 MW reactor.

Keywords: Flownex®, MTR, LOFA, EES, Steady State, Transient.

Opsomming

Die doel van die projek was om die nodige kennis en ervaring op te doen vir die simulering van ‘n Poel Tipe Navoringsreaktor. Die simulasies is gedoen met die termiese hidrouliese sagteware pakket Flownex®. Tydens die studie is die volgende aspekte van Flownex® geëvalueer:

- Die assessering van die vereenvoudigde aannames en moontlike tekortkominge in die safteware.
- Die definisie van die toepaslike modelleringsmetodologie en die vereenvoudigde aannames wat gemaak moet deur die verbruiker tydens die simulasies.
- Die evaluering van die akkuraatheid en die verenigbaarheid met die Poel Tipe Navorsingsreaktor.

- Vergelyking van resultate met soortgelyke literatuur studies

Vir die studie is die IAEA (Internasionale Atoom Energie Organisasie) se MTR (Materiaal Toetsreaktor) 10 MW navorsingsreaktor gebruik (IAEA, 1992b). ‘n Gestadigde toestand simulasie van ‘n enkele brandstofstaaf is gedoen met die sagteware pakket Flownex® en die resultalte is vergelyk met ‘n model wat in EES (“Engineering Equation Solver”) ontwikkel is. Daar was ‘n goeie ooreenkoms in die vergelyking tussen die twee sagteware simulasies.

Na die verifikasie, is daar ‘n gestadigde toestand simulasie gedoen op die totale hart van die reaktor om die gedrag van die reaktor te bepaal tydens die normale toestand. Vir die finale simulasie is daar ‘n transiënte simulasie gedoen waar die reaktor se verkoelingsvloei verminder het a.g.v ‘n probleem op die primêre verkoelingspomp. Die resultate van die transiënte simulasie is vergelyk met studies wat reeds op die veld gedoen is.

Soekwoorde: Flownex®, MTR, LOFA, EES, Gestadigde Toestant, Transient.

Acknowledgements

Firstly I want to thank my Heavenly Father Jesus Christ for giving me the strength, knowledge and ability to do a research study at the North West University.

I want to thank my supervisor Dr. Vishnu Naicker and Co-supervisor Prof. Pieter Rousseau for their interesting discussions and support throughout the entire project. Thank you for the interesting project this year.

Thank you for M-Tech Industrial (PTY) LTD for the ability for using their software package Flownex®. I want to thank the Flownex® support crew for the training on the software package which has helped me throughout my project.

Thank you to all of my friends and family who have supported and motivated me the whole time throughout my project. Your support was very helpful.

Lastly I want to thank the North West University (Potchefstroom Campus) and NRF for their financial support. Without your help this project would not be able to be done.

Table of Contents

List of figures

List of tables

Nomenclature

Symbols	Description	Unit
A	Constant	-
A	Area	m^2
A_{fuel}	Contact area of fuel	m^2
A_{flow}	Flow area	m^2
β	Beta radiation	-
β	Fraction neutrons	-
D_H	Hydraulic diameter	m
$F_i(t_\alpha, T_\alpha)$	Sum of decay heat	MeV/fission
f	Friction factor	-
$G(t)$	Correction factor	-
g	Gravity force	$kg.m/s^2$
γ	Gamma radiation	-
h_{0e}	Total enthalpy on exit	kJ/kg.K
h_{0i}	Total enthalpy on inlet	kJ/kg.K
h_c	Convention heat transfer coefficient	W/m^2K
H	Height of fuel assembly	m
k_1	Constant in the x-direction	-
k_2	Constant in the y-direction	-
k_3	Constant in the z-direction	-
$\sum K$	Sum of secondary losses	-
k	Conductivity	W/m.K
L	Length	m
L_f	Total fuel length	m
L_c	Total flow channel length	m
$\dot{m}_e$	Mass flow rate on exit	kg/s
$\dot{m}_i$	Mass flow rate on inlet	kg/s
$P_d(t,T)$	Total fission product decay heat power at t seconds after shutdown	kW
$P'_{di}(t,T)$	Uncorrected decay heat power	kW

$P_d'(t,T)$	Decay heat power	kW
$P_{i\alpha}$	Constant power of reactor	kW
P_0	Total power in reactor	kW
PF_x	Peaking factor in x-direction	-
PF_y	Peaking factor in y-direction	-
PF_z	Peaking factor in z-direction	-
p_{0e}	Total pressure on exit	kPa
p_{0i}	Total pressure on inlet	kPa
Δp_{0L}	Pressure loss	kPa
Q_i	Total energy per fission	MeV/fission
Q	Heat input	kW
R_f	Fouling factor	-
R_w	Conduction thermal resistance	K/W
T_s	Water temperature on secondary side	°C
T_p	Water temperature on primary side	°C
T_{ws}	Wall temperature on secondary side	°C
T_{wp}	Wall temperature on primary side	°C
T_∞	Fluid temperature	°C
T	Time period while the reactor was operating	sec
t	Time after shutdown	sec
t_w	Thickness of flow channel	m
$\frac{1}{(UA)}$	Thermal resistance	W/m².K
$(UA)_s$	Thermal resistance of fluid on secondary side	W/m².K
$(UA)_p$	Thermal resistance of fluid on primary side	W/m².K
V	Velocity	m/s
w_f	The width of a single fuel plate	m
w_c	The width of the cladding of a single fuel plate	m
x	x-direction	-
y	y-direction	-
z	z-direction	-
z_e	Position on exit	m

z_i	Position on inlet	m
ψ	Fissions per initial fissile atom	-
Λ	Neutron lifetime	s
λ	Mean free path	cm
Φ	Flux	neutrons/cm^2·s
$\Phi_x^{\max}$	Maximum flux	neutrons/cm^2·s
Φ_x^{ave}	Average flux	neutrons/cm^2·s
ρ	Reactivity	-
ρ	Fluid density	kg/m^3
η_0	Overall surface efficiency	-
n	Number of fuel plates per fuel assembly.	-
Nu	Nusselt	-
Re	Reynolds	-
Pr	Prandtl	-
3-D	Three dimensional	-

LIST OF ABBREVIATIONS

CFA	Control Fuel Assemblies
CFD	Computational Fluid Dynamics
EES	Engineering Equation Solver
FLOFA	Fast Loss of Flow Accident
FRIA	Fast Reactivity Insertion Accident
HEU	High Enriched Fuel
IAEA	International Atomic Energy Association
IPCM	Implicit Pressure Correction Method
LEU	Low Enriched Fuel
LOCA	Loss of Coolant Accident
LOFA	Loss of Flow Accident
LOFAs	Loss of Flow Accidents
LPD	Local Power Density
MTR	Materials Testing Reactor
NCV	Natural Convection Valve
PBMR	Pebble Bed Modular Reactor
PID	Proportional Integral Derivative
RIA	Reactivity Insertion Accident
SCFD	Systems-Computational Fluid Dynamics
SFA	Standard Fuel Assemblies
SLOFA	Slow Loss of Flow Accident
SRIA	Slow Reactivity Insertion Accident

Chapter 1

1 Introduction

1.1 Background

Nuclear energy is a very fast growing technology that is still under development. It is used, amongst others, in medical isotope production, power generation, for use in weapons and for submarine propulsion. Safety is one of the most important considerations in nuclear engineering and there are many safety requirements that must be adhered to in the design and licensing of a nuclear project.

Currently there are a variety of research reactors in the world. According to the IAEA (International Atomic Energy Association) there are more than 651 research reactors in the world that were built in more than 56 countries. Of these, 284 research reactors are still in operation, 109 have been decommissioned (IAEA, 2004) and 258 were shut down (Lu *et al.*, 2009a). These research reactors are not used for power generation. The reactors are designed according to stringent specifications so that the models comply with all the safety requirements necessary to operate a nuclear research reactor. In most cases safety factors are defined in accordance with guidelines laid down by the IAEA. The final design that would be accepted as satisfying a specific licensing requirement would have undergone a series of evaluations, of which simulation by means of software would have been one.

In the nuclear engineering industry various computational software codes are used to conduct thermal-fluid analyses/simulations of reactors as part of the licensing process. These reactors have different designs, and the plate type fuel is one of the most common designs that are used for research reactors (Lu *et al.*, 2009a). Over the years many codes like RELAP, RETRAN, CATHARE and ATHLET were developed for analysing some of the transients and accidents associated with nuclear reactors.

As part of the training of a nuclear engineer working in the South African nuclear industry, it is essential to gain a good understanding of both the licensing requirements for operating nuclear

reactors and the applicable thermal hydraulic software codes that can be used for simulation in terms thereof.

In the nuclear industry the nuclear energy is commonly used for commercial and research purposes. The research reactors are used for medical isotope production for cancer candidates and for future development on different types of nuclear fuel and power plants. A typical illustration of a research reactor in South Africa is the SAFARI 1 reactor of NECSA just outside Hartebeestpoort namely Pelindaba. The commercial nuclear reactors are used for electricity production. In South Africa a typical example of a commercial reactor namely Koeberg outside Cape Town is operated by Eskom.

It is essential during the design process of a nuclear reactor to do the adequate simulations to determine the behavior of the reactor during normal operation and during different accidents that may occur. The purpose of these simulations is to note what the effect will be in case of an accident. Currently, various software codes are being used to simulate and optimize the operation of a nuclear power plant during the different situations.

1.2 Problem Statement and Objectives of this study

The purpose of this study was to serve as a starting point to gain sufficient understanding and experience using the thermal hydraulic code Flownex® SE (Simulation Environment) (also just referred to as Flownex®) in simulations of a nuclear reactor. The evaluation of the suitability of Flownex® for this purpose was in terms of aspects that include:

- Assessing the simplifying assumptions built into and possible shortcomings of the software.
- Defining the applicable modelling methodology and further simplifying assumptions that have to be made by the user.
- Evaluating the accuracy and compatibility with the pool type research reactor.

- Comparing the results of this study with similar studies found in the open literature.

For this specific project of analysing the IAEA (International Atomic Energy Association) MTR (Materials Testing Reactor) 10 MW benchmark research reactor, the suitability of the software code Flownex® was investigated. The reason for the chosen MTR reactor was that various

studies and simulations were done on this specific reactor. The results of the MTR 10 MW are good set points to compare the results with Flownex® during this study.

It should be noted that parallel studies using COBRATF and RELAP5 mod 4 software codes have also been conducted (Fourie 2011, Kriel 2012). A follow-up study by the School would therefore be to compare the effectiveness of the different software codes being tested using the various simulation models.

1.3 Outline of this mini-dissertation

Chapter 2 presents a literature survey on different studies that were done on the IAEA MTR 10 MW during different postulated accident scenarios.

Chapter 3 presents the theoretical background that is relevant to the study. A description of the basic layout of a research reactor is discussed. For the purpose of safety analysis various different accidents may be postulated. Some of these accidents are discussed. The methods of determining the reactor power after a trip, the power distribution in the core and the heat transfer in the reactor are explained. Basic information pertaining to the software code Flownex® is discussed.

Chapter 4 gives a detailed explanation of the IAEA MTR 10 MW reactor that was simulated. A typical layout diagram of a MTR 10 MW research reactor is shown with a description of each component. The method of how the simulation model was set up is also described together with the assumptions that were made. The basic principles of Flownex® are explained and how the reactor model was built. Different steady state simulations were done on the reactor and the results are explained.

Chapter 5 presents transient simulations on the IAEA MTR 10 MW reactor core. Different LOFAs were simulated using 10 MW and 12 MW reactor power scenarios. The results are discussed in terms of the hottest section in the reactor core. The results of Flownex® were compared with results found in the open literature.

Chapter 6 is the conclusion chapter where the outcomes of the project are discussed. Future development and work resulting from this project are also discussed.

Chapter 2

2 Literature survey

2.1 Studies of different accident scenarios

Over the years various simulation models were set up according to the specifications of the IAEA MTR 10 MW reactor case study. Some of the simulations on LOCAs (loss of cooling accidents) and LOFAs (loss of flow accidents) will be discussed. Some of the results of this study were compared to that of previous studies for verification purposes.

2.1.1 Safety analysis of the IAEA reference research reactor during loss of flow accident using the code MERSAT (Hainoun et al., 2010)

The purpose of the study by Hainoun *et al.* (2010) was to do a detailed simulation of the IAEA MTR 10 MW research reactor using the thermal hydraulic code MERSAT. For their study the primary and secondary loops were modelled. The model enabled the simulation of the estimated neutronics and thermal hydraulic performance in the case of normal operation, reactivity and loss of flow accidents. In this study two different LOFA accidents were simulated, namely FLOFA (fast loss of flow accident) and SLOFA (slow loss of flow accident).

The transient and steady state operations in this study were for the thermal hydraulic simulations of the model to confirm the capability of the MERSAT code. For the steady state operation, the following boundary condition was specified similar to the IAEA MTR: water flows through the core with a mass flow of 1000m^3/h, an inlet temperature of 38°C and a pressure of 170 kPa. For the steady state simulation the temperature distribution, pressure losses and flow velocities were simulated. It was found during the steady state simulation that the core had a maximum water temperature of 61.2°C on the outlet of the hottest fuel channel for the 10 MW reactor. The results were physically realistic and there was a good comparison with studies that were done previously.

There are different actions that can cause a LOFA, including failure of the primary pump due to a loss of electrical failure on the pump or by a flow reduction through the fuel channel due to a failure of a valve or a blockage in the channel. For the study of Hainoun *et al.* (2010) a pump failure was assumed for the loss of flow through the core.

According to the IAEA (IAEA, 1992a), the reactor controller applies certain protection criteria in case of a LOFA. The criteria require that the core must shut down when the flow rate through the core is less than 85% of the nominal value. When 15% of the nominal flow rate is reached, a safety valve opens for natural circulation through the core.

For both of the LOFA simulations the model was subjected to the following conditions:

- Transient start at a power of 12 MW and downward cooling flow.
- Steady state duration before transient 50 s.
- Safety trip point: 85% of nominal core coolant flow.
- Delay time before linear shutdown reactivity insertion: 0.2 s.
- Shut down reactivity: -$10/0.5 s.
- Natural convection valve (NCV) opens at 15 % of nominal core coolant flow rate.

The results of this study is given in Appendix A

2.1.2 Simulation and analysis of IAEA benchmark transients (Gaheen et al., 2007)

The purpose of the Gaheen *et al.* (2007) study was to simulate the coupled kinetics and thermal hydraulics of the IAEA MTR 10 MW research reactor. The model was simulated for different accident scenarios.

Only the LOFA scenarios will be discussed here.

For the LOFA simulation the reactor was operating at 12 MW. In the case of the LOFA, the reactor was scrammed and the power level, fuel and cladding temperature dropped quickly. Then the temperatures started to increase due to decay heat and degradation of heat transfer. Two different LOFA simulations were done. One simulation had a time constant of 25 s and the other a time constant of 1 s. For each of these LOFA simulations LEU and HEU were used.

The results of this study is given in Appendix B

2.1.3 Dynamic calculations of the IAEA safety MTR research reactor benchmark problem using the RELAP5/3.2 code (Hamidouche et al., 2004)

A thermal hydraulic dynamic simulation was done by Hamidouche *et al.* in 2004 on the IAEA MTR 10 MW benchmark reactor. The purpose of this study was to evaluate the reactor's behaviour in the case of a reactivity induced accident and a loss of flow accident. The results were compared with previous data as determined with various software codes.

Only the LOFA accidents will be described here.

For the LOFA transient simulation, the IAEA MTR 10 MW reactor was set to trip with a delayed time of 0.2 seconds if the mass flow was 85% of the nominal value. The simulation was done for the 12 MW reactor. The mass flow was reduced according to the exponential equation exp (-t/T) with the period (T) of 1 second for FLOFA and 25 seconds for SLOFA. If the mass flow reached 15% of its nominal value the NCV (natural convection valve) would open to remove the passive decay heat by natural circulation of water.

The results of this study is given in Appendix C

During this study it was found that there was a good comparison between the results that were simulated with RELAP5 and the other software codes. The RELAP5 software was more realistic during the simulation and it took the interactions between the coolant loop and core dynamics into account.

2.1.4 Analysis of loss of coolant accidents in MTR pool type research reactor (Hamidouche & Si-Ahmed, 2010)

An analysis of a LOCA on a MTR pool type reactor was done by Tewfik Hamidouche and El-Khinder Si-Ahmed. In their simulation, they assumed a total loss of coolant accident on a MTR pool type research reactor. The purpose of this study was to examine the core behaviour during the LOCA and see if there is any visible damage to the fuel elements. The thermal hydraulic software code RELAP5/mod3.2 was used for this study.

During the study, simulations were done on different power levels before the accident was initiated. The purpose was to see what the maximum operating power can be when a LOCA occur so that there will be no damage on the cladding.

It was assumed that a breakage on the primary coolant pipe occurred. The reactor was operating full power on the time the accident happened. It was allowed that the reactor would scram when the water level of the reactor pool started to decrease, or if the mass flow rate reached 85 % of its normal flow rate. The core was analyzed at different power levels to determine the maximum power where the fuel would be damaged. The power level was varied between 1 MW and 10 MW.

The results of this study is given in Appendix D

It was found that when the reactor power was smaller than 4MW that there will be no need for an emergency cooling system. The reason for this assumption was that the maximum cladding temperature was not greater than the melting point of the aluminium cladding when the reactor was operating at a power lower than 4 MW.

2.1.5 Flow blockage analysis of a channel in a typical material test reactor core (Lu *et al.*, 2009b)

The purpose of study by Lu *et al*.,2009b was to simulate a partial and total blockage in one of the flow channels of a material test reactor without scramming the reactor. The simulation was done with the software package RELAP5/Mod3.3. The reactor core was specified according to the IAEA MTR 10 MW reactor.

For this simulation it was important to consider the interaction between the reactor cooling and core kinetics during the blockage of the channel. Only 9 of the channels and fuel plates were modeled for this study. The power and mass flow of the coolant was specified as the normal initial conditions of the reactor.

A transient simulation was done to determine the effect of the blockage over time. For the validation of the simulation model, the result of a FLOFA which was defined in IAEA TECDOC 643 (1992) was used for the study. The power of the core was initiated at 12 MW which included the 1.2 overpower factor. For the transient simulation the reactor was set to trip if the mass flow was 85% of the nominal value. The mass flow was reduced according to the equation exp (-t/T) with the period (T) of 1 second for FLOFA.

The simulation was divided into two different simulations. The first simulation was where the flow channels was partially block with 95% of the nominal mass flow and the second where the flow was totally blocked. For the transient simulation the reactor was operated for 500s under normal conditions until the blockage was initiated. The boundary conditions of the simulation is given in Table 1

Table 1: Main initial and boundary conditions

Transient key parameters	Partial blockage (95%)	Total blockage (100%)
Total core power (MW)	10	10
Total mass flow rate (kg/s)	1000	1000
Flow direction	Downward	Downward
Blocked channel	3	3
Steady state duration time before transient (s)	500	500
Transient duration time (s)	9.5	10
Scram	Disabled	Disabled

The results of this study is given in Appendix E

During this study it was found that there was no boiling in the channel even when the channel was totally blocked.

2.1.6 Comparison between the simulation results of the different studies

In terms of the scope of this study, only the LOFA will be discussed. The LOFA results of studies discussed above will be used to compare with the simulation results of the present study. All of these studies have used the same simulation approach, core layout and core specifications. These approaches, parameters, etc, will be discussed in detail in chapters 3 and 4. Further, all the studies used the same approach for the reduction of the mass flow during the LOFA.

The experimental setup of the different literature studies has given a good guideline for the preparation and development of the simulation model in Flownex®. The results of the studies can be used for the comparison and validation of the accuracy of Flownex®.

Chapter 3

3 Theory

3.1 Introduction

This chapter provides basic information of the IAEA MTR 10 MW and the function of the primary and secondary coolant loops. The different accident scenarios that can be postulated under normal operating conditions are explained and how each one of the actions can take place. The calculations on how to determine the power distribution in a reactor core and the effects of the delayed neutrons and fission products on the power after a reactor trip are explained. Flownex® was used for this study and the basic principles of the software code are therefore discussed. Flownex® solves the conservation equations and heat transfer for any thermal- hydraulic simulation. Basic principles of the conservation equation and heat transfer equations are explained. A literature survey is presented on different studies that were done on the IAEA MTR 10 MW during different accident scenarios.

3.2 IAEA MTR 10 MW Benchmark Reactor

The IAEA MTR 10 MW reactor is a light water pool type research reactor that has been specified by the IAEA as a benchmark case (IAEA, 1980). The reactor is moderated and cooled by circulating light water downwards through the core. The removal of heat is done by forced convection when the reactor is operating under normal conditions (Hamidouche *et al.*, 2010). After shutdown, natural convection is used to remove the residual heat in the core. Figure 3-1 is a representation of a typical layout of the reactor with the primary coolant loop of an MTR research reactor. The water is heated by the reactor and is circulated through the primary coolant hot leg to the heat exchanger. The heat is removed from the primary coolant side by circulating colder water from the secondary coolant loop through the heat exchanger. After the heat is removed in the primary coolant loop, the water is pumped back into the reactor core via the cold leg. The coolant loop has backup systems in case of a pipe block or pipe break to keep the reactor fuel temperatures within acceptable limits.

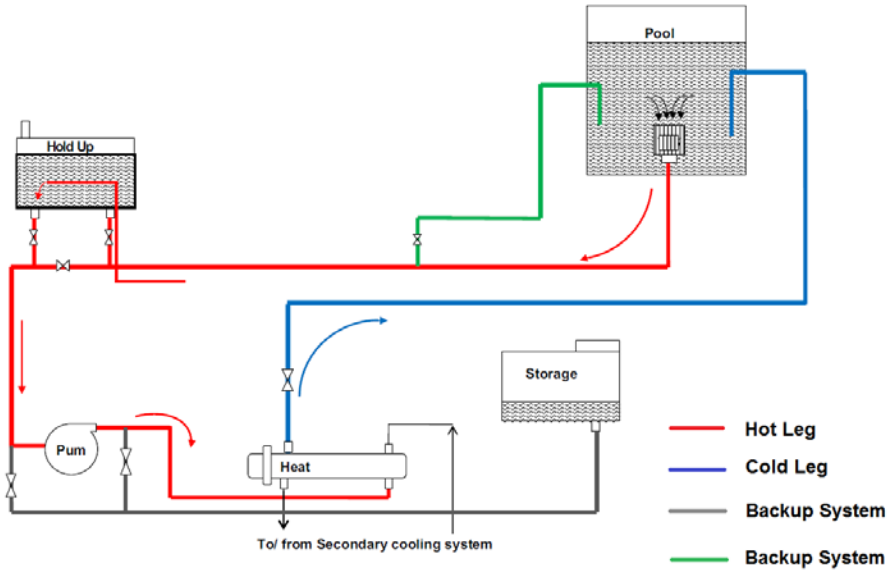

Figure 3-1: Representation of MTR coolant loop (Hamidouche et al., 2010).

It should be noted that SAFARI -1, which is the South African research reactor at NECSA, is also a MTR type reactor.

3.3 Postulated accidents

For this study, accident scenarios in terms of loss of fluid flow (LOFA) will be simulated to determine the effect thereof on the heat transfer in the core. As background, it would be fitting to give a brief description of the different accidents that can be postulated for a reactor core together with their effects. In most of the research studies that were done on the thermal-hydraulic analysis for research reactors, the cases for LOCA (loss of coolant accident) and LOFA (loss of flow accident) were simulated. Other studies included simulation of RIA (reactivity insertion accidents). In this study only the LOFA situations will be simulated in the analysis of the MTR 10 MW pool type research reactor. In the following subsections, a short description of the types of accidents that were simulated in other studies is presented.

3.3.1 Loss of coolant accident (LOCA)

LOCA is a loss of coolant from the reactor core and this can lead to serious damage to the reactor core and the plant. Such a loss of coolant can occur when there is a rupture or leak in one of the cooling pipes. During the LOCA, the temperature of the reactor core will start to

increase, and may exceed its maximum design specification. This could lead to a core meltdown. Furthermore, after a certain time, the molten fuel together with the structural material could melt its way through the pressure vessel, then through the concrete and into the ground (Lamarsh, 2001).

3.3.2 Loss of flow accident (LOFA)

LOFA is similar to LOCA. It happens in case of a failure of the primary coolant pump or other accident cases. However, the difference is that the fluid is not lost from the system. The effects of a LOFA are similar to that of a LOCA. The temperature starts to increase, and the core could start to melt should the emergency cooling system fail.

3.3.3 Reactivity insertion accident (RIA)

Normally with the research reactor, a RIA may happen during the refuelling stage when new fuel assemblies are loaded or when the control rods in the core are suddenly removed. Positive reactivity enters the core and the core becomes supercritical. The temperature and the power start to increase and if the heat removal system cannot remove the excess heat fast enough the core may be damaged, which can lead to a severe accident (Lu *et al.*, 2009a).

3.4 Loss of flow accident

According to the IAEA, the following flow transient scenarios should be considered in the case of a LOFA as different accident scenarios (IAEA, 1992b).

- Failure of primary pump.
- Primary coolant flow reduction (e.g. valve failure, blockage in piping or heat exchanger).
- Influence of experiment failure or mishandling.
- Failure of emergency cooling system.
- Primary coolant boundary rupture (pipe or vessel) leading to loss of flow.
- Fuel channel blockage.
- Improper power distribution due to, for example, unbalanced rod positions, in-core experiments or fuel loading.
- Coolant reduction due to core bypass.
- Malfunction of reactor power control.

- System pressure deviation from normal limits.
- Loss of heat sink (e.g. valve or pump failure, system rupture).

For this study the LOFA scenario due to the failure of a primary pump was simulated.

3.5 Analysis chain

For the thermal-hydraulic simulation model, the conservation laws together with the heat transfer equations are solved. To determine the heat transfer, the total power input in the core would be needed. The power has a fixed value in the case of a steady state simulation, but in the case of a transient simulation, the power input decreases after the reactor has tripped. The rate of decreasing of power is determined by the neutronics and fission products of the fuel and will be discussed in section 3.6. The neutronic and fission product decay modelling gives the power at each time step after the reactor trip. The power at these different time steps is then used to solve the heat transfer equations for the transient simulation model. A discussion follows on how the core power after the trip can be calculated.

3.6 Neutronics and decay heat power

3.6.1 Reactor power behaviour after trip

In case of a LOFA, LOCA or RIA the reactor has a protection setting which causes the control fuel elements to be inserted into the core which trips the reactor. After the trip, the reactor power reduction is effected by three main parameters, namely: reactivity feedback, decay heat and delayed neutron fission. In terms of the scope of this study only delayed neutron fission and decay heat were taken into account. The reactivity feedback coefficients were not included in the scope of this study. A discussion of the decay heat and delayed neutron follows in the next sections.

3.6.1.1 Decay heat

During the operation of a nuclear reactor, β- and γ radiation is produced by the decaying fission products. A total of around 7% of the norminal thermal power output of the reactor is produced in the form of decay heat. After shutdown, energy is released by the continuing decay of fission products. The power that is generated by the decay of fission product can be

substantial and the reactor should be cooled permanently for the safety of the reactor (Lamarsh, 2001).

The total decay heat power at t seconds after shutdown can be calculated using the following equation (ANS, 2005).

$$P_d(t,T) = P'_d(t,T) \times G(t) \tag{3.1}$$

where $P'_d(t,T)$ is the total fission product decay heat power and $G(t)$ the factor that accounts for the neutrons that are captured by fission products. This factor is given in Eq (3.5).

In Eq (3.2) the sum of the uncorrected decay heat power $P'_{di}(t,T)$ for the different fission products is calculated using

$$P'_d(t,T) = \sum_{i=1}^{4} P'_{di}(t,T) \tag{3.2}$$

The fission products that are normally used are $^{235}U, ^{239}Pu, ^{238}U$ and ^{241}Pu.

The uncorrected decay heat power $P'_{di}(t,T)$ can be solved with Eq (3.3) given below, where $P_{i\alpha}$ is the total power of the reactor and $F_i(t_\alpha, T_\alpha)$ is the decay heat power that is t seconds after shutdown while the reactor was operating for T seconds. $F_i(t_\alpha, T_\alpha)$ is calculated with Eq (3.4) given below by the decay heat given in the tables of the American Nuclear Society Report and Q_i is the energy (normally 200 MeV/fission) that will be released by fission(ANS, 2005).

$$P'_{di}(t,T) = \sum_{\alpha=1}^{N} \frac{P_{i\alpha} F_i(t_\alpha, T_\alpha)}{Q_i} \tag{3.3}$$

$$F_i(t_\alpha, T_\alpha) = F_i(t_\alpha, \infty) - F_i(t_\alpha + T_\alpha, \infty) \tag{3.4}$$

$$G(t) = 1.0 + (3.24 \times 10^{-6} + 5.23 \times 10^{-10} t) T^{0.4} \psi \tag{3.5}$$

3.6.1.2 Delayed neutrons

In the fission reaction several neutrons are produced. Most of these fission neutrons are immediately produced within a time of 10^{-14} seconds and is known as prompt neutrons. A few neutrons (less than 1%) are produced after a delayed time by radioactive fission products. These neutrons are knows as delayed neutrons (Duderstadt & Hamilton, 1976).

Normally, the delayed neutrons are arranged into six groups according to the time that the precursor fission product takes to decay.

In this study, it is assumed that the six delayed neutron groups can be represented/replaced by one delayed neutron group.

In Stacey (2007:151), the following equations are used to solve the delayed neutron population and precursor population for the transient simulation model. The derivation of these equations is discussed in Stacey (2007).

$$n(t) = n_0 \left[\frac{\rho}{\rho - \beta} \exp\left(\frac{\rho - \beta}{\Lambda} t \right) - \frac{\beta}{\rho - \beta} \exp\left(\frac{-\lambda \rho}{\rho - \beta} t \right) \right] \tag{3.6}$$

$$c(t) = n_0 \left[\frac{\rho \beta}{(\rho - \beta)^2} \exp\left(\frac{\rho - \beta}{\Lambda} t \right) - \frac{\beta}{\Lambda \lambda} \exp\left(\frac{-\lambda \rho}{\rho - \beta} t \right) \right] \tag{3.7}$$

For a light water reactor the following parameters can be used without much loss of accuracy:

β =0.0075, λ =0.08 s^{-1} and Λ =6 x 10^{-5} s (Stacey, 2007).

3.7 Reactor power spatial distribution

In an operating nuclear reactor, the power in the core is not distributed in a uniform way. The power could be more concentrated towards the middle of the core. The reason for this is because the core is finite, and the isotopic concentrations might differ in different parts of the core and reflector. This means that the neutron flux would not be evenly distributed in the core. It is necessary for this study to know the power distribution for each fuel assembly. The power

distribution can be solved analytically or numerically. The numerical calculation is a very complex solution and is normally solved with software codes like SCALE and CITATION. For this study the power distribution was solved analytically using the approximation of a finite homogenous block. The flux profile listed in the textbook Nuclear Reactor Physics of Westom M. Stacey was used as the starting point for the power distribution calculations (Stacey, 2007). Discussion of the calculation method follows in the next paragraphs.

It can be assumed to a first approximation that the MTR is a finite homogenous block with a total power of P_0.

The flux profile is then given by the following equation (see Stacey (2007) for derivation):

$$\Phi(x, y, z) = A\cos(k_1 x)\cos(k_2 y)\cos(k_3 z) \tag{3.8}$$

If we assume that the power is represented by the flux profile, then the power profile will have the same shape as the flux profile.

Let the dimensions of the reactor be 2a, 2b and 2c in the x, y and z directions. Then the total power of the reactor is given by Eq (3.9).

$$P_0 = \iiint_{-a,-b,-c}^{a,b,c} A\cos k_1 x \cos k_2 y \cos k_3 z \, dxdydz \tag{3.9}$$

Given a 3-D calculation grid, the power P_{ij} in any volume element of the grid can be calculated using Eq (3.10).

$$P_{ij} = \iiint_{x_i-\Delta x/2, y_j-\Delta y/2, z_k-\Delta z/2}^{x_i+\frac{\Delta x}{2}, y_j+\frac{\Delta y}{2}, z_k+\Delta z/2} A\cos k_1 x \cos k_2 y \cos k_3 z \, dxdydz \tag{3.10}$$

The constants k_1, k_2 and k_3 of Eq (3.10), can be determined in many ways. Here, the peaking factors are used to determine, k_1, k_2 and k_3

The peaking factor is defined as the ratio between the LPD (local power density) and the average power density in the entire core (Bae *et al.*, 2008). The LPD is defined as the hottest point in the core and must be calculated to confirm that the core will not melt (Bae *et al.*, 2008). This definition can be extended to peaking factors in specific directions.

If only the radial peak factor was given, it can be assumed that the radial peaking factor would be the same in the x- and y-direction.

For any y and z value, the maximum flux in the x-direction can be determined by Eq (3.11).

$$\Phi_x^{\max} = A\cos(k_2 y)\cos(k_3 z) \tag{3.11}$$

The average value of the flux for the function can be determined with the following equation:

$$\Phi_x^{ave} = \frac{\int_a^b A\cos(k_1 x)dz}{\int_a^b dx} \tag{3.12}$$

The peaking function can then be determined as follows:

$$PF_x = \frac{\Phi_x^{\max}}{\Phi_x^{ave}} \tag{3.13}$$

For given peaking factors PF_x, PF_y, PF_z, the values of k_1, k_2, k_3 can be determined for each of the directions. Once the values for k_1, k_2 and k_3 have been determined, the constant A can then be found by performing the integral of Eq (3.9) for a given power.

3.8 Thermal-hydraulic theory

If there is flow through a control volume with boundaries at the inlet and outlet, then there would be a change in the mass, momentum and energy due to different factors that have an effect on the fluid. These changes in the mass, momentum and energy can be solved by the conservation laws which will be discussed below.

3.8.1 Conservation equations

Figure 3-2 presents a diagram of an infinitesimal control volume that was used for the derivation of the conservation laws (Rousseau & Van Eldik, 2011). Only the final equations of the conservation equations will be described together with the meaning of each term and the derivations of these equations are not repeated here.

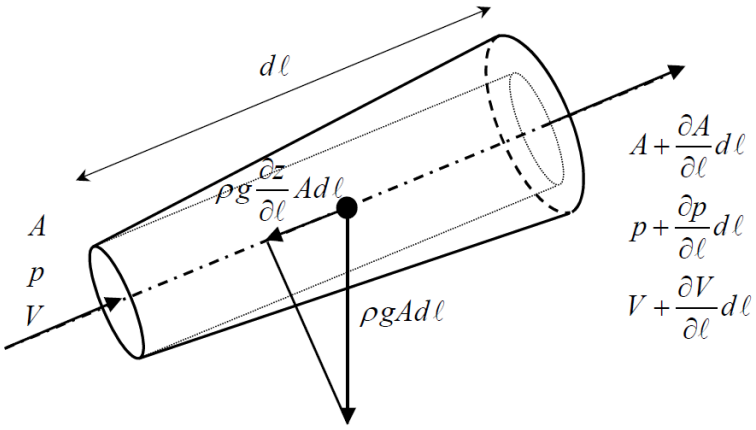

Figure 3-2: Diagram of an infinitesimal control volume (Rousseau & Van Eldik, 2011).

3.8.1.1 Conservation of mass

The conservation of mass equation is also known as the continuity equation. The conservation of mass can be defined as the rate of change of mass through the control volume and is derived for Figure 3-2. The derived equation is given by Eq (3.14).

$$\cancel{V}\frac{\partial \rho}{\partial t} + \dot{m}_e - \dot{m}_i = 0 \tag{3.14}$$

The first term of Eq (3.14) can be presented as the rate of change of mass within the control volume over time, the second term is the mass flow that exits the control volume and the last term is the mass flow that enters the control volume (Rousseau & Van Eldik, 2011).

3.8.1.2 Conservation of momentum

The conservation of momentum equation is derived from the well-known Navier-Stokes equations. The equation can be derived for compressible and incompressible flow. For this study only incompressible flow was used, because water was used as the coolant fluid. The conservation of momentum equation for incompressible flow is given by Eq (3.15).

$$\rho L \frac{\partial V}{\partial t} + (p_{0e} - p_{0i}) + \rho g (z_e - z_i) + \Delta p_{0L} = 0 \tag{3.15}$$

The first term of Eq (3.15) represents the rate of change of momentum within the control volume over time. The second term is the difference in the total pressure between the inlet and outlet of the control volume and the third term represents the gravitational force. The last term is the total pressure loss through the control volume (Rousseau & Van Eldik, 2011). The pressure drop calculation will be discussed in section 3.8.2.

3.8.1.3 Conservation of energy

The conservation of energy is also known as the first law of thermodynamics. The equation can be defined as the change of energy within the control volume. The conservation of energy equation is given by Eq (3.16).

$$\dot{Q} + \dot{W} = \cancel{V} \frac{\partial}{\partial t} (\rho h_0 - p_0) + \dot{m}_e h_{0e} - \dot{m}_i h_{0i} + \dot{m}_e g z_e - \dot{m}_i g z_i \tag{3.16}$$

The equation can be explained as the total work and heat in the control volume that is equal to the rate of change in energy over time plus the losses of energy throughout the control volume (Rousseau & Van Eldik, 2011).

3.8.2 Pressure Drop

In any normal flow channel a pressure drop is present which is caused by friction and secondary losses in the control volume (Rousseau & Van Eldik, 2011). The pressure drop term in Eq (3.15) can be solved by the following equation given in the Flownex® Library User Manual 2011 (Anon, 2011):

$$\Delta p_{0L} = \left(\frac{fL}{D_H} + \sum K \right) \frac{1}{2} \rho V |V| \tag{3.17}$$

where:

f	-	Friction factor.
L	-	Length (m) of the pipe.
D_H	-	Hydraulic diameter (m) of the flow channel.
ρ	-	Density of the fluid (kg/m^3).
$\sum K$	-	Sum of the secondary losses.
V	-	Mean velocity (m/s).

The mean velocity V in Eq (3.17) can be solved with the following equation:

$$V = \frac{\dot{m}}{\rho A} \tag{3.18}$$

where A is the flow area of the pipe and $\dot{m}$ the mass flow through the channel. By substituting Eq (3.18) into Eq (3.17), the pressure drop through a flow channel is given by the following equation (Anon, 2011).

$$\Delta p_{0L} = \left(\frac{fL}{D_H} + \sum K \right) \frac{1}{2} \rho \frac{\dot{m}|\dot{m}|}{\rho^2 A^2} \tag{3.19}$$

3.8.3 Heat transfer

The definition of heat transfer is the transition of thermal energy due to spatial temperature difference (Incropera *et al.*, 2007). There are 3 different types of heat transfer, namely conduction, convection and radiation. Only heat transfer through conduction and convection will be taken into account for the simulation in this project. Since all the fuel plates in a fuel assembly will be assumed to be at the same temperature, there will be no radiation between the plates.

Conduction is known as the heat transfer of energy between volumes with higher to volumes of lower energy by the interactions of the particles of the different volumes (Incropera *et al.*, 2007). It can be expressed as the heat transfer between two solid materials. For this project the conduction heat transfer is used to determine the total heat transfer between the uranium fuel and aluminium cladding in the MTR. It will be used to determine the wall temperature of each material that is connected to each other.

Convection is defined as the energy transfer due to the molecules moving from one place to another (Incropera *et al.*, 2007). It contributes to the heat transfer between a solid and a fluid. In this project, the convection heat transfer will be used to determine the heat transfer between the water coolant of the reactor and the aluminium cladding of the fuel plates. With this approach the surface temperature of the aluminium cladding can be determined.

A discussion on how to calculate the conduction and convection heat transfer in a simulation model follows. Newton's Law of cooling states that when a fluid with a temperature T_∞ flows over a surface with no fins with a surface temperature T_s and a surface area A, then

$$Q = h_c A(T_s - T_\infty) \tag{3.20}$$

where h_c is the convection heat transfer coefficient and Q the total heat input (Rousseau & Van Eldik, 2011).

Figure 3-3 gives a diagram of a heat exchanger with a wall in the centre and fluid entering the primary and secondary sides. In Figure 3-3 the subscripts p and s indicate the primary and

secondary sides respectively, and the temperatures on the wall are indicated by T_{wp} and T_{ws} for the primary and secondary sides respectively (Rousseau & Van Eldik, 2011).

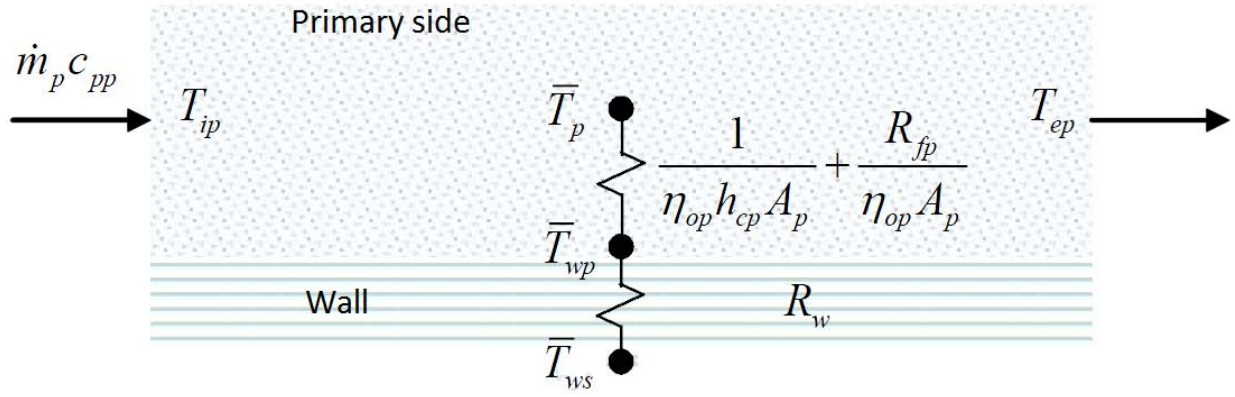

Figure 3-3 : Diagram of thermal resistances in a heat exchanger (Rousseau & Van Eldik, 2011).

This method that will be described is for the convection heat transfer calculations. The thermal resistance of the primary side can be determined by using the following equation:

$$\frac{1}{(UA)_p} = \frac{1}{\eta_{op} h_{cp} A_p} + \frac{R_{fp}}{\eta_{op} A_p} \tag{3.21}$$

where in Eq (3.21)

$\frac{1}{(UA)}$	-	Thermal Resistance.
η_0	-	Overall surface efficiency.
h_c	-	Convention heat transfer coefficient.
A	-	Total heat transfer area.
R_f	-	Fouling factor.

To determine the convection heat transfer coefficient the Nusselt must be calculated with the Dittus-Boelter equation for turbulent flow (Rousseau & Van Eldik, 2011). The Dittus-Boelter Equation is given by the following:

$$Nu = 0.023 \mathrm{Re}^{0.8} \mathrm{Pr}^{0.4} \tag{3.22}$$

where Re is the Reynolds number and Pr is the Prandtl number. The Reynolds number Re can be calculated with Eq (3.23).

$$\mathrm{Re} = \frac{\rho V D_H}{\mu} = \left| \frac{\dot{m} D_H}{\mu A} \right| \tag{3.23}$$

where

ρ	-	Density of the fluid.
μ	-	Viscosity of the fluid.
$\dot{m}$	-	Mass flow of the fluid.
D_H	-	Hydraulic diameter of the flow channel.

The Prandtl number Pr is solved with Eq (3.24) where C_p is the specific heat of the fluid.

$$\mathrm{Pr} = \frac{C_p \mu}{k} \tag{3.24}$$

The convection heat transfer coefficient is then calculated with Eq (3.25):

$$Nu = \frac{h_c D_H}{k} \tag{3.25}$$

For conduction heat transfer, the thermal resistance of a wall can be determined by the following equation as described by Incropera *et al.* (2007:98):

$$R_w = \frac{L}{kA} \tag{3.26}$$

where L is the thickness of the wall, k the thermal conductance of the solid material and A the total heat transfer area. The temperatures of the fluid and the wall on the primary side can be solved with the following equations:

$$Q = (UA)_p (T_{wp} - T_P) \tag{3.27}$$

with

$$T_p = \frac{1}{2}(T_{ip} + T_{ep}) \tag{3.28}$$

where the subscript i and e are the inlet and outlet temperatures of the fluid in the flow channel. The heat transfer in the wall can be calculated with the following equation:

$$Q = \frac{1}{R_w}(T_{ws} - T_{wp}) \tag{3.29}$$

The overall heat transfer coefficient UA between the two fluid streams can be determined by

$$\frac{1}{UA} = \frac{1}{\eta_{op} h_{cp} A_p} + \frac{R_{fp}}{\eta_{op} A_p} + R_w \tag{3.30}$$

The same approach was used for this study. The only difference was that the heat transfer was calculated for one flow channel for the convection heat transfer and two different solid materials for the conduction heat transfer. The different materials that were used for this study were aluminium cladding and uranium fuel.

3.8.4 CFD and SCFD

3.8.4.1 CFD approach

"CFD (computational fluid dynamics) approach is the solution of the differential equations for the conservation of mass, momentum and energy on a per unit volume basis." (Rousseau & Van Eldik, 2011).

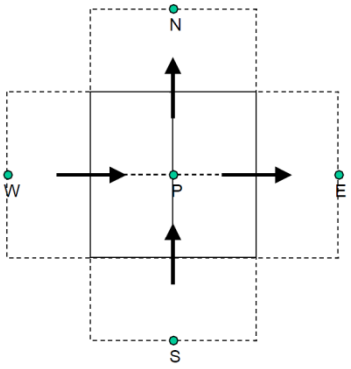

Figure 3-4: Control volume for CFD approach (Landman & Greyvenstein, 2004).

In Figure 3-4 a typical two dimensional control volume is shown that is used for the CFD approach. An assumption is made that pressure, velocity and temperature properties vary smoothly over the control volume. The average property values of the control volume are then represented by a nodal point P in the middle of the control volume. The properties such as the temperature, velocity and pressure can be represented by the nearest neighbours (N, E, S, and W). The mass momentum and energy vary over the boundary of the control volume (Landman & Greyvenstein, 2004).

The conservation of mass and energy is written around point P for a control volume but the conservation of momentum is written for flows over the boundary at the interface of the control volume. This is known as a staggered grid approach (Landman & Greyvenstein, 2004).

3.8.4.2 SCFD approach

The difference between CFD and SCFD (systems computational fluid dynamics) is that SCFD uses one dimensional elements that are connected to nodes. In Figure 3-5 it can be seen that the elements and nodes can be linked up in an unstructured method (Rousseau & Van Eldik, 2011).

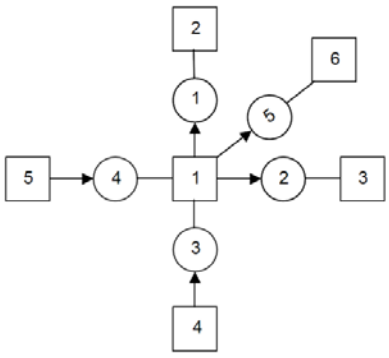

Figure 3-5: Node element configuration of SCFD approach method (Rousseau & Van Eldik, 2011).

In Figure 3-5 the square blocks represent the nodes and the circle represents the elements. The elements can be specified as any type of thermal-fluid component like pipes, pumps, fans, compressors, turbines or heat exchangers. The nodes can be used for the connection between elements or to specify a boundary condition method (Rousseau & Van Eldik, 2011).

One of the similarities of the CFD and SCFD approach is that the node represents the average fluid properties. Another similarity is that the conservation of mass and energy are also written in terms of a node and the conservation of momentum equations are written in terms of the elements method (Rousseau & Van Eldik, 2011).

It is assumed that the limits of the SCFD method are that it can only solve one-dimensional flow. However, two or three dimensional flow fields can be built up from the one-dimensional case with appropriate assumptions. The correct combinations of elements and nodes must be used to build the network for the different directions on the coordinate system method (Rousseau & Van Eldik, 2011).

Flownex® is based on the System-CFD approach or the so called network approach.

3.9 Flownex®

For this project the software code Flownex® was used to set up a simulation of a typical MTR 10 MW Research Reactor.

Over the years Flownex® has been developed by M-Tech industrial (South Africa, Potchefstroom) in association with PBMR. This software helps the user to perform detailed analysis and design of complex thermal-fluid simulations and structures such as power plants and thermal-fluid networks (Van Niekerk *et al.*, 2006). In Flownex® the system is divided into a number of spatial or conceptual volumes in a way that is similar to the conventional CFD code. The system is then solved by a number of equations. Flownex® does not solve the three-dimensional Navier-Stokes equations like normal CFD software. A number of basic one-dimensional momentum equations are applied into the three-dimensional spatial control volumes. This method is similar to how the flow through a porous medium is approached in standard CFD codes (Van Niekerk *et al.*, 2006). Flownex® is based on an IPCM (implicit pressure correction method) that solves the momentum equation in each element and the continuity and energy equation at each node in large arbitrarily structured networks for both steady-state and dynamic situations (Landman & Greyvenstein, 2004). This gives the software a pseudo-CFD capability and allows Flownex® to analyse complex scenarios such as temperature and pressure gradient through pipes and buoyancy effects in packed beds (Landman & Greyvenstein, 2004).

Flownex® is capable of calculating the steady-state and the dynamic simulations of systems that consist of any combination of the following (Anon, 2009):

- Liquids systems.
- Gas systems.
- Mixtures of gases.
- Two phase system with phase changes.
- Incondensable mixtures of two phase fluids with gases.
- Slurry systems.
- Heat transfer between systems.
- Mechanical systems like shafts and gearboxes between systems.
- Combustion.
- Control systems.
- Electric systems.
- Excel workbooks.
- User coding and scripts.

"The solver that is optimized for steady-state and transient flows, can deal with both fast and slow transients" (Van Ravenswaay *et al.*, 2006). The code is able to solve multiple gas and liquid networks that are connected through a heat exchanger at the same time. The code uses the fundamental principle approach that will be discussed in section 3.9.1, that allows prediction of phenomena such as choking, natural convection and Joule heating (Van Ravenswaay *et al.*, 2006).

In Flownex®, a feature called a model builder helps the user to build any advanced model by using complex components or sub-systems such as nuclear reactors and heat exchangers. The standard component models include a comprehensive pipe model, orifice models, a reservoir model, a turbine model, various heat exchanger models, a compressor model, two reactor models, a PID (proportional integral derivative) controller, valve models and pump models (Van Ravenswaay *et al.*, 2006).

3.9.1 Fundamental approach

In Flownex® the thermal-fluid networks are based on the numerical solution of the governing equations. The solution is based on solving the fluid dynamics equations for compressible gas, incompressible liquids, two phase fluids and heat transfer through solid structures (Theron, 2011).

In a Flownex® network the mass flow, pressure and temperature of solids and fluids are obtained by solving the conservation of mass, momentum and energy equation. Flownex® can predict phenomena like the buoyancy effect and temperature and pressure waves (Theron, 2011). “The Fundamental Approach is normally used for simulation, design, optimization of thermal-fluid networks.” (Theron, 2011).

3.9.2 Heat transfer in Flownex®

The following effects can be taken into account in Flownex® when heat transfer simulations are done (Theron, 2011):

- The effects of cooling and heating of fluids on pipes and component walls.
- Determination of the total heat loss to the atmosphere through walls and pipes.
- During dynamic simulation the thermal inertia and heat capacitance of materials and fluids can be determined.
- The total heat loss or gain when there is a change to the atmospheric temperatures.
- The determination of the heat transfer of the fluids through the wall and plate in heat exchangers.
- The optimal calculation of the insulation of pipes, components and housings.
- The effect of the heat transfer of solar heating systems.

Flownex® uses a heat transfer element to convey the effect of the heat transferred to other elements. The calculation of the heat transfer element is done on the same principle that was explained in section 3.8.3. This heat transfer element allows the user to specify convection, conduction and radiation in two different directions (Theron, 2011). More than one type of heat transfer can be specified at the same time in the element. This enables the user to determine the total heat transfer in an insulated pipe, with water flowing through it.

Chapter 4

4 Numerical model setup, results and discussion

4.1 Introduction

In this chapter a full description of the numerical model will be discussed. First the assumption made in developing the model is presented. The detailed specifications of the IAEA MTR 10 MW reactor are then given with a description of the basic principles of the reactor core and components. This is followed by the method of the simulation model setup in Flownex® and the different assumptions that were made for the different simulations. Steady state simulations on the single fuel assembly are done and the results of Flownex® are compared with a model in EES (Engineering Equation Solver) to determine the validity thereof. The core is also built in Flownex® for a steady state simulation and the simulation results were validated. The different calculations and assumptions used to determine the power distribution are discussed

4.2 Assumptions

For the simulation model a few assumptions were made to reduce the complexity of the project.

- The point kinetics equations with one delayed neutron group were used without reactivity feedback.
- A cosine power profile was used due to the fact that the calculation of the neutronic flux profile was beyond the scope of this study.
- The average power in each of the 23 fuel plates in a fuel assembly was assumed to be equal. This eased the difficulty in the discritization of the problem
- No heat transfer between the fuel assemblies was assumed and also between the individual fuel plates in a fuel assembly.
- The heat source must be specified at the boundary.

4.3 Reactor core specifications and experimental setup

4.3.1 IAEA MTR 10 MW benchmark reactor specifications

Figure 4-1 illustrates the core configuration of the MTR 10 MW reactor, showing the layout of each assembly. In the core there are 23 standard fuel assemblies (SFAs) and 5 control fuel assemblies (CFAs) (IAEA, 1992a). Graphite blocks on two of the opposite sides of the core reflect the neutrons back into the core. The core is cooled by two water channels and the core is surrounded by light water. Light water enters the core at a temperature of 38°C and a pressure of 170 kPa. The core is cooled by circulating this light water through the vessel at a rate of 1000 m^3/h.

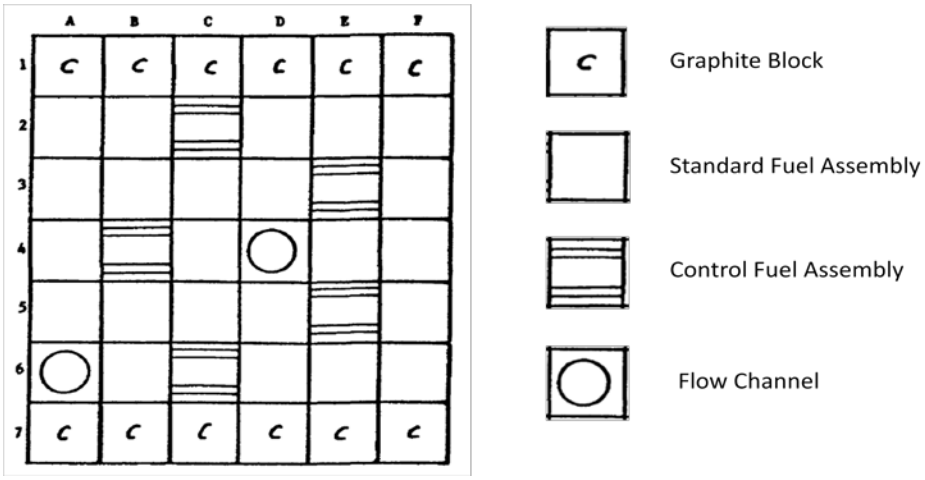

Figure 4-1: Core Configuration (IAEA, 1992a).

In Figure 4-2 it can be seen how a typical fuel assembly is structured with flow paths and fuel plates. Each of the SFAs contains 23 standard fuel plates and the CFAs contain 17 standard fuel plates and 4 aluminium absorber plates (IAEA, 1992a).

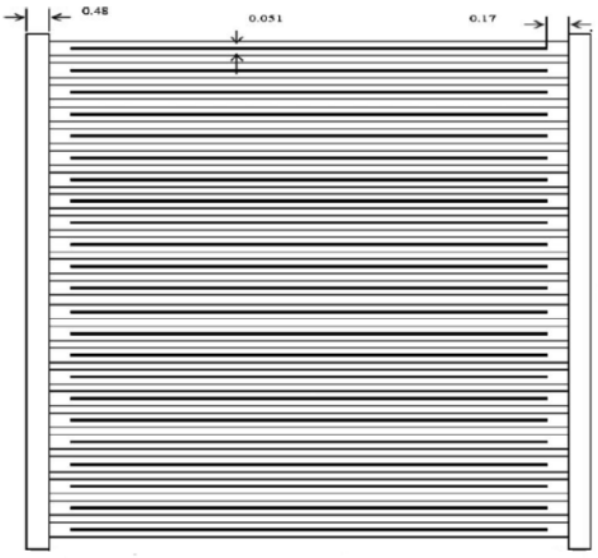

Figure 4-2: Cross sectional view of MTR fuel assembly (Bousbia-salah et al., 2006).

Figure 4-3 shows the dimensional cross sectional view of the SFA and CFA. Figure 4-3 gives a clear representation of the different dimensions according to the specifications of the MTR fuel assembly (IAEA, 1992a). The unit of the dimensions in Figure 4-3 is in centimetres. In Table 2 a full description of the core specifications of the fuel assemblies is given. For this study only Low Enriched Uranium (LEU) was simulated.

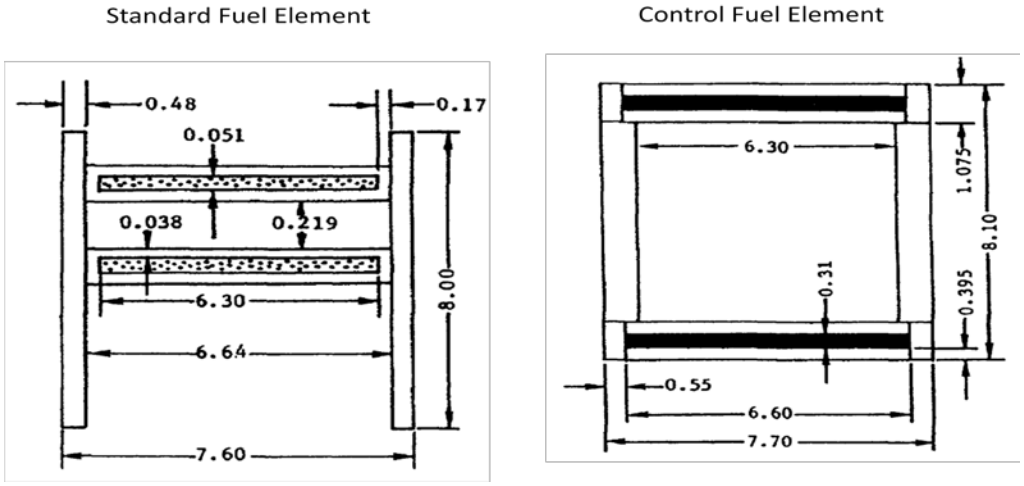

Figure 4-3: Cross-sectional view of MTR SFA and CFA (IAEA, 1992a).

Table 2: Reactor fuel specifications (IAEA, 1992a).

IAEA 10 MW generic reactor specifications	
Coolant	Light water
Coolant flow direction	Downward

Fuel thermal conductivity (W/cm K)	0.5
Cladding thermal conductivity (W/cm K)	1.8
Fuel specific heat (J/g K)	0.728
Cladding specific heat (J/g K)	0.892
Fuel density (g/cm^3)	0.68
Cladding density (g/cm^3)	2.7
Radial peaking factor	1.4
Axial peaking factor	1.5
Engineering peaking factor	1.2
Inlet coolant temperature (°C)	38
Operating pressure (bar)	1.7
Length (cm)	8
Width (cm)	7.6
Height (cm)	60
Number of fuel elements SFE/SCE	23/5
Number of plates SFE/SCE	23/17
Plate meat thickness (mm)	0.51
Width (cm) active/total	6.3/6.64
Height (cm)	60
Water channel thickness (mm)	2.19
Plate clad thickness (mm)	0.38
Mass Flow (m^3/h)	1000

4.3.2 IAEA prescription of transient accidents

Studies have been done by the IAEA on the different transient accidents that can occur during the operation of a nuclear reactor. The most common are the LOFA and the slow reactivity insertion that may happen during the start-up of the reactor. These actions were simulated with the software core PARET for the benchmark calculations, and the results will be discussed in the next section.

4.3.2.1 Loss of flow accident

In case of a LOFA the flow rate decay is postulated as exponential with a time constant of 1 s dropping from a power level of 12 MW. The reactor has a trip setting with a time delay response of 0.2 s in the case of the coolant flow rate through the core becoming less than 85% of its nominal flow rate. For the simulation in PARET by the IAEA the mass flow was reduced by an exponential (exp(-t/T)) decline with the period (T) equal to 1 s for a FLOFA and 25 s for a

SLOFA. After the reactor trip a negative reactivity of $10/05.s is inserted to keep the core under control (IAEA, 1992a).

During the LOFA the cladding reached peak temperatures of 114°C using HEU fuel and 113°C when LEU fuel was used. According to the design specifications of 6061 aluminium, which was used in the simulation, the temperatures that were reached are far below the maximum allowed design temperature of the material (IAEA, 1992a).

4.3.3 IAEA MTR 10 MW reactor core simulation model

For this study only the reactor core was modeled according to the specifications of the IAEA MTR 10 MW reactor. The primary and secondary cooling systems were not included but the effect of the pump was simulated via varying flow rate boundary conditions.

As discussed in the previous section, the IAEA MTR 10 MW reactor core has 23 SFAs and 5 CFAs. One of the difficulties in analysing the core using the core layout in Figure 4-1 is that the core is unevenly structured, i.e. the core is not symmetrical in the radial direction. As in previous studies (Hainoun *et al.*, 2010), the core was restructured so that the core could be symmetric along certain radial directions. Figure 4-4 shows the core configuration that is used for the simulation models. It can be seen that the core is symmetrical and can be divided into four similar quadrants. This allows significant simplification of the simulation model since only one of the quadrants has to be modelled rather than the whole core. In this core configuration that was used for the simulation, there are 21 SFAs, 4 CFAs, a central water channel and 4 other water flow channels. Each reactor fuel assembly has 23 fuel plates, whilst the control elements have 17 fuel plates.

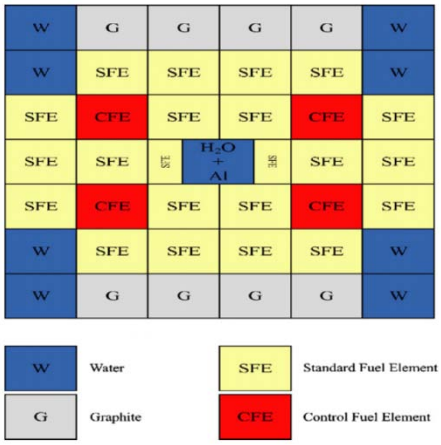

Figure 4-4: Core configuration (Hainoun et al., 2010).

Between each fuel plate, water is circulated downwards through the fuel assembly for cooling purposes.

4.3.4 Reactor core experimental setup

For the simulation model such as in Figure 4-4 a few assumptions were made to build the most straightforward fuel assembly. The justification for these assumptions was to reduce the complexity in simulating each fuel assembly, whilst keeping the model as realistic as possible. It was assumed that in the fuel assembly the mass flow through each flow channel was uniformly distributed. This meant that the mass flow rate through each of the 23 flow channels in a single fuel assembly had the same value.

In a single fuel assembly, it is assumed that the heat is uniformly distributed over each plate, which means that each fuel plate has the same amount of power. Figure 4-5a shows the cross-sectional top view of a single fuel plate in a single fuel assembly where the axial direction (z-direction) is out of the page. With the assumption that the heat and flow are uniformly distributed, each plate has an adiabatic symmetry line through its centre in the y-direction. For each flow channel we therefore only need to simulate half of the fuel plate on each side, as shown in Figure 4-5b. Since all the flow channels in a single fuel assembly are assumed to look exactly the same with no heat conduction across the width of the plates, the 23 fuel plates can now be placed side-by-side to form one single wide flow channel with a flow area equal to that of all the flow channels combined, as shown in Figure 4-5c. Note that a 3-D picture of this is shown in Figure 4-5d. However, it is crucial that the axial height of the plate and the width of the

flow channel be maintained at the correct physical values in order for the model to be a valid representation of the reality.

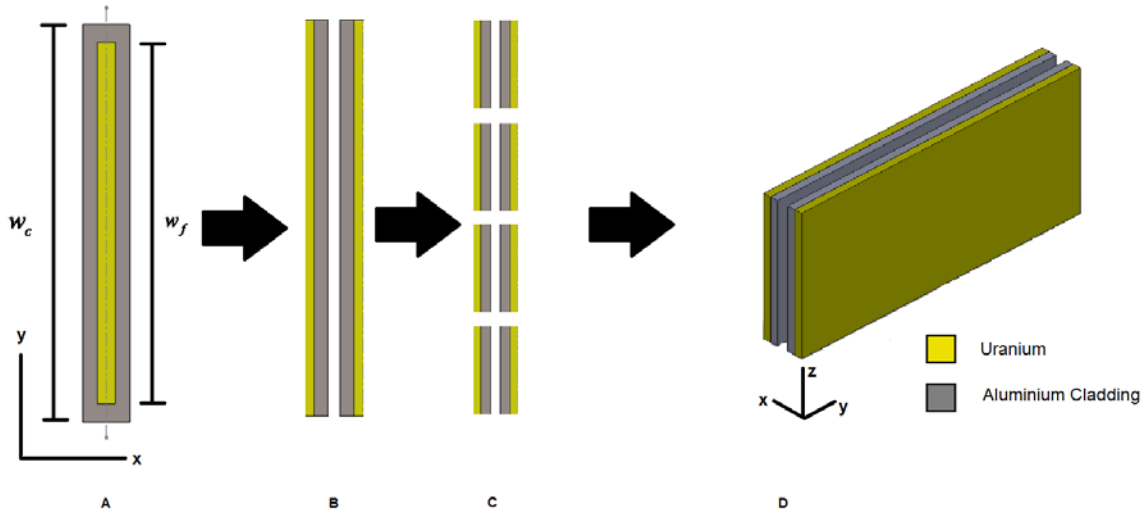

Figure 4-5: Fuel assembly assumption

Figure 4-6 gives the explanation of each symbol that was used for the calculations given below. Each symbol will be explained throughout the discussion. Figure 4-7 shows the water flow from the top to the bottom of the fuel assembly.

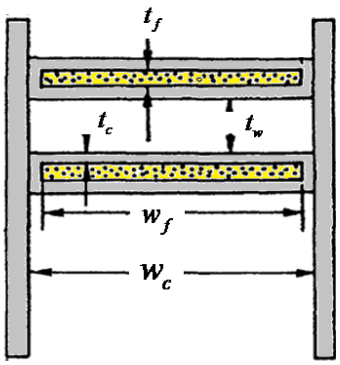

Figure 4-6: Cross section of core symbol configuration.

For the simulation, the total height H of the fuel assembly was kept at 0.6 m to determine the correct pressure drop through the fuel assembly. The total flow channel length can be defined as the total length of the cladding in a single fuel assembly as seen in Figure 4-7.

The total flow channel length L_c of the fuel assembly was determined by adding together the length w_c of each plate. In Figure 4-3 the length w_c of a single fuel plate of the aluminium cladding is shown, which is 66.4 mm. The total flow channel length L_c of the combined plates is determined by the following equation.

$$L_c = w_c \times n \tag{4.1}$$

In Eq (4.1) w_c is the width of the cladding of a single fuel plate and n is the number of fuel plates per fuel assembly. The total fuel length L_f can be calculated on the same method that was used for the calculation of the total flow channel length, because w_c and w_f is not equal to each other as seen in Figure 4-3. The total fuel length L_f was calculated with the following equation.

$$L_f = w_f \times n \tag{4.2}$$

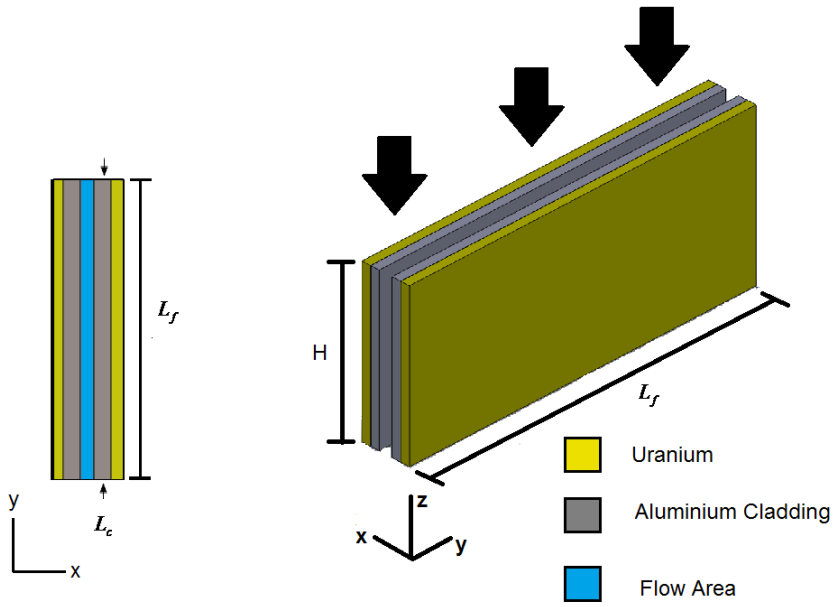

Figure 4-7: Single fuel assembly flow path.

To do an accurate heat transfer simulation, it is necessary to use the correct flow area of the fluid, the correct contact area where the water has contact with the wall surface, and the correct contact area between the different layers of uranium fuel and aluminium cladding. The total flow

area is defined in Figure 4-7 as the total area where the coolant flows through the fuel assembly to cool it down. The flow area can be calculated by multiplying the total flow channel length L_c with the water channel thickness t_w that is given in Figure 4-6 and Table 2. The total flow area was calculated with the following equation, where L_c is the total flow channel length of the fuel assembly and t_w the thickness of the water channel. The thickness t_w of the channel is 2.19 mm.

$$A_{flow} = L_c \times t_w \tag{4.3}$$

To simulate a duct in Flownex® it is necessary to calculate the circumference of the wetted perimeter of the fuel assembly. The circumference was calculated by the following equation:

$$Circumference = (2L_c + 2t_w) \tag{4.4}$$

The total contact area is defined as the total area where surface of the uranium fuel makes contact with the surface of the aluminium cladding. It can also be explained as the area where the heat is transferred from the fuel through the cladding to the water. Because the two parallel plates on either side of the representative flow channel are identical, the plates can be repositioned next to each other to calculate the total contact area.

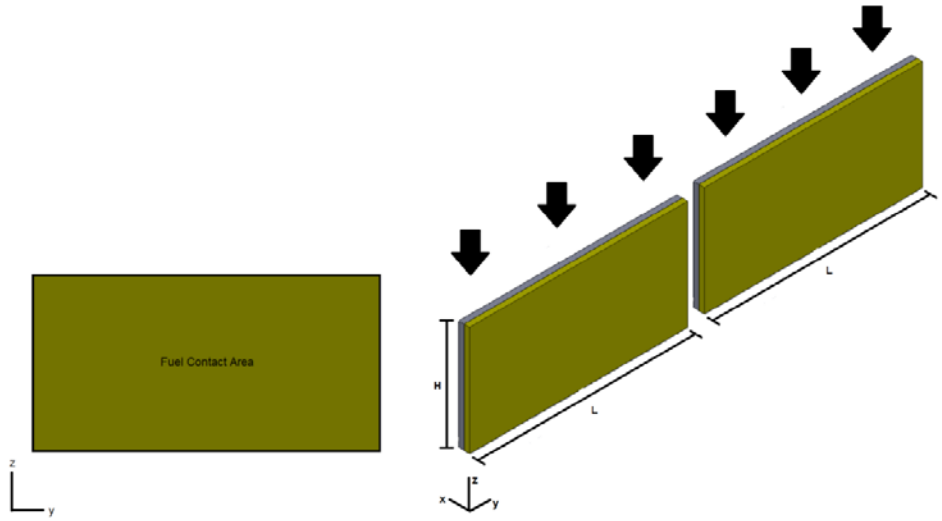

Figure 4-8: Single fuel assembly contact area calculation.

In Figure 4-8 it can be seen how the contact area of the fuel was determined. The fuel contact area was calculated with multiplying double the total fuel width L_f the height H of the fuel. The total contact area of the fuel can be calculated by the following equation:

$$A_{fuel} = 2 \times L_f \times H \tag{4.5}$$

The contact area of the aluminium cladding was calculated in the same way as for determining the contact area of the fuel. The only difference was that the total flow channel length L_c was used for the calculation of the contact area in aluminium cladding.

4.4 Flownex® library and nodalization

Flownex® is a very user friendly software package for model simulation. The Flownex® library contains a variety of elements that can be used for different simulation model developments. Some of the elements that can be used for a model simulation are shown in Figure 4-9.

The different elements in Figure 4-9 can simply be dragged from the library into a window to design a model according to the user's specifications. The different elements can then be linked with each other via a node to calculate the flow and heat transfer through the model. The most common elements that were used for this study were the pipe element, heat transfer element and boundary condition element. Figure 4-10 shows a diagram of how the different elements can be linked on the Flownex® canvas. Figure 4-10 also shows how a single fuel assembly can be simulated in Flownex®.

Each element has a subscript identifying it. A full description of each element that was used during this study follows. The discussion describes the different specifications that were specified in the simulation model.

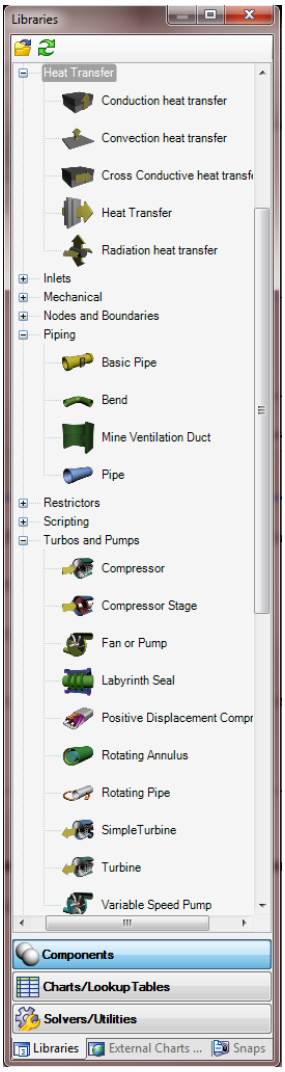

Figure 4-9: Flownex® library.

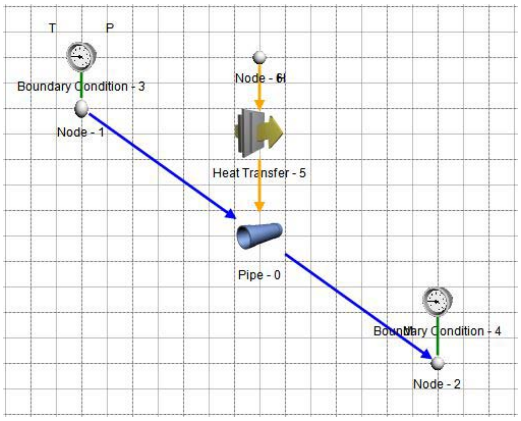

Figure 4-10: Flownex® Canvas.

4.4.1 Pipe element

For this study a pipe element was used in Flownex® to represent the flow of the coolant through the fuel assembly. Some values needed to be specified for the simulation of the flow through the fuel assembly. The most important value was the flow area of the water through the fuel assembly. The pipe element in Flownex® has a function which could be used for either a pipe or a duct. The difference between these two functions is that one could specify the diameter for the pipe whilst for the duct the flow area and the circumference had to be specified. For this study the duct element was used. The flow length of the fuel assembly was specified as the total height H for the fuel assembly.

During flow through a fuel assembly, there will be pressure drop caused by friction forces on the surface, secondary losses and by gravity. In Flownex®, in order to determine the correct pressure drop, the surface roughness of the material that is to be simulated, is specified according to the material specifications.

The pipe element can be divided into increments to determine the effects at different points along the flow channel.

A number of pipe elements can be specified parallel to each other to model bundles of elements.

4.4.2 Boundary conditions element

The boundary condition element was used to specify the boundary conditions of the fuel assembly. For the simulation models the temperature and pressure were specified at the inlet of the fuel assembly and the mass flow was specified at the outlet. The mass flow at the outlet node was given a negative value to represent the correct direction of flow through the fuel assembly.

4.4.3 Heat transfer element

Figure 4-10 shows how the heat transfer element was linked to the fuel assembly. It is necessary in the heat transfer element, that the upstream and downstream nodes are selected correctly. The upstream node is the node where the inlet value must be specified and the

downstream is the outlet properties where it connects to the outlet node. In this model, the fuel assembly was connected to the downstream node of the heat transfer element and node 6 on the upstream node as seen in Figure 4-10 .

The heat transfer element has a function where multiple layers of a certain material can be specified. This means that more than one layer can be modelled with different contact areas and material specifications. Flownex® also has a built in function where different materials can be selected. For this simulation, two different materials were selected. One of the layers was aluminium that was used as the cladding between the uranium and the water and other layer for the simulation was the uranium. In the heat transfer element, the contact area must be specified between each of the contact layers.

For this study it was assumed that the face of the uranium connected to the node representing the outside was adiabatic as seen in Figure 4-11.

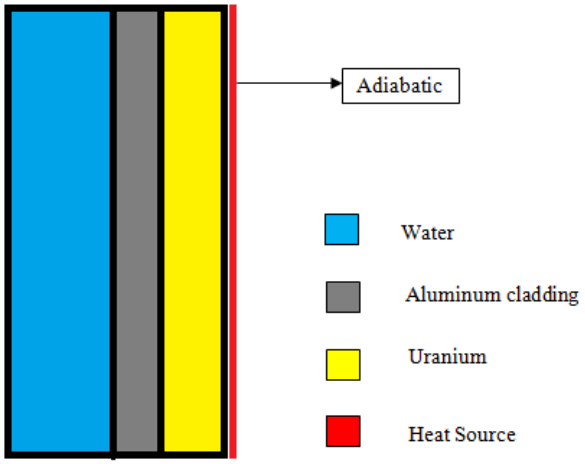

Figure 4-11: Fuel assembly layout

4.4.4 Node

Nodes are used to link the elements with each other. A node can also be used to specify certain boundary conditions like mass flows, temperatures and pressures at different points. For the simulation nodes were used to specify the evaluation of the core inlet and outlet to determine the correct pressure drop. The evaluation was specified according to the core flow height H and ground level (0 m) on the outlet node. It should be noted that a node was also used to specify the power on the heat transfer element as shown in Figure 4-10. The heat source can also be

set on the surface of the pipe element in Flownex®. The reason why the heat source was set on the node was so that the outside surface could be specified as adiabatic as discussed in section 4.4.3 and the temperature distribution on the fuel and aluminium could be calculated. This would not be possible if the heat source is specified on the pipe surface.

4.5 Steady state simulation of a single fuel assembly: Uniform power distribution

4.5.1 Model parameters

Part of a complex simulation model is to start with a less complex model and to build it up as the work progresses. This makes it easier to identify faults and/or problems in the model. As a first step, a single fuel assembly was modelled with the simplifying assumption that the power is distributed uniformly throughout the height and width of the fuel plate. The purpose was to learn how the software worked and to compare the results with a solution using the Engineering Equation Solver (EES) software.

The fuel assembly was built according to the IAEA MTR 10 MW reactor specifications that were given in Table 2. For this simulation it was assumed that the heat was uniformly distributed in the axial direction. This meant that each fuel assembly had the same amount of power concentration. The CFA has less power than normal SFA and is used to control the behaviour of the core. For this simulation only the normal SFAs were simulated.

The power for a SFA was determined by the following method. Each SFA has 23 fuel plates and the CFA has 17 fuel plates. As mentioned in section 4.3.3 the core has 21 SFAs and 4 CFAs, which have a total of 551 fuel plates in the core. The total power in the core was divided by the total plates in the core to determine the power per single fuel plate. The power per single fuel plate was calculated as 18.14882 kW. The power per fuel plate was multiplied with the total plates per SFA. The power per SFA was determined as 417.422 kW.

For the single fuel assembly simulation, it was assumed that the mass flow through each fuel assembly was uniformly distributed. The mass flow of a single fuel assembly was determined by dividing the total mass flow by the total fuel assemblies. There are 25 fuel assemblies including those with control elements and 9 water channels which give a total of 34 flow channels. The calculated mass flow was given in Table 3.

Section 4.3.4 discusses how each variable of the flow channel and the heat transfer element was calculated. The calculation results are given in Table 3 and were used for the input specification of the simulation model in Flownex®. The surface roughness of aluminium was taken to be 1.5 μm (Guillen & Yoder, 2008). Figure 4-12 shows how the simulation model was built in Flownex®. The pipe in the model was divided into 10 equal increments in the axial direction to account for the variations in fluid properties, pressure drop, temperature, etc. along the height of the flow channel. One of the features in Flownex is that the pipe can automatically be incremented in any number of increments along the flow direction. The pressure drop, water temperature and surface temperatures at the outer wall of the cladding and the fuel centreline temperature were calculated for each of the different increments.

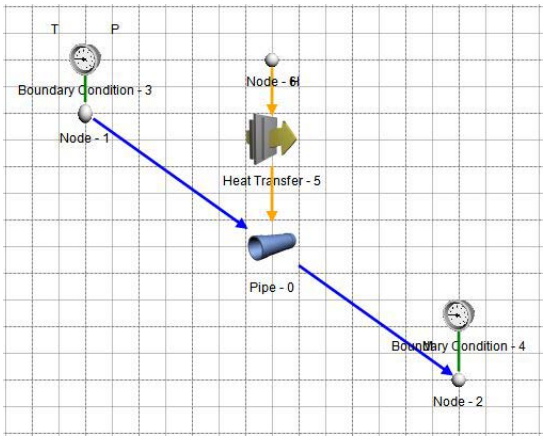

Figure 4-12: Flownex® single fuel assembly with heat transfer model.

Table 3: Flownex® input calculations per single flow channel.

Description	Value
Flow Channel	
Water channel thickness (mm)	2.19
Height H (mm)	600
Flow channel length (m)	1.5272
Number of increments	10
Increment flow height (mm)	60
Flow area (m^2)	0.0033446
Circumference (m)	3.05878
Surface roughness (μm)	1.5

Description	Value
Boundary Conditions	
Inlet coolant temperature (°C)	38
Inlet pressure (kPa)	170
Mass flow(kg/s)	8.169934
Heat Transfer Element	
Power (kW)	417.422
Cladding thickness (mm)	0.038
Cladding contact area (m^2)	1.83264
Cladding thermal conductivity (W/mK)	180
Cladding capacitance (kJ/m^3K)	2408
Fuel thickness (mm)	0.0255
Fuel contact area (m^2)	1.7388
Fuel thermal conductivity (W/mK)	50
Fuel capacitance (kJ/m^3K)	495

4.5.2 Results and discussion

For this first case only a steady state simulation was done using Flownex®. In order to verify that the model was implemented correctly in Flownex®, an EES model was programmed according to the same specifications that were used in the Flownex® model. The result from Flownex® was compared with the EES model and there was a very good comparison between the EES and Flownex® models. The results of these models are given in Table 4. The EES model calculations are given in Appendix F.

From Table 4 it can be seen that there was a very small difference between the results of the EES and Flownex® models. The reason for the difference is the fact that Flownex® and EES use different fluid properties. The fluid properties differing between the software codes are the fluid density, viscosity, specific heat and conductivity. The different values of the fluid properties of Flownex® and EES are provided in Table 5. In section 3.8.3 it was explained how the heat transfer can be calculated using the different equations. It can be seen from section 3.8.3 that the fluid properties will affect the following equations (3.23-3.26). This effect will cause the two simulation models to have different Reynolds - , Prandtl - and Nusselt numbers. These

differences will affect the convection heat transfer coefficient which will lead to the difference in the temperatures.

Table 4: Single fuel assembly results (uniform heat distribution).

Increments	EES Static Pressure (kPa)	Flownex® Static Pressure (kPa)	EES Water Temperature (°C)	Flownex® Water Temperature (°C)	EES Wall Temperature (°C)	Flownex® Wall Temperature (°C)	EES Cladding Temperature (°C)	Flownex® Cladding Temperature (°C)	EES Fuel Centreline Temperature (°C)	Flownex® Fuel Centreline Temperature (°C)	EES Convection coefficient (W/m².K)	Flownex® Convection coefficient (W/m².K)	EES Nusselt number	Flownex® Nusselt number
1	166.707	166.706	38.610	38.611	56.181	56.421	56.688	57.100	57.300	57.544	13662.369	13795.705	97.020	96.006
2	166.133	166.132	39.832	39.834	57.213	57.436	57.719	58.115	58.332	58.559	13812.175	13962.585	97.813	96.886
3	165.565	165.564	41.054	41.057	58.249	58.451	58.756	59.130	59.368	59.575	13961.260	14133.222	98.603	97.789
4	165.002	165.002	42.276	42.280	59.290	59.514	59.797	60.193	60.409	60.638	14109.624	14267.341	99.388	98.474
5	164.444	164.443	43.498	43.502	60.336	60.576	60.843	61.255	61.455	61.699	14257.265	14405.004	100.169	99.180
6	163.891	163.889	44.720	44.724	61.386	61.636	61.893	62.316	62.505	62.760	14404.184	14546.387	100.947	99.909
7	163.343	163.340	45.942	45.947	62.441	62.695	62.948	63.375	63.560	63.819	14550.379	14691.678	101.721	100.660
8	162.800	162.796	47.165	47.169	63.500	63.753	64.007	64.432	64.619	64.877	14695.849	14841.392	102.491	101.438
9	162.261	162.256	48.387	48.392	64.563	64.809	65.070	65.489	65.682	65.933	14840.596	14995.447	103.258	102.242
10	161.726	161.722	49.609	49.614	65.629	65.864	66.136	66.544	66.748	66.988	14984.617	15154.063	104.022	103.073
Average	164.187	164.1852	44.1094	44.1131	60.8789	61.1155	61.3857	61.794	61.9978	62.2392	14327.8317	14479.2824	100.543	99.5658

Table 5: Flownex® vs. EES fluid properties.

	Uniform Power Distribution							
	EES Density (kg/m^3)	**Flownex® Density (kg/m^3)**	**EES Viscosity (kg/m.s)**	**Flownex® Viscosity (kg/m.s)**	**EES Specific Heat (kJ/kg.K)**	**Flownex® Specific Heat (kJ/kg.K)**	**EES Conductivity (W/m.K)**	**Flownex® Conductivity (W/m.K)**
1	992.8	992.6967	6.707E-04	6.743E-04	4.182	4.179348	0.6159	0.62849
2	992.3	992.2664	6.553E-04	6.572E-04	4.182	4.179513	0.6176	0.630314
3	991.8	991.832	6.405E-04	6.403E-04	4.182	4.17968	0.6193	0.632126
4	991.3	991.3122	6.263E-04	6.277E-04	4.182	4.179848	0.6209	0.633684
5	990.9	990.7924	6.126E-04	6.151E-04	4.182	4.180017	0.6225	0.635242
6	990.4	990.2727	5.993E-04	6.025E-04	4.182	4.180187	0.6241	0.636801
7	989.8	989.7529	5.865E-04	5.899E-04	4.181	4.180359	0.6256	0.638359
8	989.3	989.2331	5.742E-04	5.773E-04	4.181	4.180753	0.6271	0.639917
9	988.8	988.7134	5.622E-04	5.647E-04	4.181	4.181154	0.6286	0.641476
10	988.2	988.1936	5.507E-04	5.521E-04	4.181	4.181552	0.63	0.643034

4.5.3 Different Discretisation calculations

To determine the accuracy of the previous simulation the fuel assembly was discretized into 20 equal increments. The model was simulated in Flownex® with the same condition as the previous simulation. The only difference was the single fuel assembly was set for 20 equal increments. The simulation results of the 20 equal increments were compared with the previous simulation with 10 equal increments. Figure 4-13 shows the static pressure simulation results of the different increments. Figure 4-14 and Figure 4-15 shows the simulation results of the water temperature through the channel, the wall temperature in the flow channel, the cladding and maximum temperatures of the fuel.

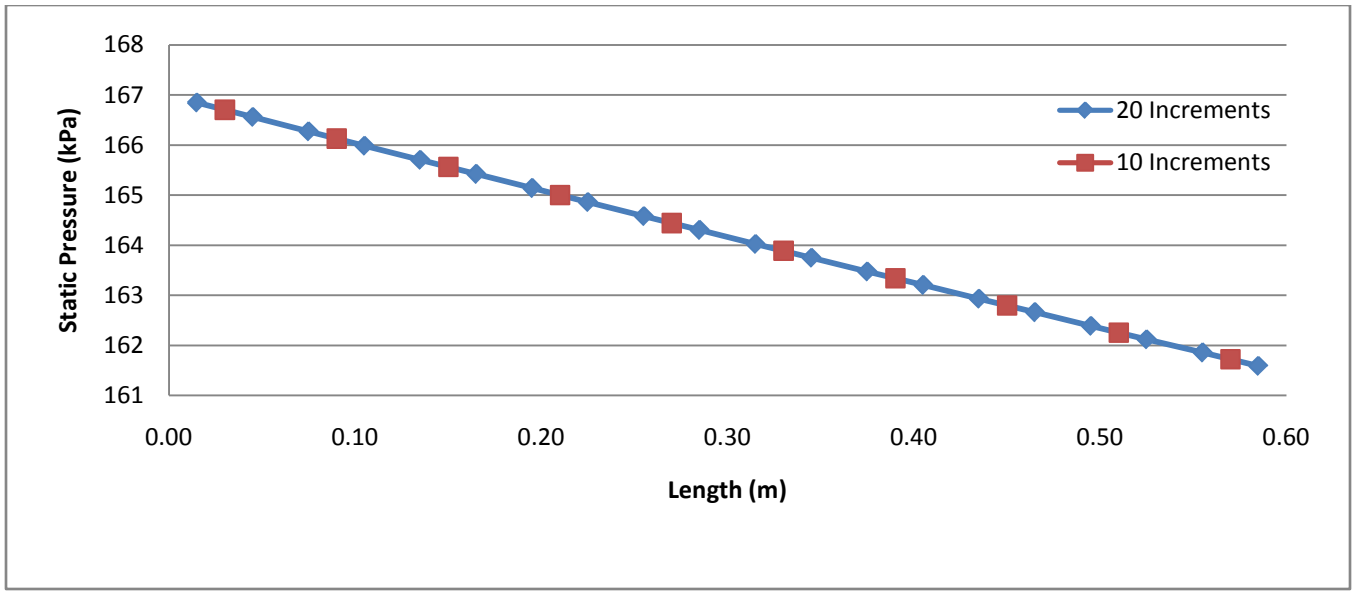

Figure 4-13: 10 vs 20 Increments Static Pressure

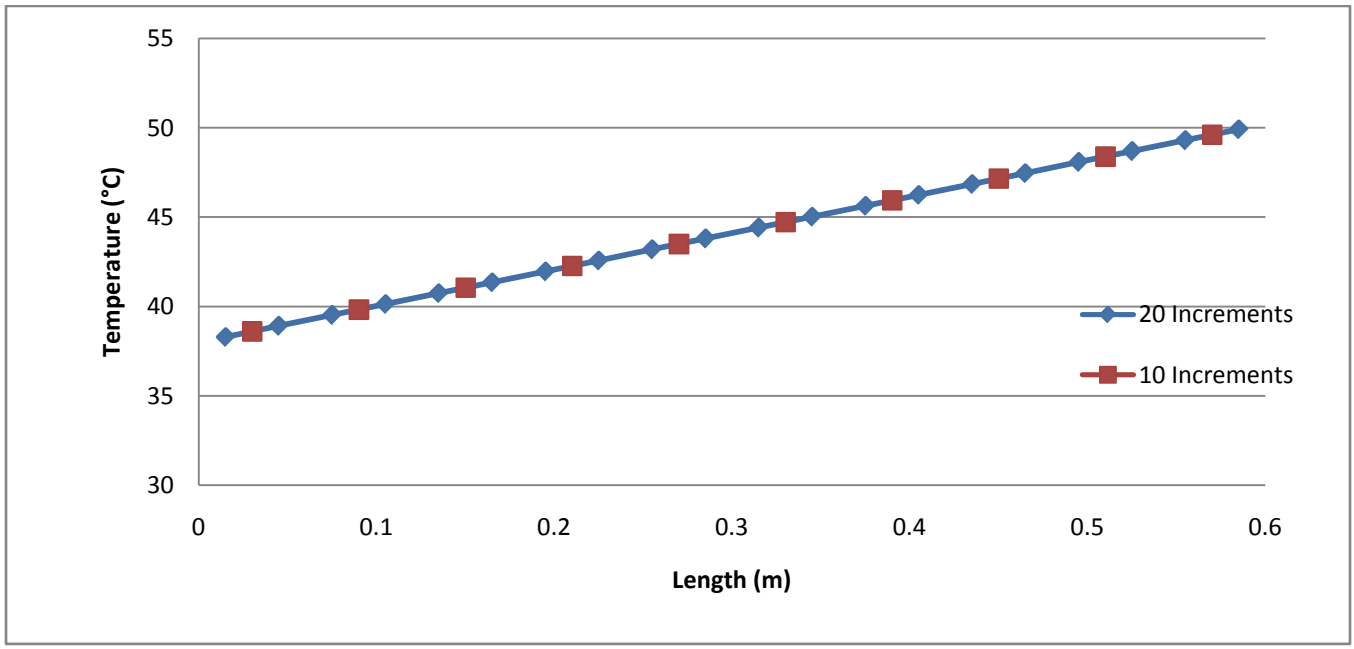

Figure 4-14: 10 vs 20 Increments Water Temperature

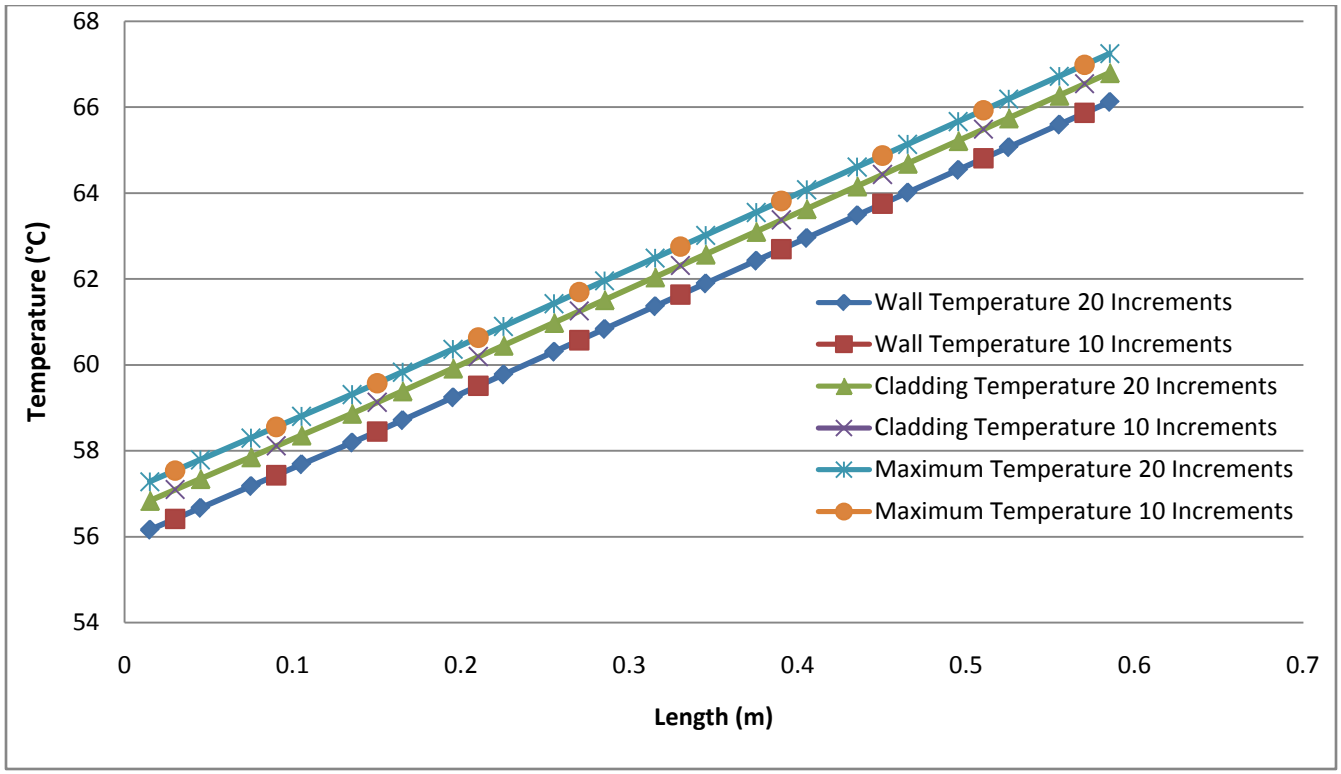

Figure 4-15:10 vs 20 Increments Wall, Cladding and Maximum Temperatures

For the Figure 4-13 -Figure 4-15 it can be seen that there was an accurate comparison between 10 and 20 Increments. For the convenience of this study for simulating the model it was decided to use 10 increments for each simulation of this study.

4.6 Steady state simulation of a single fuel assembly: Sinusoidal power distribution

The next level of complexity that was modelled is the case where the variation in the power distribution along the height of the fuel assembly is taken into account.

4.6.1 Model parameters

The axial power distribution was calculated with the method that was explained in section 3.7. The equation was only solved for the z-direction of a single fuel assembly. In Table 2 it can be seen that the MTR has an axial peaking factor of 1.5. With this value given, the value k_3 in Eq (3.9) was determined with the peaking factor equation, and the power level for each increment was calculated. The x and y direction was disregarded due to the fact that only the z-direction was considered. The total power of 417.422 kW that was used for a single standard fuel

assembly in the previous simulation was used for the sinusoidal power distribution calculation. Appendix G contains more information on how the sinusoidal power distribution was calculated for each increment. Figure 4-16 illustrates the sinusoidal power distribution of a single fuel assembly at each increment.

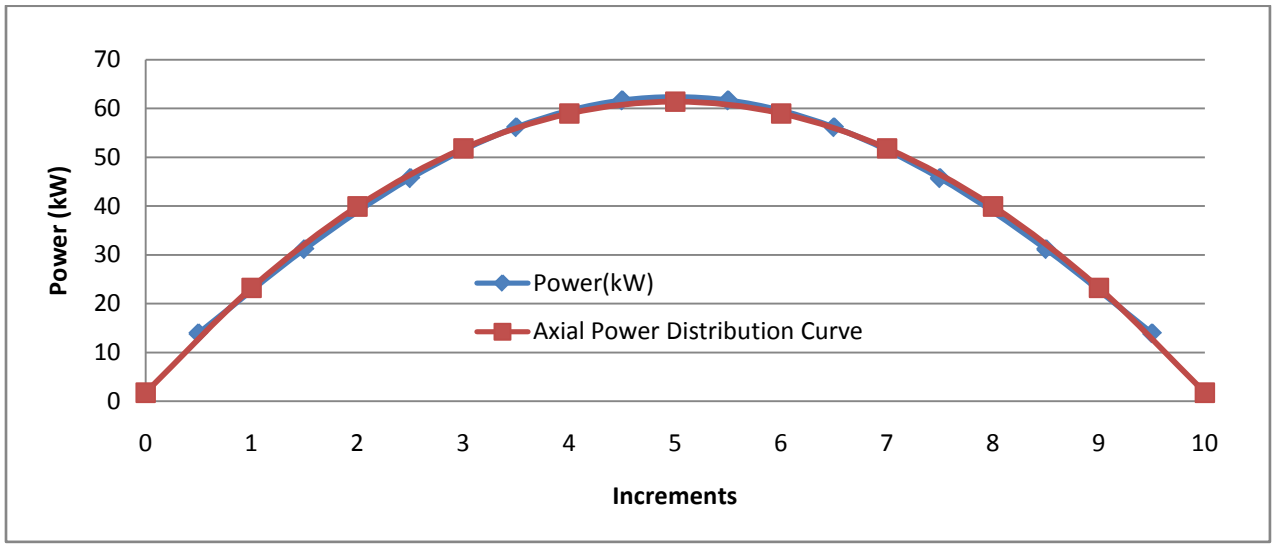

Figure 4-16: Axial heat distribution curve.

4.6.2 Flownex® single fuel assembly model (Sinusoidal heat distribution)

A single fuel assembly was modelled in Flownex® to investigate the effect of the sinusoidal heat distribution. As mentioned earlier, the heat source was specified on a node connected to the heat transfer element. This node then represented the heat source due to the fission in the uranium fuel. One of the shortcomings in Flownex® is that the heat transfer element and the node do not have a feature where a sinusoidal power generation profile can automatically be specified for the automatic increments. To overcome this, the model had to be developed such that 10 separate pipe elements were used in series with each other, simulating the axial length of the fuel assembly. Each pipe element had its own heat transfer element and power node connected to it. Figure 4-17a shows how this was set up in Flownex®. With this approach the sinusoidal heat distribution in the axial direction could be approximated at each increment. Due to this shortcoming in Flownex® a model in EES was developed with the same specifications to verify this calculation. The input specifications that were used for the Flownex® and EES models are given in Table 6

Table 6: Flownex® input specifications for sinusoidal power distribution.

Description	Value
Flow Channel	
Water channel thickness (mm)	2.19
Height H (mm)	600
Flow channel length (m)	1.5272
Number of increments	10
Increment flow Height (mm)	60
Flow area (m^2)	0.0033446
Circumference (m)	3.05878
Surface roughness (µm)	1.5
Boundary Conditions	
Inlet coolant temperature(°C)	38
Inlet pressure (kPa)	170
Mass flow(kg/s)	8.169934
Heat Transfer Element	
Power (kW)	417.422
Power per increment (kW)	Figure 4-16
Cladding thickness (mm)	0.038
Cladding contact area (m^2)	1.83264
Cladding contact area per increment(m^2)	0.183264
Cladding thermal conductivity (W/mK)	180
Cladding capacitance (kJ/m^3K)	2408
Fuel thickness (mm)	0.0255
Fuel contact area (m^2)	1.7388
Fuel contact area per increment (m^2)	0.17388
Fuel thermal conductivity (W/mK)	50
Fuel capacitance (kJ/m^3K)	495

Figure 4-17b shows how the model was set up for the simulations in Flownex®. This model was built using the same method as the uniform heat distribution model. The inlet- and outlet boundary conditions were specified at the inlet and outlet nodes. The coolant water entered the fuel assembly with a temperature of 38°C and a pressure of 170 kPa. For each pipe element

the flow area and circumference was the same as the previous simulation. The only difference was that only a tenth of the total of flow length was set at each pipe, which was 0.06 m.

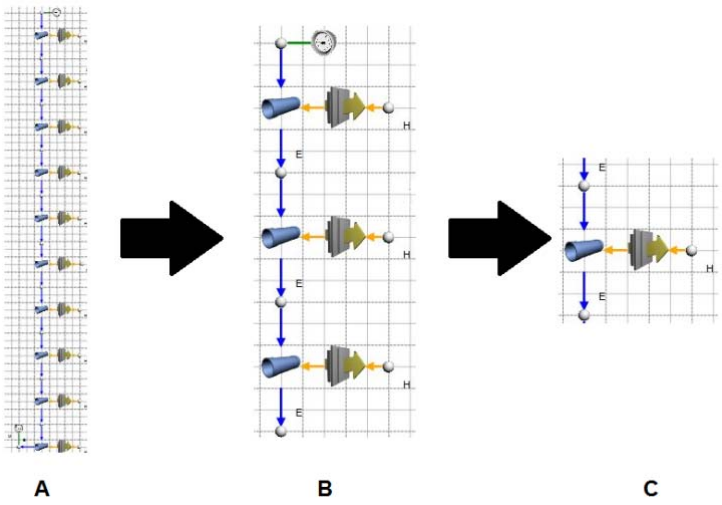

Figure 4-17: Flownex® single fuel assembly with sinusoidal heat distribution model.

For the heat transfer element the same approach was used as in the previous simulation. The different layers were specified according to the specifications, with the difference that only a tenth of the total contact area was specified for each element. In Figure 4-17c it can be seen how the heat transfer element is connected to the duct. In Figure 4-17c the “H” indicates that a heat source was specified at the specific element. The different power levels at each node were specified according to the axial heat distribution calculations at each increment in Figure 4-16. In Flownex®, if a property is specified at the specific node, there will be an indication to show what was specified at the node. On each node that links the ducts, there was an “E” indication that showed that the elevations were specified at each node. For any simulation it is necessary to specify the correct elevation at each node due to the fact that buoyancy and gravitational forces will influence the fluid behaviour. The reason for specifying the correct elevation was in order to determine the correct pressure drop through the fuel assembly for the simulation purposes.

4.6.3 Results and discussion

The pressure drop, water temperature, surface temperature, aluminium cladding and maximum temperatures were calculated along the height of the channel at each increment. An EES model was developed according to the same specifications as the model that was simulated in

Flownex®. The result in Flownex® was compared with the EES model at the different increments and is given in Table 7. The EES model calculations is given in Appendix H

It can be seen from Table 7 that there was a difference between the results of Flownex® and EES. The reason for this difference is the same as was discussed in section 4.5.2. The different values of the fluid properties of Flownex® and EES can be seen in Table 8. The good comparison between the two simulation models showed that the power distribution profile was correctly implemented in the Flownex® model and the method could be expanded to the simulation of the entire core.

Table 7: Single fuel assembly results (Sinusoidal heat distribution)

Increments	EES Static Pressure (kPa)	Flownex® Static Pressure (kPa)	EES Water Temperature (°C)	Flownex® Water Temperature (°C)	EES Wall Temperature (°C)	Flownex® Wall Temperature (°C)	EES Cladding Temperature (°C)	Flownex® Cladding Temperature (°C)	EES Fuel Centreline Temperature (°C)	Flownex® Fuel Centreline Temperature (°C)	EES Convection coefficient (W/m².K)	Flownex® Convection coefficient (W/m².K)	EES Nusselt number	Flownex® Nusselt number
1	166.707	166.706	38.203	38.204	44.078	44.162	44.247	44.394	44.451	44.546	13612.271	13741.297	96.750	95.720
2	166.130	166.129	38.863	38.865	51.969	52.146	52.347	52.653	52.805	52.986	13693.450	13829.805	97.180	96.185
3	165.558	165.556	39.989	39.992	59.004	59.245	59.560	59.990	60.230	60.477	13831.395	13984.465	97.920	97.002
4	164.990	164.988	41.481	41.484	64.545	64.827	65.227	65.741	66.051	66.340	14013.200	14179.707	98.880	98.026
5	164.429	164.427	43.207	43.210	68.146	68.493	68.895	69.497	69.799	70.154	14222.096	14371.816	100.000	99.010
6	163.876	163.873	45.012	45.016	69.577	69.946	70.326	70.950	71.230	71.606	14439.154	14580.707	101.100	100.086
7	163.329	163.325	46.737	46.742	68.806	69.146	69.488	70.061	70.312	70.659	14645.100	14788.582	102.200	101.164
8	162.789	162.784	48.230	48.235	65.974	66.244	66.529	66.989	67.200	67.476	14822.029	14975.383	103.200	102.137
9	162.254	162.249	49.356	49.361	61.356	61.330	61.735	61.691	62.192	62.403	14954.868	15120.837	103.900	102.899
10	161.723	161.718	50.016	50.022	55.336	55.325	55.505	55.486	55.709	55.804	15032.482	15208.001	104.300	103.357
Average	164.178	164.176	44.109	44.113	60.879	61.086	61.386	61.745	61.998	62.245	14326.604	14478.060	100.543	99.559

Table 8: Flownex® vs. EES fluid properties (Sinusoidal power distribution).

	Sinusoidal Power Distribution							
	EES Density (kg/m^3)	**Flownex® Density (kg/m^3)**	**EES Viscosity (kg/m.s)**	**Flownex® Viscosity (kg/m.s)**	**EES Specific Heat (kJ/kg.K)**	**Flownex® Specific Heat (kJ/kg.K)**	**EES Conductivity (W/m.K)**	**Flownex® Conductivity (W/m.K)**
1	992.9154	992.84	6.759E-04	6.800E-04	4.182	4.179294	0.6153	0.627882
2	992.6694	992.6074	6.675E-04	6.708E-04	4.182	4.179383	0.6163	0.628868
3	992.2427	992.2109	6.534E-04	6.550E-04	4.182	4.179537	0.6178	0.630549
4	991.6631	991.6501	6.355E-04	6.359E-04	4.182	4.17974	0.6199	0.63267
5	990.973	990.9164	6.158E-04	6.181E-04	4.182	4.179978	0.6221	0.63487
6	990.2285	990.1486	5.962E-04	5.995E-04	4.181	4.180227	0.6245	0.637173
7	989.4961	989.4149	5.784E-04	5.817E-04	4.181	4.180609	0.6266	0.639373
8	988.8465	988.7804	5.637E-04	5.663E-04	4.181	4.1811	0.6284	0.641276
9	988.3463	988.3014	5.530E-04	5.547E-04	4.181	4.181468	0.6297	0.642712
10	988.0491	988.0204	5.469E-04	5.479E-04	4.181	4.181684	0.6305	0.643554

4.7 Steady state simulation of the complete MTR reactor core

For the modelling of a nuclear reactor it is necessary to do a simulation of the entire core to determine its behaviour in different situations. As seen from Figure 4-18 the reactor core is symmetrical around the x and y coordinate axis. It was therefore assumed that the reactor core could be divided into four similar quadrants with symmetry boundaries in between and the model was only set up for one of these quadrants. This reduced the size of the model for the complete reactor core. It was assumed that the symmetry boundaries of the quarter cores were adiabatic. This was because of the neutronics and thermal-hydraulic symmetry that was assumed between the four quarters of the core.

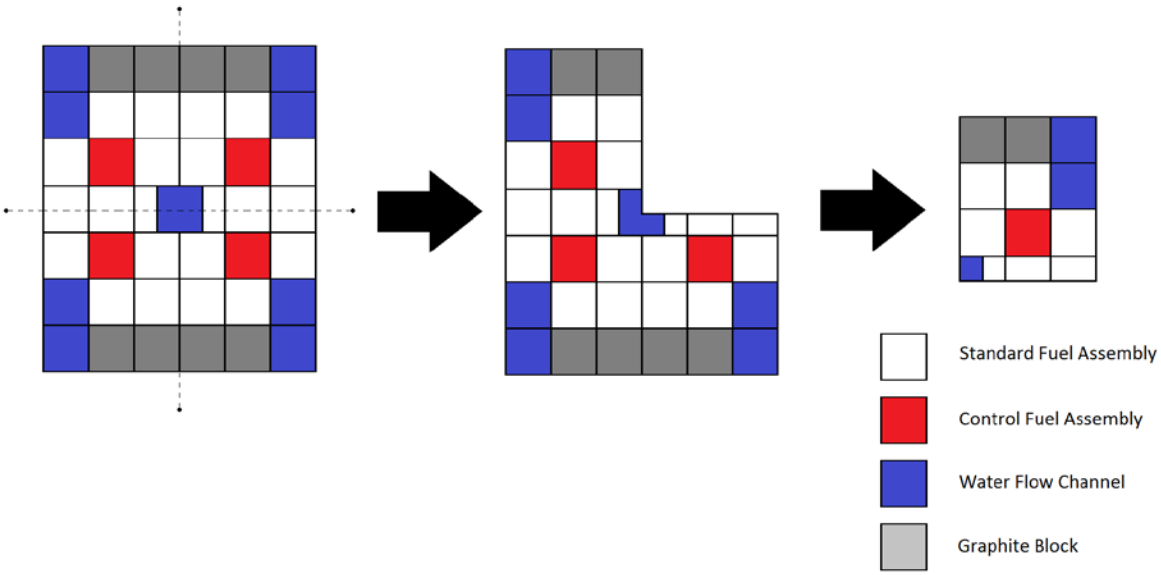

Figure 4-18: Core simulation assumption.

4.7.1 Reactor core power distribution

The power distribution of the core was calculated by solving the method that was explained in section 3.7. For the simulation it was assumed that the reactor core was homogenous. The program was written in EES to solve the integral equation for the power distribution. Figure 4-19 gives the calculated power distribution of the core. The power in Figure 4-19 is arranged according to the normal core layout of the MTR. It can be seen from Figure 4-19 that in this first calculation the power is present in the water channels at the corners of the core layout and in the water channel at the centre of the core. This is not totally physically realistic since there is no fuel in these regions where heat is generated.

120.7	225.5	283.8	283.8	225.5	120.7
225.9	421.9	531.2	531.2	421.9	225.9
264.8	494.6	622.6	622.6	494.6	264.8
225.9	421.9	531.2	531.2	421.9	225.9
120.7	225.5	283.8	283.8	225.5	120.7

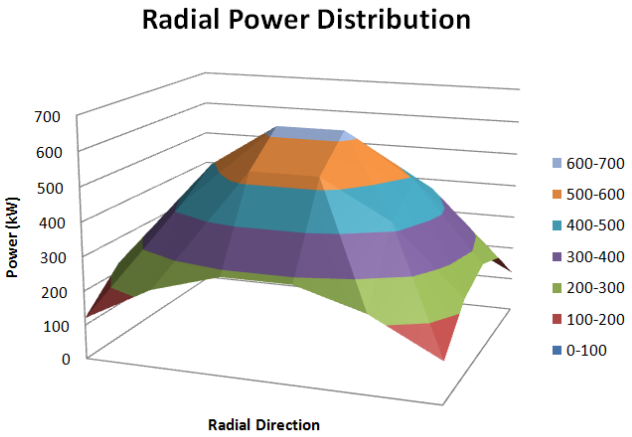

Figure 4-19: Radial power calculation.

The power profile was therefore adjusted by zeroing the power in the water channels whilst keeping the total power to the specified value. Each fuel assembly power was therefore multiplied by the differencing factor of 1.050729206. With this approach the differencing factor compensated for the power that was removed from the water channels. The result of these modifications can be seen in Figure 4-20.

0.0	253.9	319.7	319.7	253.9	0.0
254.4	475.3	598.3	598.3	475.3	254.4
298.2	557.0	341.2	341.2	557.0	298.2
254.4	475.3	598.3	598.3	475.3	254.4
0.0	253.9	319.7	319.7	253.9	0.0

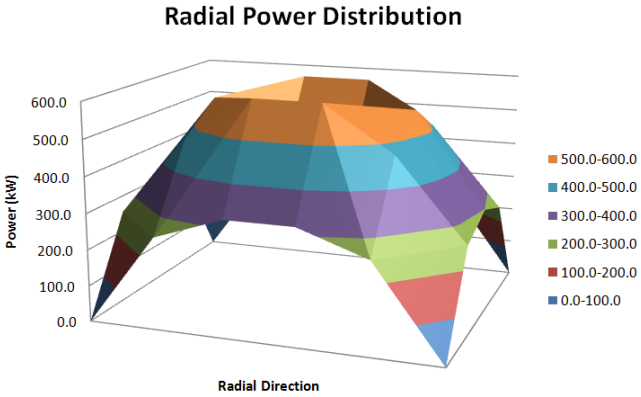

Figure 4-20: Radial power distribution calculations.

The same approach was used for the assemblies containing with control plates (i.e. the CFA plates). As mentioned the CFA has only 17 fuel plates and 4 absorber plates. The 4 CFAs were multiplied with a 17/23 factor to determine the core power in the CFA. A second differencing factor was calculated and multiplied with each fuel assembly, keeping in effect the total power at 10 MW. The new calculated axial power distribution is shown in Figure 4-21.

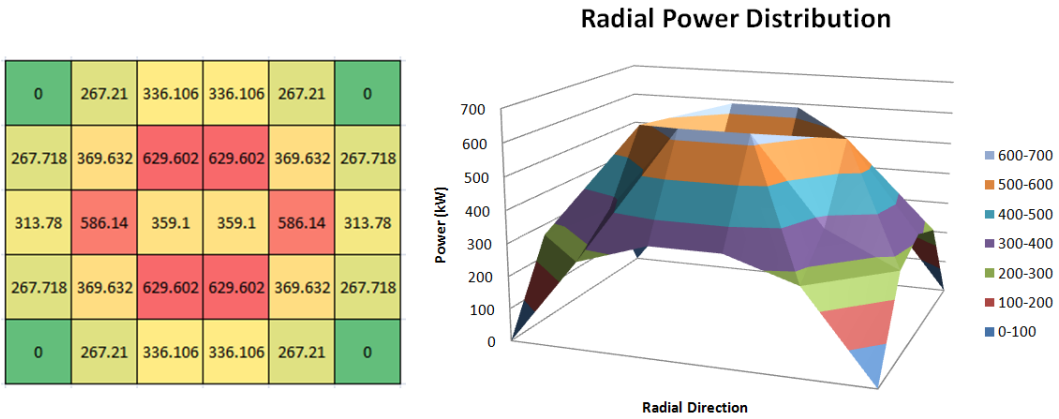

Figure 4-21: Radial power distribution.

As seen from Figure 4-21 there is a dip in centre of the curve. The reason for the dip was due to the water flow channel that runs through the centre of the core. This can be seen from Figure 4-18. Due to this flow channel, only half of the normal fuel assembly could be accommodated on both sides of the flow channel. In effect the fuel plates in the two fuel assemblies in the centre of the core have the highest power distribution per plate. These two assemblies are the hottest fuel assemblies in the core during operating conditions.

Thus far in Figure 4-21 only the radial power profile has been discussed. As mentioned a model in EES was developed for the calculations in both the axial and radial directions. The axial power distribution was calculated on the same principle as in section 4.6.1.

The power distribution was only calculated for the quarter core configuration. A notarization scheme was used for the calculation of the different fuel assemblies. The notarization scheme was used to number each fuel assembly for the simulation model. In Figure 4-22 it can be seen how the core was numbered for the simulation model.

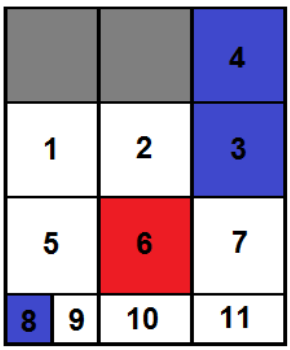

Figure 4-22: Quarter core numbering.

The axial power distribution was calculated according to the numbering scheme that is shown in Figure 4-22. The calculated result of the power distribution of each fuel assembly is given in Table 9. The calculations of the power distribution of the 10 MW and 12MW reactor are given in the Appendix I.

Table 9: Axial power distribution calculations.

	Fuel Assembly Number							
Increment	**1**	**2**	**5**	**6**	**7**	**9**	**10**	**11**
1	11.207	8.902	20.974	12.314	8.919	5.981	9.763	5.227
2	25.147	19.975	47.065	27.631	20.013	13.422	21.908	11.728
3	36.855	29.274	68.976	40.495	29.33	19.671	32.107	17.188
4	45.29	35.974	84.763	49.763	36.042	24.173	39.456	21.122
5	49.704	39.48	93.023	54.613	39.555	26.528	43.301	23.18
6	49.704	39.48	93.023	54.613	39.555	26.528	43.301	23.18
7	45.29	35.974	84.763	49.763	36.042	24.173	39.456	21.122
8	36.855	29.274	68.976	40.495	29.33	19.671	32.107	17.188
9	25.147	19.975	47.065	27.631	20.013	13.422	21.908	11.728
10	11.207	8.902	20.974	12.314	8.919	5.981	9.763	5.227
Total (MW)	**336.406**	**267.21**	**629.602**	**369.632**	**267.718**	**179.55**	**293.07**	**156.89**
Power (MW)	**2500.078**							

4.7.2 Core model setup in Flownex®

The quarter core simulation model was built on the same principles as the single fuel assembly with sinusoidal power distribution in section 4.6.2. The model was built according to the number of fuel assemblies and flow channels in the quarter. Each fuel assembly was specified according to its calculated power distribution. The water channel areas were set as the area of a single fuel assembly. The area of the fuel assembly was 7.6 cm x 8 cm as given in Table 2. It was assumed that the heat transfer between fuel assemblies could be neglected due to the fact that the heat transfer between the elements was very small. The model that was simulated in Flownex® can be seen in Figure 4-23. The values that were specified in the Flownex® model are given in Table 10.

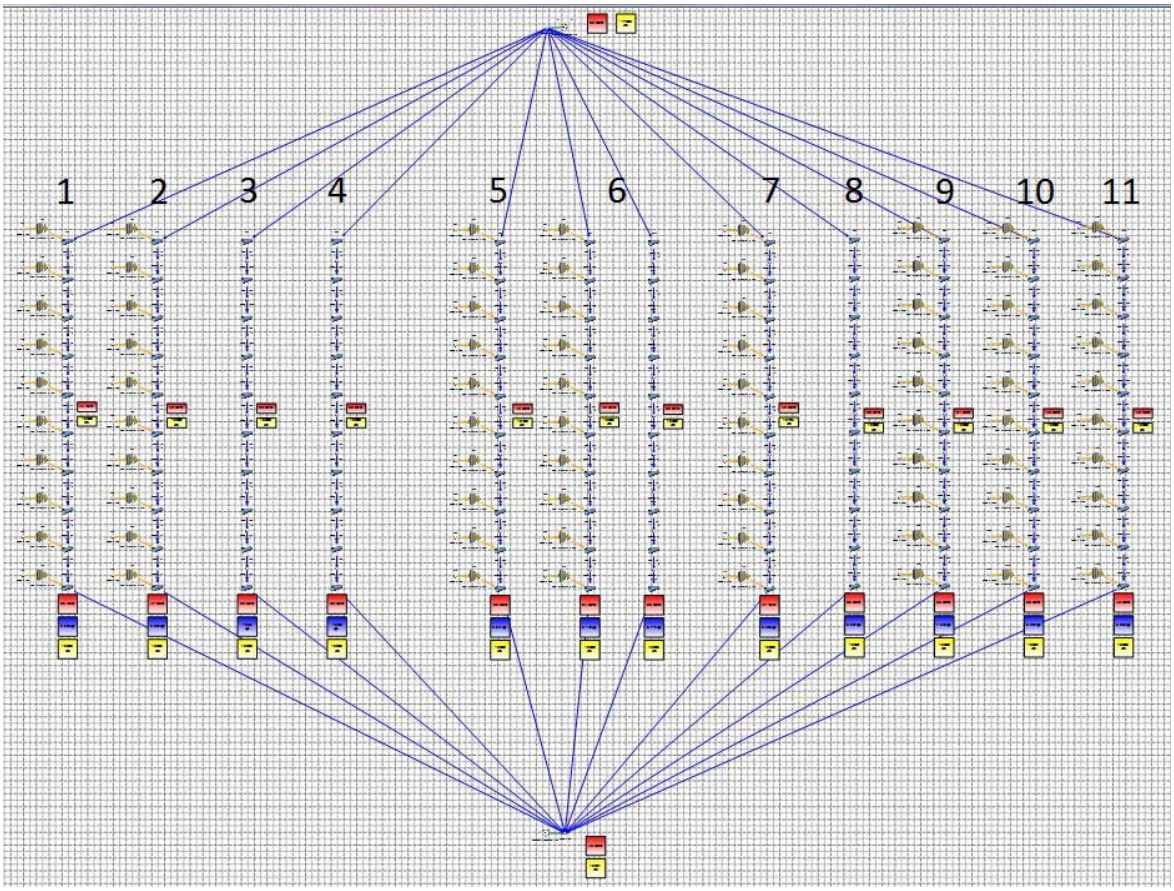

Figure 4-23: Flownex® core simulation model.

In Figure 4-22 and Figure 4-23 the number 6 represents the CFA. As seen in Figure 4-23 the CFA is modelled using two different flow channels. The reason for this configuration is that the CFA can be separated into two flow channels, one for the 17 fuel plates and the second for the absorber plates where no power was generated. The calculation of the flow area and contact area of channel 6 is given in Table 10.

In Figure 4-22 and Figure 4-23 it can be seen that channel 8 represents the centre water flow channel of the core. For the simulation only a quarter of the normal flow area was specified in Flownex® due to the fact that only a quarter of the core was simulated. For channel 9 only a quarter of the flow area of the normal fuel assemblies was specified for the same reason. For channel 10 and 11 only half of the normal flow area of the normal fuel assembly area was specified.

The inlet boundary condition was specified according to the inlet conditions of the core. The inlet temperature was 38°C with a pressure of 170 kPa. A negative mass flow 69.444 kg/s was

specified on the outlet boundary condition node. During the simulation the distribution of the mass flow rates between the different fuel assemblies is automatically calculated according to its flow area and pressure drop. The pressure drop is calculated by taking into account the friction loss factors and the secondary loss factors. The friction loss factors are dependent on surface roughness, hydraulic diameter, viscosity, density, speed of the fluid, etc. The secondary loss factors are due to the geometrical form of the component.

A secondary loss factor k = 1 was specified on the outlet and 0.5 at the inlet of each fuel assembly and water channel for the secondary pressure loss of curvature and recirculation.

Table 10: Flownex® inputs for core simulation

Description	1	2	3	4	5	6	7	8	9	10	11
Flow Channel											
Height H (mm)	600	600	600	600	600	600	600	600	600	600	600
Number of increments	10	10	10	10	10	10	10	10	10	10	10
Increment flow height (mm)	60	60	60	60	60	60	60	60	60	60	60
Flow area (m^2)	0.00334	0.00334	0.00608	0.00608	0.0033446	0.0024721	0.0033446	0.00152	0.00084	0.00167	0.00167
Circumference (m)	3.05878	3.05878	0.312	0.312	3.05878	2.26083	3.05878	0.078	0.7647	1.52939	1.52939
Surface roughness (μm)	1.5	1.5	1.5	1.5	1.5	1.5	1.5	1.5	1.5	1.5	1.5
Boundary Conditions											
Inlet Coolant Temperature(°C)	38	38			38	38	38		38	38	38
Inlet Pressure (kPa)	170	170			170	170	170		170	170	170
Mass Flow(kg/s)											
Heat Transfer Element											
Power (kW)	336.406	267.21			629.602	369.632	267.718		179.55	293.07	156.89
Power per increment (kW)	Table 9										
Cladding thickness (mm)	0.038	0.038			0.038	0.038	0.038		0.038	0.038	0.038
Cladding contact area (m^2)	1.83264	1.83264			1.83264	1.35456	1.83264		0.45816	0.91632	0.91632
Cladding contact area per increment(m^2)	0.18326	0.18326			0.183264	0.135456	0.183264		0.04582	0.09163	0.09163
Cladding thermal conductivity (W/mK)	180	180			180	180	180		180	180	180
Cladding Capacitance (kJ/m^3K)	2408	2408			2408	2408	2408		2408	2408	2408
Fuel thickness (mm)	0.0255	0.0255			0.0255	0.0255	0.0255		0.0255	0.0255	0.0255
Fuel contact area (m^2)	1.7388	1.7388			1.7388	1.2852	1.7388		0.4347	0.8694	0.8694
Fuel contact area per increment (m^2)	0.17388	0.17388			0.17388	0.12852	0.17388		0.04347	0.08694	0.08694
Fuel thermal conductivity (W/mK)	50	50			50	50	50		50	50	50
Fuel capacitance (kJ/m^3K)	495	495			495	495	495		495	495	495

4.7.3 Results and discussion

A steady state simulation was done with the core model in Flownex®. At each increment of every fuel assembly and water channel the pressure drops and water- , wall- , cladding and fuel temperatures were calculated.

For this model simulation of the core, the results of the hottest fuel assembly and the assembly representing the average fuel assembly were determined and discussed. The reason for the analysis on the average fuel assembly was to understand the normal effects in a fuel assembly. In the case of an accident the hottest fuel assembly will be most appropriate to study since it is necessary to keep the fuel and cladding temperatures below their specified limits. The average fuel assembly was found to be fuel assembly 1 in Figure 4-22 and fuel assembly 9 was the hottest fuel assembly.

The results of these two fuel assemblies are given in Table 11. Figure 4-24 gives an illustration of the behaviour of the fuel assembly as the water flows through the channel.

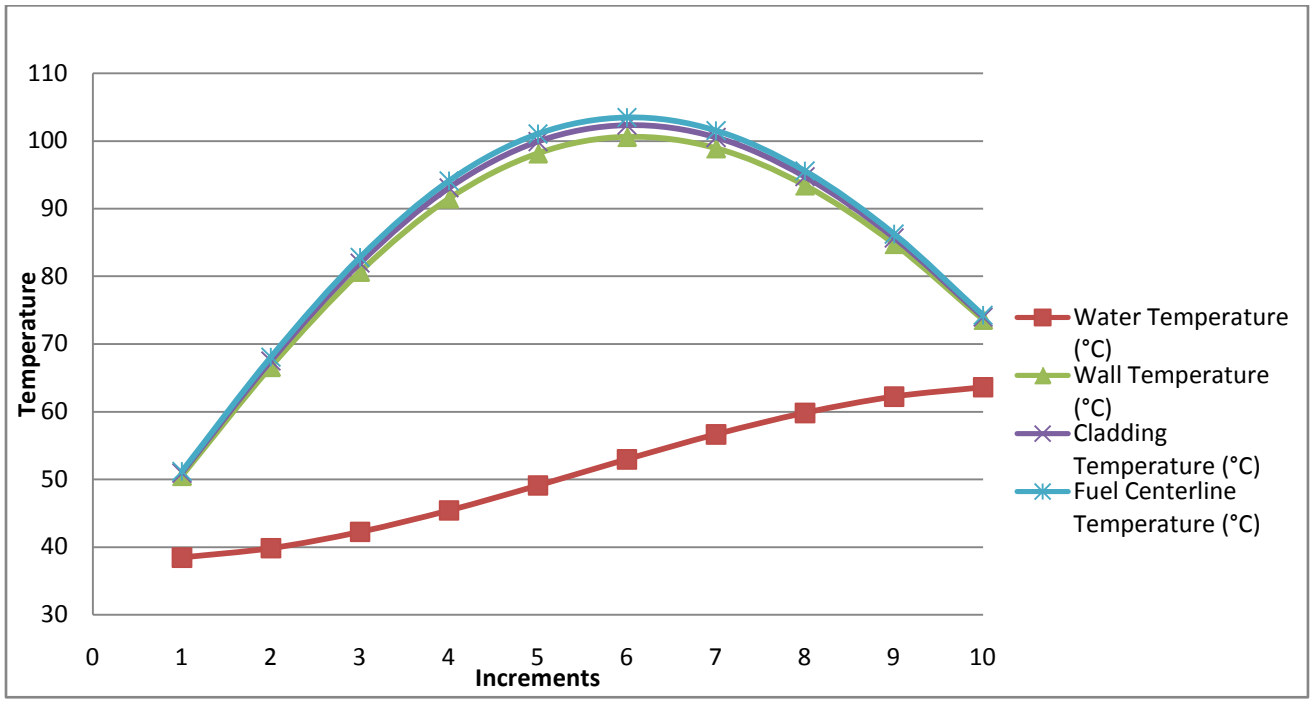

Figure 4-24 : Flownex® quarter core graph of fuel assembly 9 (hottest).

Table 11: Flownex® quarter core calculations of fuel assembly 9 (hottest) and fuel assembly 1 (average).

	Fuel Assembly 9 (Hottest)							Fuel Assembly 1 (Average)						
Increments	Static Pressure (kPa)	Water Temperature (°C)	Wall Temperature (°C)	Cladding Temperature (°C)	Fuel Centerline Temperature (°C)	Convection coefficient (W/m².K)	Nusselt number	Static Pressure (kPa)	Water Temperature (°C)	Wall Temperature (°C)	Cladding Temperature (°C)	Fuel Centerline Temperature (°C)	Convection coefficient (W/m².K)	Nusselt number
1	164.529	38.434	50.533	50.923	51.177	11597.353	80.741	164.571	38.205	43.919	44.102	44.221	11500.902	80.113
2	160.909	39.844	66.629	67.503	68.074	11758.930	81.593	160.967	38.870	51.611	52.021	52.288	11575.474	80.506
3	160.704	42.246	80.694	81.975	82.813	12011.387	82.909	160.768	40.005	58.474	59.074	59.466	11705.818	81.194
4	160.506	45.429	91.519	93.093	94.122	12319.616	84.496	160.574	41.508	63.897	64.634	65.116	11869.810	82.054
5	160.316	49.110	98.185	99.912	101.042	12705.610	86.506	160.384	43.245	67.492	68.301	68.830	12031.778	82.883
6	160.136	52.960	100.612	102.339	103.469	13094.080	88.533	160.198	45.063	68.967	69.776	70.306	12207.944	83.791
7	159.965	56.638	98.953	100.527	101.556	13444.521	90.359	160.017	46.801	68.280	69.017	69.499	12383.306	84.700
8	159.801	59.819	93.457	94.737	95.575	13770.165	92.072	159.840	48.303	65.567	66.167	66.559	12540.915	85.522
9	159.643	62.218	84.800	85.674	86.245	14001.878	93.295	159.668	49.437	61.105	61.514	61.782	12663.667	86.165
10	158.500	63.625	73.601	73.990	74.245	14125.859	93.949	158.531	50.102	55.272	55.455	55.272	12737.257	86.552

It can be seen from Table 11 and Figure 4-24 that the temperatures of the wall, cladding and fuel increase from the inlet to the centre of the fuel assembly and start to reduce towards the end of the fuel assembly. The reason for this behaviour is due to the sinusoidal power distribution that has the highest power concentrated in the centre of the fuel assembly. The temperature profile of the fluid does not display the same behaviour as the wall, cladding and fuel temperature. The gradient in the water temperature distribution increases as the fuel gets warmer towards the centre of the fuel assembly. The same with the outlet of the fuel assembly, the gradient decreases as the power starts to get lower towards the outlet. The average fuel assembly displays the same effects as the graph in Figure 4-24. The difference is that fuel assembly 1 has lower temperatures that that of fuel assembly 9, because this assembly has a lower concentration of power.

4.8 Comparison of results

To determine the validity of the Flownex® results, the simulation models can be verified either by hand calculations and/or comparisons with previous research studies.

4.8.1 Verification of the core water outlet temperature

The coolant water is used to cool the reactor down during the operation of the plant. The heat is transferred to the water and the water is heated up through the core. For the simulation the water was specified as 38°C on the inlet of the core. To prove the validity of Flownex® the outlet temperature of the 12 MW and 10 MW models can be calculated with the following equation:

$$\dot{Q} = \dot{m} C_p (T_e - T_i) \tag{4.6}$$

where $\dot{Q}$ is the power in the reactor, $\dot{m}$ the mass flow through the core, C_p the specific heat of the fluid, T_e the temperature at the outlet and T_i the temperature at the inlet. Table 12 gives the variables that were used for Eq (4.6) and the comparison between the calculated and Flownex® outlet temperatures for the 10MW and 12 MW reactors respectively.

Table 12: Core water outlet temperature.

	12 MW	**10 MW**
Mass flow rate (kg/s)	277.77	277.77
Power (kW)	12000	10000
Specific heat (kJ/kg.K)	4.18	4.18
Inlet temperature (°C)	38	38
Calculated outlet temperature (°C)	48.33493	46.61244
Flownex® outlet temperature (°C)	48.33753	46.61508

From Table 12 it can be seen that there was a good comparison between the two different calculations.

In section 2.1.1 it was mentioned in the study of Hainoun *et al.* (2010) that the hottest fuel channel has a maximum water temperature of 61.2°C for the 10 MW reactor. The water temperature of the hottest fuel assembly in Flownex® for the 10 MW reactor was calculated as 63.625°C.

This provides good confidence in the results of the outlet water temperatures in Flownex® for this study.

4.8.2 Verification of water/cladding temperature difference

Table 13 gives the steady state results that were determined by Flownex and other studies for the 12 MW case. These fuel and cladding temperature results were determined at the hottest increment in the core. For this specific case it was channel 9 at increment 6. The water temperature was determined on the outlet of channel 9 to be consistent with the other studies. Thus the temperatures of the previous studies were also determined at the same point where the results in Flownex® were measured.

Table 13: Comparison between different software codes for steady state simulations

	Power (MW)	Water (°C)	Clad (°C)	Fuel (°C)
MERSAT	12	65	96	110
MATLAB SIMULINK	11.87	55	80	85
RELAP5/mod3.2	n/a	40	78	n/a
Flownex®	12	68.7	113.9	115

In Table 19 of Appendix A it is clear that the temperature difference between the water and the cladding is between 25-30°C. The temperature difference between the cladding and water is almost 40°C in Flownex® for both the 10 MW and 12MW reactors.

One of the explanations can be that a different power profile was used for this study as compared to those listed in the literature study in chapter 2, i.e the profile in this study should have been flatter. During the literature research no suitable power profile was found that was used for the simulations. One of the methods that can be used for solving the power profile is with MCNP calculations. These calculations was not part of the scope of this study, and only a essential explanation will be discussed

The flatter power can be explained from Figure 4-25. If the reactor was considered to have homogenous isotopic distributions in the core and the reflector, it can be seen from Figure 4-25 that a reactor with a reflector has more thermal neutrons on the edges that is reflected back into the core as compared to the reactor without the reflector. The total power in a reactor can be determined as the total area below the graph. This indicates that a reactor with a reflector has a flatter power profile as compared to a bare core. This is because the power in the centre of core will be lower in a reactor with a reflector and the power on the edges of the core of the reactor with the reflector would be higher. (Stacey, 2007).

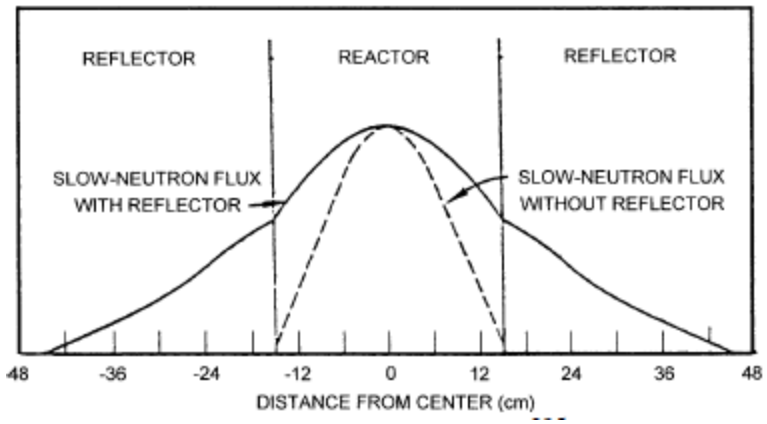

Figure 4-25: Thermal neutron flux in a reactor with and without n reflector (Stacey, 2007)

Figure 4-26 gives an illustration of the difference between the power curve in the axial direction that was used during this study and that of an estimated profile. It can be seen that power has a more even distribution and there is a lower power in the centre of the fuel assembly. In both profiles, the area under the curve was kept constant.

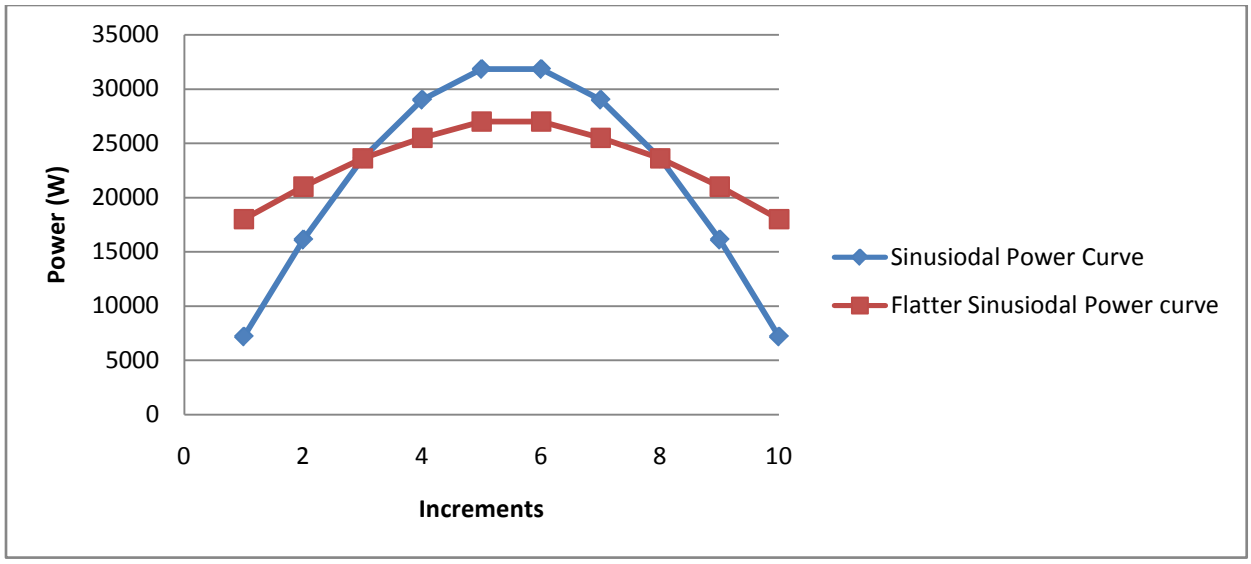

Figure 4-26: Power curve.

In Table 14 the difference in temperature using the different power profiles are shown. It can be seen that the temperature difference between the water and cladding is larger on the inlets and outlets of the channel, but smaller in the centre of the channel for the more even power profile. The temperature difference between the cladding and water was determined by Eq (4.7), where

$\dot{Q}$ is the power in the increment, h the convection heat transfer coefficient, A the wall contact area and ΔT is the temperature difference between the wall and cladding.

$$\dot{Q} = hA\Delta T \tag{4.7}$$

For the more even power profile the temperatures will be lower in the centre of the fuel channel and this can explain the difference between the temperatures observed. Consider Table 14. The temperature differences between the wall and the water are shown in the 5th and 12th columns for the sinusoidal profile and the more flatter profile respectively. It can be seen that the temperature difference between the sinosiodal profile and the more even profile is larger at the centre of the assembly. At the top and bottom of the core, the reverse happens. The temperature difference of the more even core profile is larger. This explains the lower temperature differences that were found with the literature study.

Table 14: Comparison of the temperature difference between the water and the cladding for the different power profiles.

12 MW Channel 9											
	Flownex				More even power profile						
	Water (°C)	Q (W)	Wall (°C)	Delta T (°C)	Re	Pr	Nu	Q (W)	Area (m^2)	h ($W/m^2.K$)	Delta T (°C)
1	38.521	7177.200	53.013	14.492	12773.940	4.493	80.875	16846.676	0.046	11618.956	31.644
2	40.209	16106.400	72.205	31.996	13236.421	4.319	81.905	19654.455	0.046	11814.012	36.309
3	43.089	23605.200	88.883	45.794	13932.792	4.079	83.402	22092.731	0.046	12103.291	39.837
4	46.904	29007.600	101.502	54.599	14877.415	3.792	85.364	23866.124	0.046	12482.950	41.726
5	51.314	31833.600	109.079	57.765	16119.525	3.470	87.854	25270.014	0.046	12958.646	42.559
6	55.927	31833.600	111.880	55.953	17286.612	3.213	90.086	25270.014	0.046	13388.369	41.193
7	60.335	29007.600	109.696	49.362	18571.551	2.971	92.457	23866.124	0.046	13839.330	37.637
8	64.143	23605.200	103.352	39.209	19600.500	2.801	94.291	22092.731	0.046	14186.914	33.986
9	67.018	16106.400	93.289	26.271	20413.671	2.680	95.707	19654.455	0.046	14453.630	29.678
10	68.704	7177.200	80.282	11.578	20922.704	2.610	96.581	16846.676	0.046	14617.365	25.153

Another possibility for this larger temperature difference can be attributed to the neglecting of the reactor feedback due to the Doppler effect and changes in coolant density. For example, the Doppler effect indicates that if the fuel temperature increases, the Uranium-238 will absorb more neutrons, thus reducing the number of thermal neutrons, which will cause the power to decrease in core, and vice versa. This means that the reactor power will decay quicker with reactivity feedback and the changes in the temperature will be smaller. This possibility of the reactivity feedback was not simulated because it was beyond the scope of this study.

4.8.3 Verification of cladding/fuel temperature difference

The temperature difference in Flownex® between the cladding and the fuel shows a good comparison with the previous studies except for that of the MERSAT simulation (Hainoun *et al.*, 2010).

The fuel-cladding temperature difference has also been verified using a hand calculation, as shown in Table 15.

Table 15: Temperature difference between fuel and cladding calculations.

Power per increment (W)	Thickness of Fuel (m)	Number of Fuel plates	Width (m)	Height per increment (m)	Volume (m^2)	q''' (kW/m3)	a (m)	k (W/m.K)	k x dT	Delta T
7177.2	0.00051	23	0.0664	0.06	4.67323E-05	153.581	0.000255	50	4.9933	0.09987
16106.4	0.00051	23	0.0664	0.06	4.67323E-05	344.652	0.000255	50	11.2055	0.22411
23605.2	0.00051	23	0.0664	0.06	4.67323E-05	505.115	0.000255	50	16.4226	0.32845
29007.6	0.00051	23	0.0664	0.06	4.67323E-05	620.718	0.000255	50	20.1811	0.40362
31833.6	0.00051	23	0.0664	0.06	4.67323E-05	681.19	0.000255	50	22.1472	0.44294
31833.6	0.00051	23	0.0664	0.06	4.67323E-05	681.19	0.000255	50	22.1472	0.44294
29007.6	0.00051	23	0.0664	0.06	4.67323E-05	620.718	0.000255	50	20.1811	0.40362
23605.2	0.00051	23	0.0664	0.06	4.67323E-05	505.115	0.000255	50	16.4226	0.32845
16106.4	0.00051	23	0.0664	0.06	4.67323E-05	344.652	0.000255	50	11.2055	0.22411
7177.2	0.00051	23	0.0664	0.06	4.67323E-05	153.581	0.000255	50	4.9933	0.09987

The temperature difference between the fuel and cladding was calculated from the *Thermal Hydraulic Fundamentals Vol. 1* textbook from Todreas and Kazimi (1990). The equation that was used for the calculation is given by Eq (4.3) (Todreas & Kazimi, 1990).

$$k(T_{\max} - T_{ci}) = q''' \frac{a^2}{2} \tag{5.3}$$

where k is the conductivity of the uranium, $T_{\max}$ the maximum temperature of the fuel, T_{ci} the temperature on the inside of the cladding, q''' power per cubic meters and a the distance from the centre of the fuel to the cladding. Figure 4-27 gives a representation of each of the variables that were used in Eq (4.3).

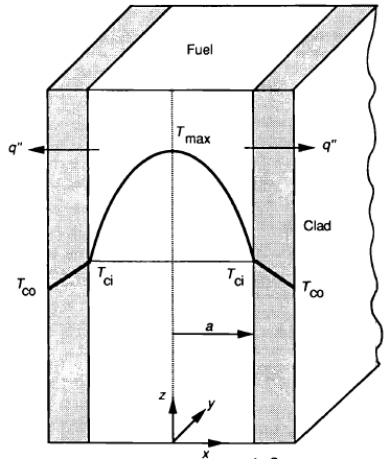

Figure 4-27: Plate fuel element (Todreas & Kazimi, 1990).

This method offered verification for the small temperature difference between the fuel and the cladding.

Chapter 5

5 Transient simulation of reactor core

5.1 Introduction

For a nuclear reactor is it necessary to know what the effects will be in the case of an accident. Simulation models are used to determine the behaviour of the core in such cases. Transient simulations were done on the IAEA MTR research reactor using the Flownex® model. The accident scenarios were taken to be LOFAs.

5.2 Simulation model

5.2.1 Loss of flow accident (LOFA)

For this study LOFAs were simulated for the 10 MW and 12 MW IAEA MTR reactors. Using the guidelines described in section 3.4, it was decided to simulate a failure of the primary coolant pump for the LOFAs.

The primary coolant pump has a safety feature in case of a pump failure. The pump is fitted with a flywheel on a main axle to increase in rotation inertia in case of a pump trip. For the simulation the mass flow of water through the core was reduced by the exponential equation (exp (-t/T)) as given in section 4.3.2.1. The SLOFA and FLOFA simulations corresponded to decline periods (T) of 25s and 1s respectively. The nominal mass flow through the core was 69.4444 kg/s.

It was assumed that the reactor operated under normal conditions for 50 seconds before the primary coolant pump failed. After 50 seconds the mass flow was set to reduce according to the exponential expression (exp (-t/T)).

The rate of change of the mass flow through the core is shown in Figure 5-1.

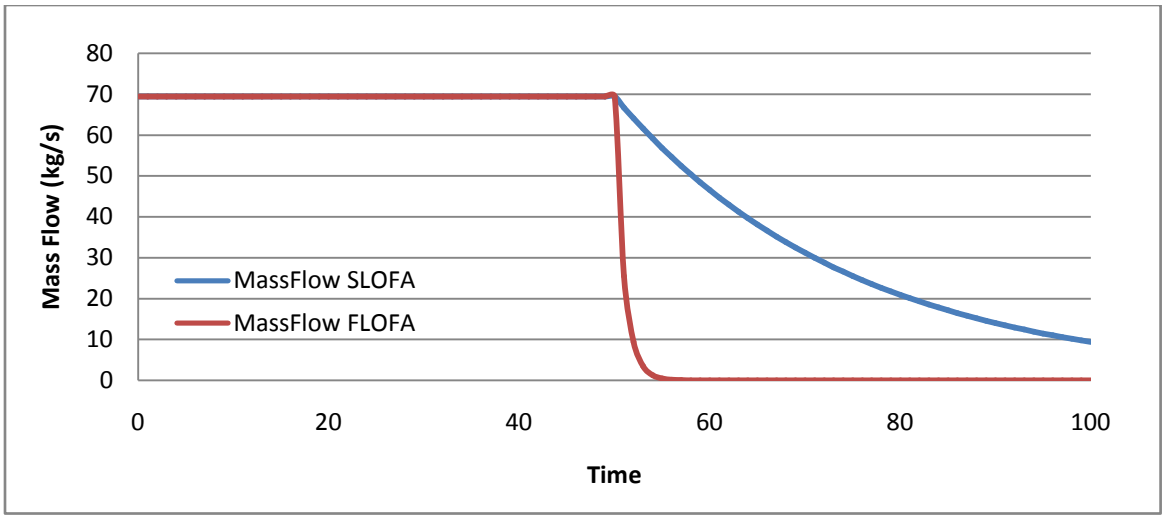

Figure 5-1: Mass flow during LOFA.

5.2.2 Power reduction during LOFA

The reactor was set to trip with a delayed time of 2 ms once the mass flow through the core was 85% of the nominal mass flow rate. After the reactor trip, an instantaneous negative reactivity of \$10 was injected into the core. This approximated the specifications of IAEA given as \$10/05s in section 4.3.2.1. The power reduction in the core was calculated from the contribution from the delayed neutron fissions and the decay heat production. It should again be noted that the reactivity feedback was disregarded for the purposes of this study. The equations in section 3.6.1.1 and 3.6.1.2 were used for the calculation of this power reduction. The different variables that were used for the calculation in section 3.6.1.1 and 3.6.1.2 are given in Table 16.

Table 16: Input variables for power reduction calculation

Variable	Value	Unit
Reactivity (ρ)	-0.075	-
Neutron lifetime (Λ)	6 x10^{-5}	sec
Mean free path (λ)	0.08	sec^{-1}
Fissions per fissile atom (ψ)	1	-
Operating time (T)	30.4	days
Energy produced per fission (Q)	200	MeV/fission
Faction delayed neutrons (β)	0.0075	-

The reason why the fissions per atom (ψ) were used as 1, is because it would not make a huge difference in the calculations of the decay heat and it was used during an example in the report of the American Nuclear Society (ANS, 2005). The total power reduction was determined by the sum of the decay heat produced by the fission products and the fission energy due to the delayed neutrons fissioning per time step. Figure 5-2 and Figure 5-3 show the power reduction calculation of the core after the reactor trip. The zero value on the x-axis represents the time when the reactor trips and the power starts to decrease. Figure 5-3 shows the effect of the power reduction in a small time interval. The calculated power percentage/fraction is multiplied with each power specified at the different nodes in Flownex® for the transient simulation.

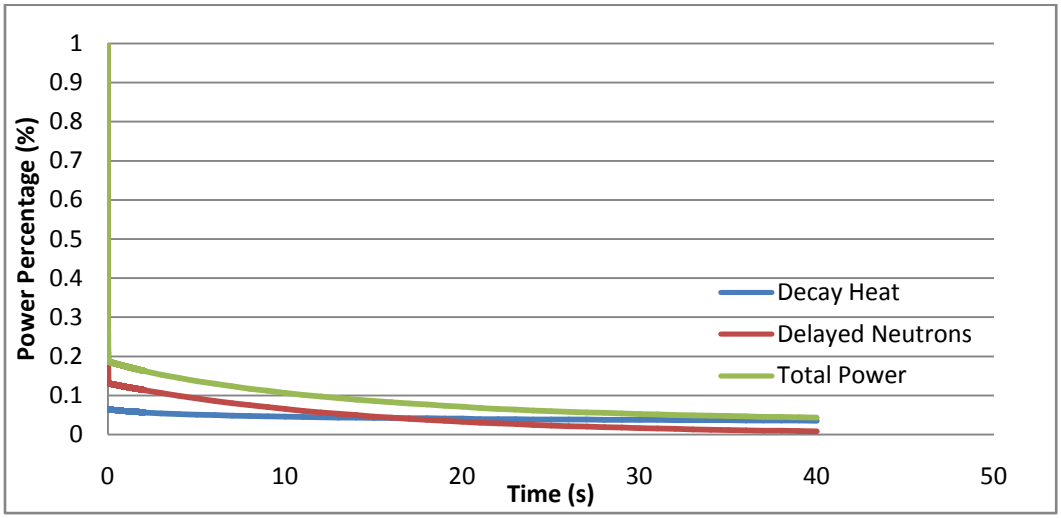

Figure 5-2: Power reduction during LOFA.

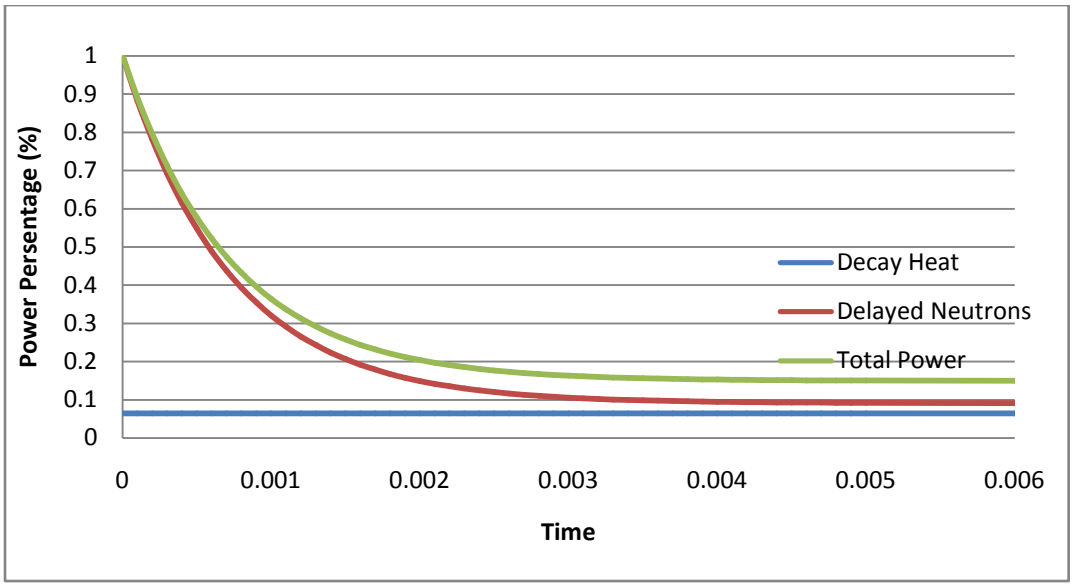

Figure 5-3: Power reduction during LOFA between 0-0.006 seconds.

5.2.3 Flownex® transient model

The Flownex® transient model was based on the steady state simulation model of the core that was used in section 4.7. A Microsoft Excel component was inserted in the model for the transient simulation. Figure 5-4 shows the simulation model of the core with the Microsoft Excel component.

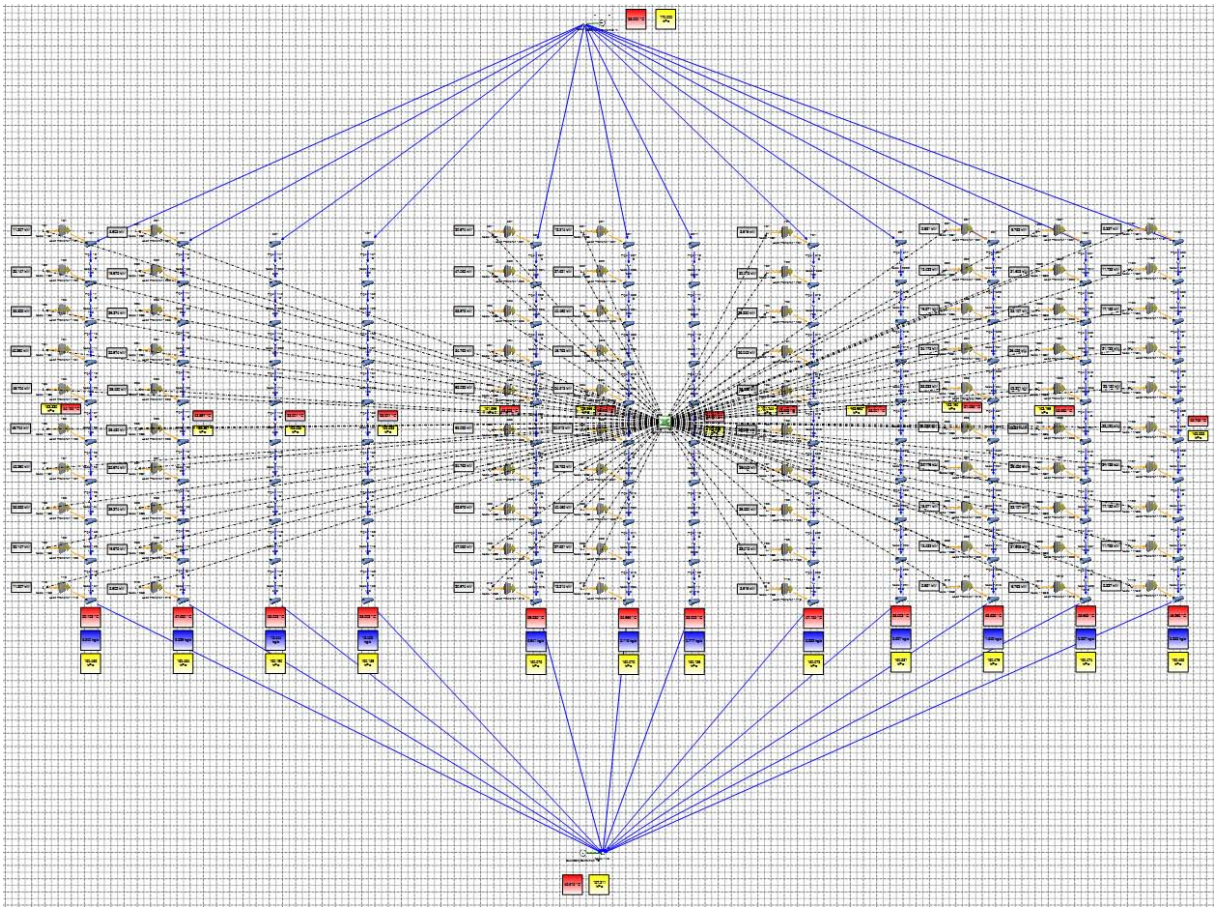

Figure 5-4: Flownex® reactor model (transient).

The Microsoft Component was used to set the power for each node for the different time steps. When Flownex® was running the transient simulation, the different powers for each node was calculated in Microsoft Excel and was sent back to Flownex® with a "Data Transfer link" for each subsequent time interval. This enabled Flownex® to determine the effect of the decrease in power on the LOFA.

It was also possible to set different actions/changes at different time steps in Flownex®. The Flownex® model of the core was set according to the setup that was discussed in section 5.2.1 and section 5.2.2. The power was set to reduce according to the calculations in section 5.2.2. The simulation was run for a total time of 100 seconds.

5.2.4 Results and discussion

5.2.4.1 SLOFA transient simulation

A SLOFA simulation was done for both the 10 MW and 12 MW cases. Only the hottest increment in the core will be discussed due to the fact that it would present the most challenging case to the fuel integrity. The hottest fuel increment is fuel assembly number 9 shown in Figure 4-22. Figure 5-5 and Figure 5-6 give the results of the core's behaviour during the transient simulation.

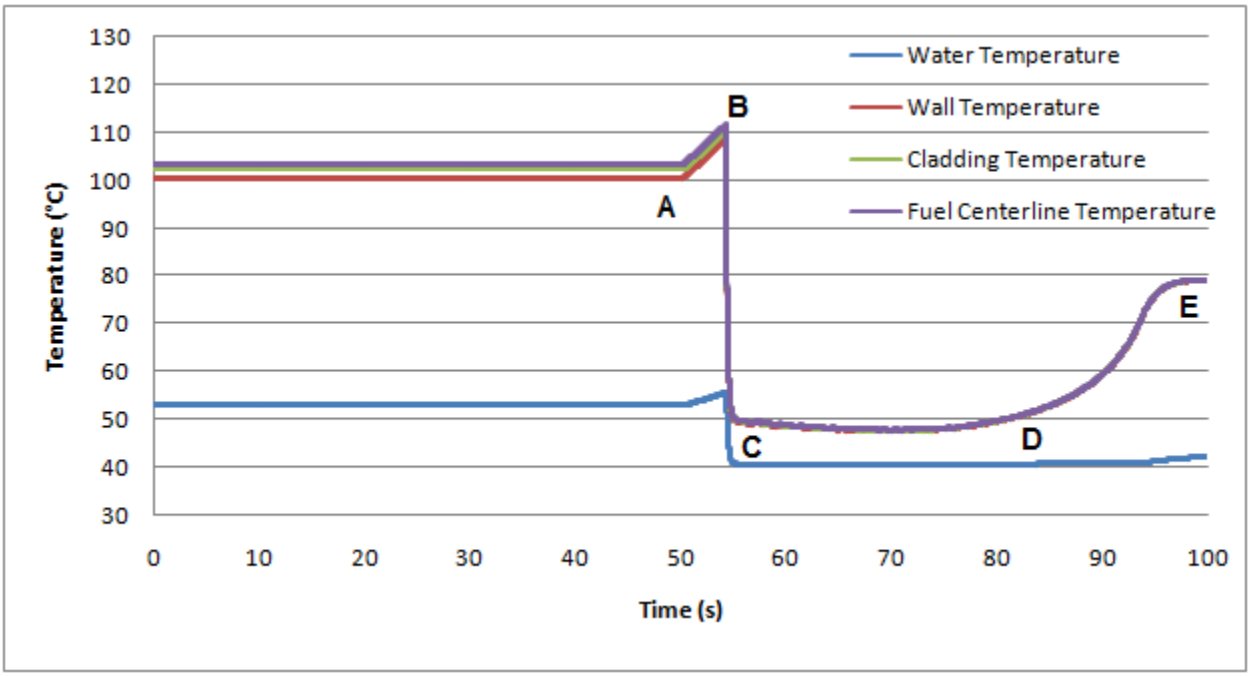

Figure 5-5: Flownex® transient simulation of SLOFA 10 MW.

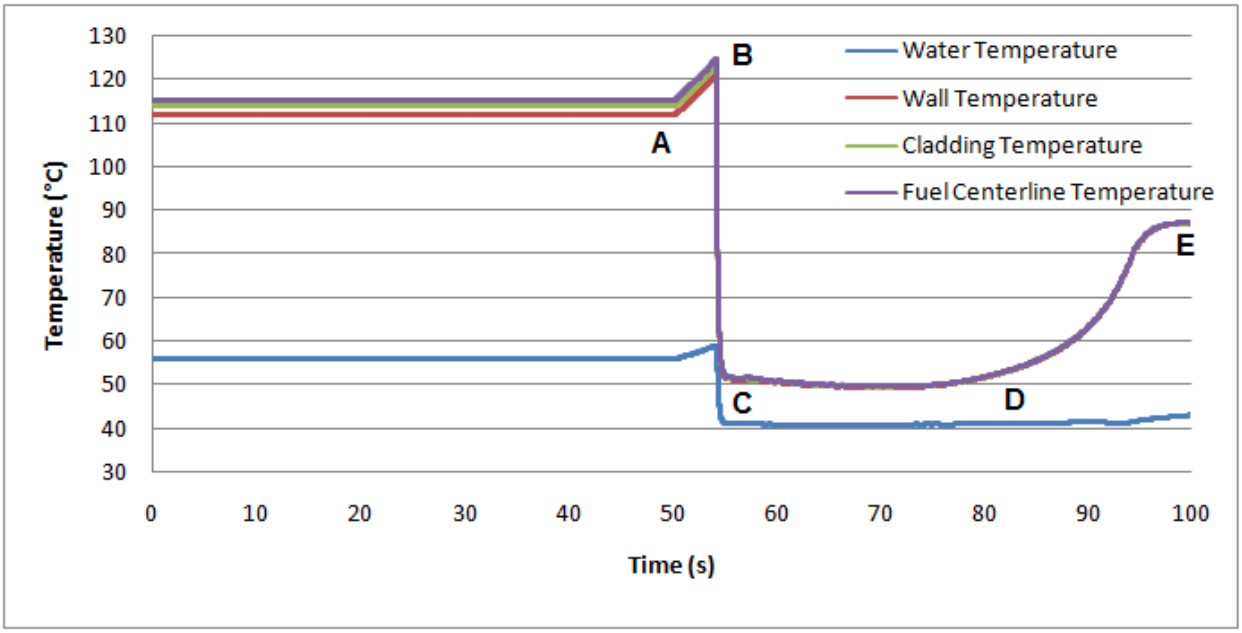

Figure 5-6: Flownex® transient simulation of SLOFA 12 MW.

From Figure 5-5 and Figure 5-6 it can be seen that the reactor was running under normal condition for 50 seconds up to point A. At 50 seconds the LOFA occurred and the mass flow in the core started to decrease. As the mass flow decreased, the water, wall, cladding and fuel centreline temperature started to increase. This is shown as the region A-B in the figures. When 85% of the mass flow was reached, the control elements were inserted, and the reactor tripped. This trip occurred 4.263 seconds after the primary coolant pump failed with the 0.2 second delay time taken into account. This is point B of the graph. As the reactor power deceased after the trip, the temperatures began to decrease until it reached the point C, where the effect of the decay heat in the core became significant compared to the cooling effect. It was explained in section 3.6.1.1 that there is about 6% decay heat still left in the core. At point D, the mass flow in the core is greatly reduced from the nominal value, but it is not sufficient to remove the decay heat being generated. As a result, the water, wall, cladding and fuel centreline temperatures begin to rise. This is indicated in the graph from point D to E.

Somewhere in the region of point D, the backup cooling system of the core should start to operate to prevent the fuel from overheating and possibly melting.

However, in terms of the scope of this project, this was not modelled.

It can be seen that for both of the reactor powers, the core behaviour is similar during the SLOFA, with the difference that the 12 MW reactor has higher temperatures due to the fact that it has a higher concentration of power. Table 17 gives the first maximum temperatures of the water, wall, cladding and fuel centreline temperatures. The first maximum temperatures were reached after 54.22 seconds at the point where the reactor has tripped.

Table 17: 10 MW and 12 MW reactors maximum temperatures during SLOFA

Reactor	Water Temperature (°C)	Wall temperature (°C)	Cladding Temperature (°C)	Fuel centreline temperature (°C)
10 MW	55.5830	108.8198	110.5408	111.6678
12 MW	59.0717	121.3010	123.3672	124.7198

5.2.4.2 FLOFA transient simulation

This simulation was similar to the simulation that was done in the previous section. The difference was that the time period T of the exponential equation that calculated the mass flow reduction, was changed to 1 second. In effect the mass flow through the core reduced much quicker and the reactor tripped at an earlier point in time. Figure 5-7 and Figure 5-8 provides graphs of the simulations that were done on the 10 MW and 12 MW reactors. A discussion on the results follows thereafter.

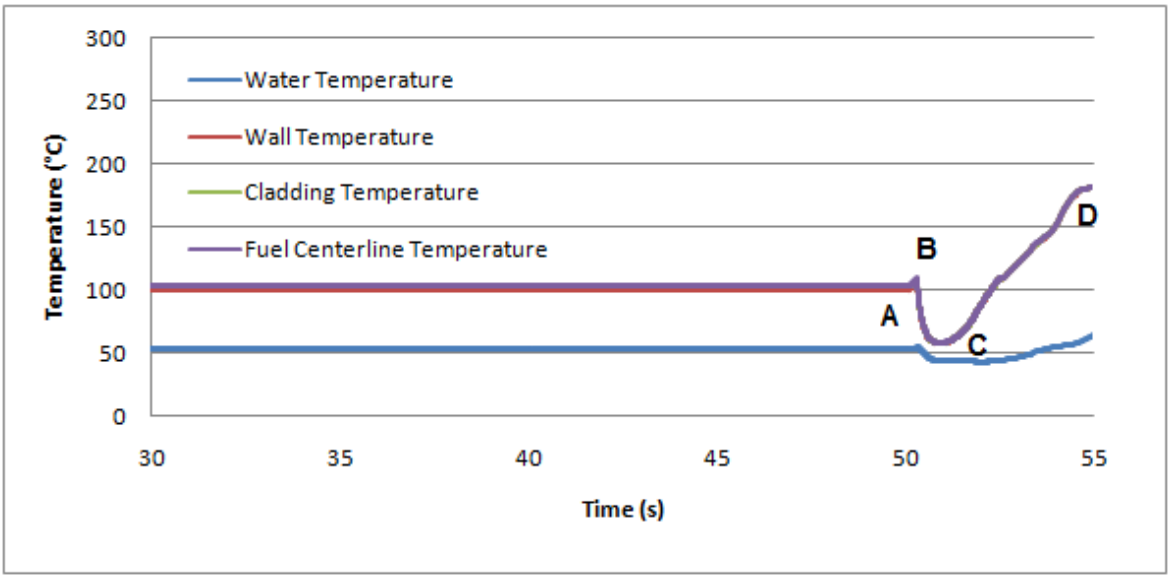

Figure 5-7: Flownex® transient simulation of FLOFA 10 MW.

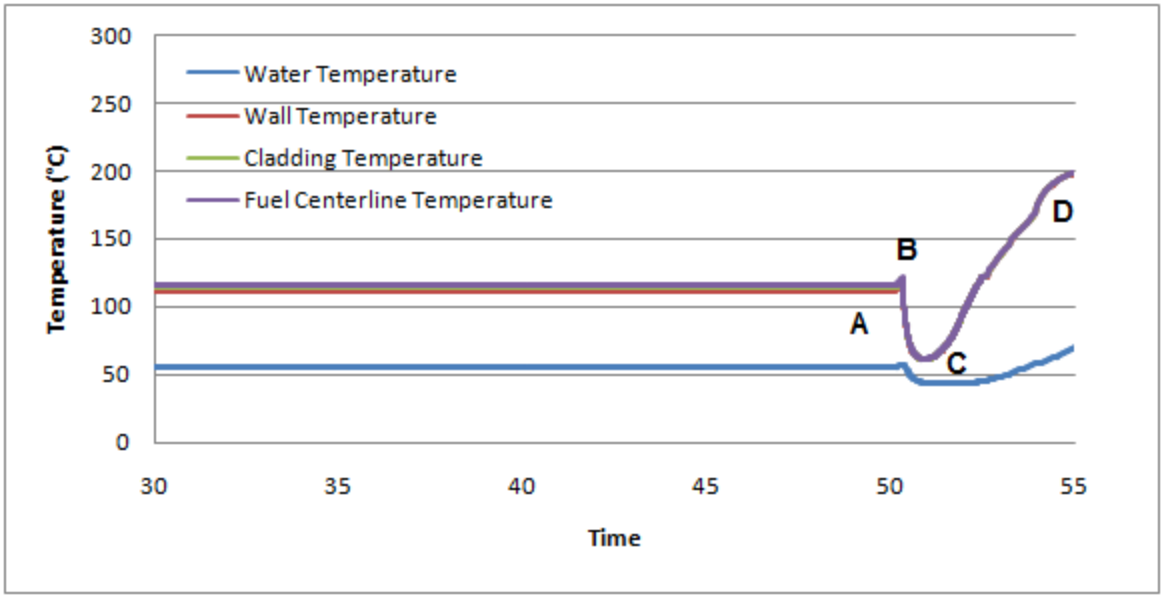

Figure 5-8: Flownex® transient simulation of FLOFA 12 MW.

From Figure 5-7 and Figure 5-8 it can be seen that the reactor was running under normal condition for 50 seconds. At 50 seconds, shown as point A in the graph, the FLOFA occurred and the mass flow in the core started to decrease. As the mass flow decreased, the water, wall, cladding and fuel centreline temperatures started to increase. This is shown as the curve A-B in the graph. The control elements were inserted when 85% of the mass flow was reached and the reactor tripped. The reactor took 0.3625 seconds to trip after the primary coolant pump failed with the 0.2 second delayed time taken into account. As the power deceased from the trip the temperature started to decrease until it reached the point C. At this point the decay heat in the core became important. About 6 seconds after the pump failed, at point D, there was almost no mass flowing through the core, and the decay heat could not be effectively removed from the core. The water, wall, cladding and fuel centreline temperatures thus began to increase until it reached the maximum.

At point D, the backup cooling system of the core should start to operate to prevent the fuel from overheating and possibly melting.

However, in terms of the scope of this project, this was not modelled.

The behaviour of the 10 MW and 12 MW reactors are similar. The only difference is that the temperatures of the 12 MW are higher than the 10 MW reactor core. Table 18 gives the first

maximum temperatures of the water, wall, cladding and fuel centreline temperatures. These temperatures were determined at the point where the reactor had tripped. The maximum temperatures were reached after 50.32 seconds.

Table 18: 10 MW and 12 MW reactors maximum temperatures during SLOFA.

Reactor	Water Temperature (°C)	Wall temperature (°C)	Cladding Temperature (°C)	Fuel centerline temperature (°C)
10 MW	54.0821	103.5252	104.9653	105.6967
12 MW	57.2832	115.2658	116.9954	117.8738

5.2.4.3 FLOFA transient simulation of the 12 MW Reactor with backup cooling system

A simulation was done on the 12 MW reactor with a backup cooling system. The purpose of the simulation was to determine at what point the backup cooling system should be activated to prevent damage to the fuel. The simulation model was based on the Flownex® model that was described in the previous section. However, this model was set to engage a core backup cooling system when the fuel centreline temperature reached a maximum value of 135°C. It was assumed that the backup cooling system has a mass flow rate of 69.44444 kg/s equal to that of the nominal flow rate and was supplied instantaneously to the core. The results of the simulation is given in Figure 5-9

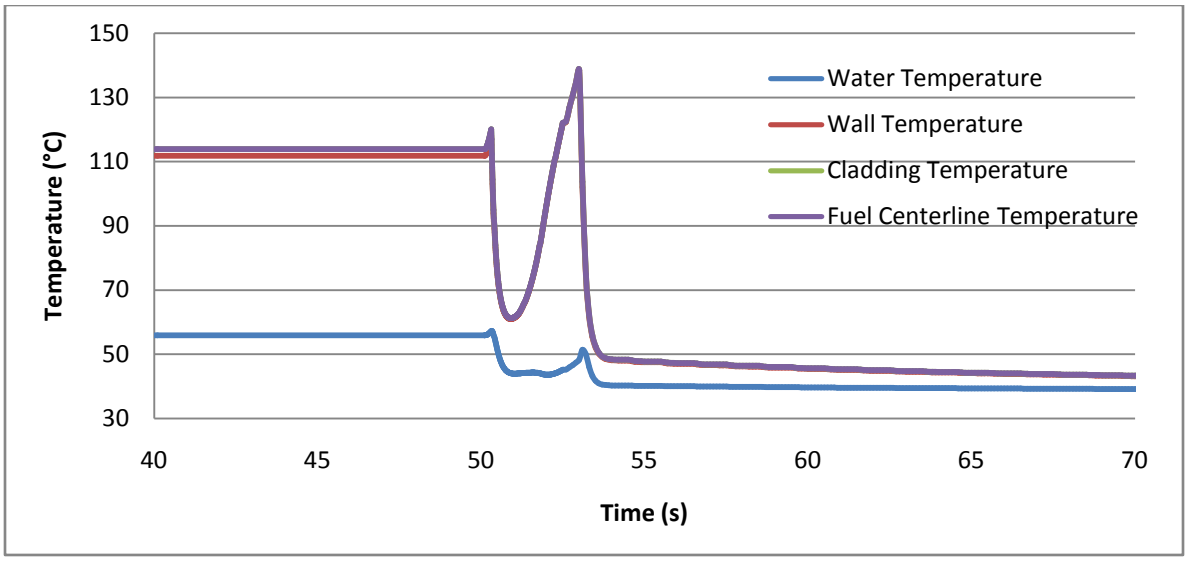

Figure 5-9: FLOFA simulation of 12 MW reactor with backup cooling system.

It can be seen from Figure 5-9 that the behaviour of the core is, as expected, exactly the same as in the previous simulation up to the point where the backup system was activated. After the backup system was activated, the fuel centreline temperature increased to a maximum of 138.55°C until it started to decrease. The temperatures then decreased until it became stable where the remaining decay heat was being effectively removed by the coolant, and thus having no adverse effects on the water, wall, cladding and fuel centreline temperatures. This simulation has shown that it is necessary to have a core backup cooling system in case of an emergency such as the FLOFA. Without such a backup cooling system, the core could have a meltdown in a few seconds. However, this was not studied in detail, due to the time constraints of this project.

5.3 Verification of the LOFAs

For the LOFAs the same method was used as in previous studies. The behaviour of the reactor during the LOFA simulations was the same as in the study done by Hainoun *et al.* in 2010. The only difference was that the temperatures in the Flownex® simulation were higher than in some of the studies in the literature. The reason for this was explained in section 4.8.2 where another power profile was used for the other simulations. Table 19 gives comparison between the results of the different LOFA simulations that have been done in previous studies, with Flownex®.

Table 19: Comparison of results during LOFAs.

	SLOFA					FLOFA				
Temperatures	**Flownex®**	**MERSAT**	**RELAP 3.2**	**RETRAC-PC LAS**	**COBRA III-C**	**Flownex®**	**MERSAT**	**RELAP 3.2**	**RETRAC-PC LAS**	**COBRA III-C**
Water (°C)	73.966	68.450	57.97	58.68	55.400	70.04	69.250	59.530	60.050	56.500
Cladding(°C)	123.3672	100.060	88.41	84.440	85.500	116.995	103.940	91.280	88.450	89.500
Fuel centre (°C)	124.7198	112.620	88.67	87.310	88.200	117.874	116.050	n/a	91.200	91.000

Chapter 6

6 Conclusions and Recommendations

6.1 Summary

During this study, the software package Flownex® was used to evaluate its ability to simulate the IAEA MTR 10 MW benchmark research reactor. Only the reactor core was simulated.

A basic simulation model of a single fuel assembly was built to determine the validity of the model that can be constructed in Flownex®. This model was compared with the results of a model that was developed in EES with the same specifications. There was good comparison between the models.

Next, a model was built for the entire reactor core

Using the model of the IAEA MTR 10 MW reactor, steady state simulations as well as transient simulations were done. The steady state results were used to determine the operating conditions. Transient simulations were done for fast and slow loss of flow accidents (LOFAs) where it was assumed that the primary coolant pump has failed. The LOFAs were simulated and compared with each other.

Finally, the results used obtained in this study were compared with results obtained from other studies.

6.2 Conclusions

The objectives of this study were assessing the simplifying assumptions that have to be made by the user and shortcomings that were built in the software. During the study a few assumptions were made. These assumptions can be split into the user and software assumptions.

The first assumption made was using the point kinetics equations without reactivity feedback. Flownex® does not calculate the heat due to the delayed neutrons, and this must be input by the user. This can be considered to be a shortcoming by the software code and could be built into the code.

The second assumption was that a cosine power profile was used and it was an assumption made by the user. A more representative power profile could be calculated using a neutronics code like MCNP (Monte Carlo N-Particle Transport Code). However, this was beyond the scope of this study.

The third assumption was that the average power in each of the 23 fuel plates in a fuel assembly was equal. This was also an assumption made by the user to ease with the discritization of the problem

The fourth assumption was that there was no heat transfer between the fuel assemblies and also between the individual fuel plates in a fuel assembly. This assumption was made by the user also to keep the complexity of the problem small.

The last assumption was that the heat source was specified at the boundary. This was an assumption made by the software code.

For the first part of the study a basic model was simulated to determine the validity of the modelling approach used in the software package. A single fuel assembly model was developed and simulated in Flownex® and EES. There was a very good comparison between the different models.

A simulation model of the entire core was built in Flownex® to determine the normal operating conditions of the reactor during steady state operating conditions.

This model was then applied to LOFA transient studies. The reactor was simulated for the 10 MW and 12 MW reactors during a SLOFA and an FLOFA. In total four simulations were done.

It was found that for the transient LOFA studies, the temperature of the fuel, cladding, and coolant behaved as expected. These temperatures rose when the flow began to decrease, whilst the reactor was still at full power. When the reactor was tripped, the temperatures began to decline. However, the mass flow rate also continued to decrease, and thus a point was

reached where the coolant could no longer adequately remove the decay heat, and thus the temperatures began to rise again.

In terms of the time response, it was seen that the reactor responded more adversely to a FLOFA than to a SLOFA, as would be expected.

It was also noted that cooling by free convection has to be considered as a backup cooling system to prevent the core from reaching excessive temperatures.

It was found during the simulations that there was no substantial difference between the temperature and pressure trends of the 10 MW and 12 MW simulations. The difference was that the 12 MW reactor had higher temperatures than the 10 MW reactor.

The results of the LOFAs in Flownex® were compared to calculations that were done in previous LOFAs on the MTR 10 MW research reactor. The behaviour of the core during the LOFAs was similar to the previous studies, except that the temperature predicted by Flownex® was higher than those in the literature.

6.3 Computational effort

For any thermal hydraulic simulation study similar to this study, Flownex® was a very user friendly software package. The user manual gives a clear understanding how each of the various elements works and how to use it in a simulations. The software package has various tutorials that the user can do to give a clear picture of model certain problems. Flownex® is a very fast solver of problems and is easy to get the answer at the different points were it is needed. For this study Flownex® has solved all the steady state simulations in a few seconds. The transient simulations were solved a bit longer than the steady state simulations. For the transient simulations Flownex® can specify different accident scenarios at different time steps. Flownex® also can be set to solve the transient simulation at different time steps which has an effect on the duration of the solving of the model. The transient simulations were solved in 4-6 minutes which is very fast for solving such an complex model.

6.4 Recommendation for future studies

As part of the modelling strategy, each fuel element was analysed as a single pipe element with the assumption that all the fuel plates in the element/assembly behave in exactly the same manner, with values for flow areas, heat transfer areas and hydraulic diameters being calculated accordingly. To fine-tune this model, each fuel plate with its surrounding water channel can be analysed as a separate pipe element. However, this would be a larger burden on the model complexity, and therefore possibly only the hottest fuel assembly could be analysed in this way.

This would give better resolved temperature distributions.

It was assumed that the heat transfer between the different fuel assemblies could be disregarded. This leads to the recommendation for a study where the heat transfer between the fuel assemblies is calculated to determine the effect that each of the fuel assemblies have on each other.

It was also assumed that the power profile has cosine profiles in the x, y and z directions. However, it is known that the flux profiles would tend to be more flattened. Therefore it is recommended that the coupled neutron thermal-hydraulic study be performed to obtain better power profiles for the Flownex® calculations.

The reactivity insertion was assumed to be instantaneous, and the point kinetics model was used with a single delayed neutron group and without reactivity feedback. This model can be improved by considering all of these effects.

During this study only the behaviour of the core was simulated. A future study should consider the entire nuclear plant with the primary and secondary loops. This will further help to determine the effect of the primary and secondary coolant loops on the plant during a LOFA.

In 2011 a few studies were done using the same principle as in this study. However, different software packages were used, viz. COBRATF and RELAP5 mod4 (Fourie L 2011 and Kriel 2012). The results of the different software packages should be compared with each other to determine which applications are most suitable for each package.

Bibliography

ANON. 2011. Flownex® library manual. Potchefstroom: M-Tech Industrial.

ANON. 2009. Flownex® version 8.0 user manual. Potchefstroom: M-Tech Industrial.

ANS (AMERICAN NUCLEAR SOCIETY). 2005. Decay heat power in light water reactors. Illinois, USA.

BAE, I.H., NA, M.G., LEE, Y.J. & PARK, G.C. 2008. Calculation of the power peaking factor in a nuclear reactor using support vector regression models. *Annals of nuclear energy*, (35):2200-2205.

BOUSBIA-SALAH, A., MEFTAH, B., HAMIDOUCHE, T. & SI-AHMED, E.K. 2006. A model for the analysis of loss of decay heat removal during loss of coolant accident in MTR pool type research reactors. *Annals of nuclear energy*, (33):406-414.

DUDERSTADT, J.J. & HAMILTON, L.J. 1976. Nuclear reactor analysis. Michigan: John Wiley & Sons.

Fourie L, 2011, Thermal-hydraulics simulation of a benchmark case for a typical Materials Test Reactor using RELAP5 Mod4, 2011, M.Eng Dissertation, North West University, South Africa

GAHEEN, M.A., ELARABY, S., ALY, M.N. & NAGY, M. 2007. Simulation and analysis of IAEA benchmark transients. *Progress in nuclear energy*, (49):217-229.

GUILLEN, D.P. & YODER, T.S. 2008. Thermal hydraulic effect of fuel plate surface roughness. *Nuclear engineering and design*, (238):2480-2483.

HAINOUN, A., GHAZI, N. & MANSOUR ABDUL-MOAIZ, B. 2010. Safety analysis of the IAEA reference research reactor during loss of flow accident using the code MERSAT. *Nuclear engineering and design*, (240):1132-1138.

HAMIDOUCHE, T., BOUSBIA-SALAH, A., ADORNI, M. & D'AURIA, F. 2004. Dynamic calculations of the IAEA safety MTR research reactor benchmark problem using RELAP5/3.2 code. *Annals of nuclear energy,* (31):1385-1402.

HAMIDOUCHE, T. & SI-AHMED, E.-K. 2010. Analysis of loss of coolant accident in MTR pool type research reactors. *Progress in nuclear energy*, (53):285-289.

IAEA (INTERNATIONAL ATOMIC ENERGY ASSOCIATION). 1980. Research reactor core conversion from the use of highly enriched uranium to the use of low enriched uranium fuels guidebook- IAEA TECDOC-233. Vienna.

IAEA (INTERNATIONAL ATOMIC ENERGY ASSOCIATION). 1992a. Research reactor core conversion guidebook - IAEA TECDOC-643. Vienna.

IAEA (INTERNATIONAL ATOMIC ENERGY ASSOCIATION). 1992b. Safety guide on safety assessment of research reactors and preparation of the safety analysis report safety series 35-G1. Vienna.

IAEA (INTERNATIONAL ATOMIC ENERGY ASSOCIATION). 2004. Safety considerations for research reactors in extended shutdown - IAEA-TECDOC-1387. Vienna.

INCROPERA, F.P., DEWITT, D.P., BERGMAN, T.L. & LAVINE, A.S. 2007. Fundamentals of heat and mass transfer. John Wiley & Sons Inc.

Kriel S, to be published in 2012, Thermal-hydraulics simulation of a benchmark case for a typical Materials Test Reactor using COBRA TF, M.Eng Dissertation, North West University, South Africa

LAMARSH, J.R. 2001. Introduction to nuclear engineering. Addison-Wesley Publishing Co. Reading, MA.

LANDMAN, W.A. & GREYVENSTEIN, G.P. 2004. Dynamic systems CFD simulation code for the modelling of HTGR power plants. (*In* 2nd International Topical Meeting on High Temperature Reactor Technology. Beijing, China, 22-24 September.)

LU, Q., QIU, S. & SU, G. 2000a. Development of a thermal-hydraulic analysis code for research reactors with plate fuels. *Annals of nuclear energy*, (36):433-447.

LU, Q., QIU, S. & SU, G. 2000b. Flow blockage analysis of a channel in a typical material test reactor core. *Nuclear Engineering and Design*, (239):45-50.

VAN RAVENSWAAY, J.P., GREYVENSTEIN, G.P., VAN NIEKERK, M. & LABUSCHAGNE, J.T. 2006. Verification and validation of the HTGR systems CFD code Flownex. *Nuclear engineering and design*, p. 491-501.

ROUSSEAU, P.G. & VAN ELDIK, M. 2011. Thermal-fluid systems modelling 1: lecture notes. Potchefstroom: North-West University.

SALAMA, A. & EL-MORSHEDY, E-D. 2010. CFD simulation of the IAEA 10 MW generic MTR reactor under loss of flow transient. *Annals of nuclear energy*, (38):564-577.

STACEY, W.M. 2007. Nuclear reactor physics. Second Edition. Weinheim: WILEY.

THERON, W.G.J. 2011. Flownex training course: lecture notes. Potchefstroom: M-Tech Industrial.

TODREAS, N.E. & KAZIMI, M.S. 1990. Nuclear systems I: thermal-hydraulic fundamentals. Taylor & Francis.

VAN NIEKERK, W.M.K., GREYVENSTEIN, G.P., LABUSCHAGNE, J.T. & SWIFT, J. 2006. Comparison of the thermal-fluid analysis code Flownex with experimental data from the pebble bed micro model. (*In* 3rd International Topical Meeting on High Temperature Reactor Technology. Johannesburg, South Africa 1 - 4 October.)

Appendix

7 The contents of the appendices are as follows:

Appendix A is the safety analysis study that what was done by Hainoun et al in 2010.

Appendix B presents the simulation and analysis study that was done on the IAEA benchmark reactor. The study was done in 2007 by Gaheen *et al*.

Appendix C presents the dynamic calculations of the IAEA safety MTR research reactor using the software code RELAP5/3.2. The study was done by Hamidouch *et al* in 2004.

Appendix D presents the analysis of loss of coolant accidents in MTR pool type research reactor. The study was done by Hamidouch *et al* in 2010.

Appendix E gives the flow blockage analysis of a channel in a typical material test reactor core. The study was done by Lu et al in 2009b.

Appendix F gives the steady state calculation of a single fuel assembly. The power was uniformly distributed and the calculation was done in EES.

Appendix G gives the EES calculation of the sinusoidal power distribution in the axial direction of a single fuel assembly.

Appendix H gives the steady state calculation of a single fuel assembly. The power was sinusoidal distributed and the calculation was done in EES.

Appendix I gives the EES calculation of the power distribution in the entire reactor core.

Appendix A: Safety analysis of the IAEA reference research reactor during loss of flow accident using the code MERSAT (Hainoun et al., 2010)

The first simulation that was done was the SLOFA. The reactor tripped after 3.99 seconds and the negative reactivity was inserted into the core. Figure 7-1 shows the power distribution after the reactor had tripped.

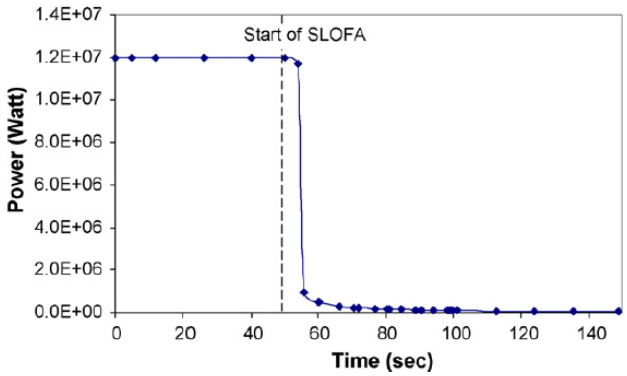

Figure 7-1: Reactor power during SLOFA.

In Figure 7-2 the change of mass flow during the accident is shown. It shows exactly where the different actions took place during the simulation.

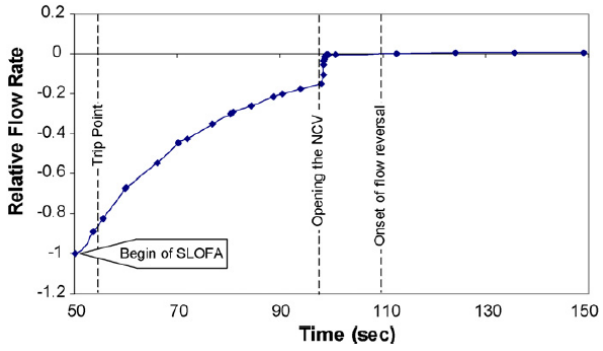

Figure 7-2: Relative flow rate during SLOFA.

Figure 7-3 presents the temperature of the fuel, cladding and coolant through the channel with the highest values. A maximum temperature of 112.62°C was reached in the fuel 3.79 seconds after the SLOFA started with 100.06°C and 68.45°C in the cladding and coolant respectively.

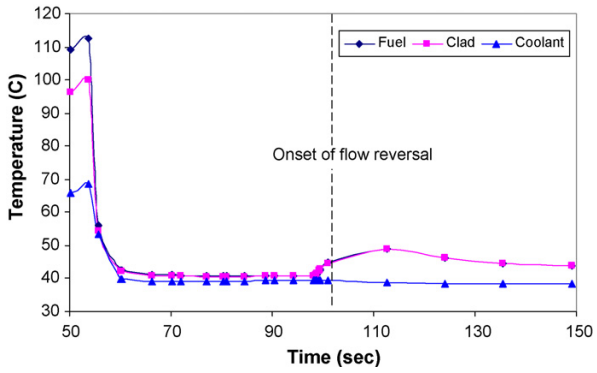

Figure 7-3: Fuel, cladding and coolant temperature during SLOFA.

In case of the FLOFA, the reactor tripped after 0.2 seconds. In the FLOFA simulation the fuel had reached a maximum temperature of 116.05°C, with 103.94°C and 69.25°C in the cladding and coolant respectively. Figure 7-4 presents the temperature of the fuel, cladding and coolant through the channel with the highest values of the FLOFA simulation.

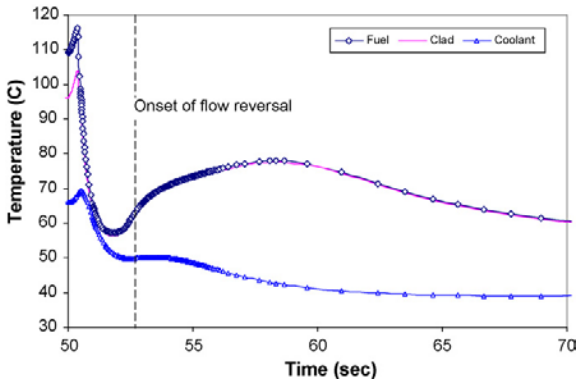

Figure 7-4: Fuel, cladding and cooling temperature during FLOFA.

The results of the two simulations that were done show that the limit of the onset of sub-cooled boiling was not reached and therefore the design limits in terms of the thermal instability were not exceeded. This implies that the core of a MTR 10 MW reactor will not result in a meltdown in case of a LOFA. Table 20 gives the results of the LOFA simulation of MERSAT compared with the different software codes applied by Hainoun *et al.* (2010).

Table 20: Results comparison of LOFA for the MTR (Hainoun et al., 2010).

Code name Institution	MERSAT (AECS)	RELAP5/3.2 (UPISA)	PARET (ANL)	RETRAC-PC (LAS)	COSTAX-BOIL (JEN)	EUREKA-PT (JAERI)	COBRA III-C (Interatom)
SLOFA							
1st Peak fuel temperature (°C)	112.62 (3.79)	n/a	n/a	n/a	91.2 (4.27)	n/a	87.4 (4.263)
2nd Peak fuel temperature (°C)	49.11 (62.53)	n/a	n/a	n/a	43.9 (45.0)	n/a	n/a
1st Peak clad temperature (°C)	100.06 (3.79)	88.67 (4.305)	84.51 (4.07)	84.69 (4.160)	90.7 (4.27)	96.4 (4.20)	85.8 (4.263)
2nd Peak clad temperature (°C)	49.03 (62.53)	98.48 (61.58)	98.23 (70.74)	77.87 (57.26)[a]	43.9 (45.0)	41.1 (10.0)	n/a
1st Peak coolant temperature (°C)	68.45 (3.79)	58.78 (4.305)	58.81 (4.075)	58.83 (4.16)	58.3 (4.27)	57.7 (4.30)	55.6 (4.263)
2nd Peak coolant temperature (°C)	39.60 (50.91)	87.11 (64.19)	98.23 (70.74)	65.20 (57.26)[a]	43.9 (45.0)	39.0 (10.0)	n/a
HC flow inversion time (s)	51.40						
NCV flow inversion time (s)	59.79	57.40	61.82	57.26[a]	n/a	n/a	n/a
FLOFA							
1st Peak fuel temperature (°C)	116.05 (0.36)	n/a	n/a	n/a	94.5 (0.37)	n/a	91.0 (0.363)
2nd Peak fuel temperature (°C)	78.00 (8.32)	n/a	n/a	n/a	123.5 (6.0)	n/a	n/a
1st Peak clad temperature (°C)	103.94 (0.36)	91.28 (0.408)	89.43 (0.505)	91.74 (0.385)	94.0 (0.37)	98.4 (0.40)	89.5 (0.380)
2nd Peak clad temperature (°C)	77.58 (8.32)	121.00 (10.20)	105.76 (8.91)	112.12 (7.36)[a]	123.5 (6.0)	106.0 (10.0)	n/a
1st Peak coolant temperature (°C)	69.25 (0.53)	59.53 (0.503)	60.94(0.602)	60.04 (0.481)	59.4 (0.43)	58.4 (0.48)	56.5 (0.460)
2nd Peak coolant temperature (°C)	50.23 (3.43)	107.06 (11.10)	101.68 (9.13)	54.37[a]	64.8 (6.0)	48.4 (10.0)	n/a
HC flow inversion time (s)	2.72						
NCV flow inversion time (s)	23.99	7.40	4.415	7.66[a]	n/a	n/a	n/a

Appendix B: Simulation and analysis of IAEA benchmark transients (Gaheen et al., 2007)

Figure 7-5a and Figure 7-5b show the power and temperature results of the LOFA in case of the different time constants. The results for the LOFA are given in Table 21.

The result of this study was that a simple model was developed that was able to do various transient actions with accurate results. The results were compared with a variety of software codes. The model had predicted that the cladding temperature was below the nucleate boiling temperature in a case of a LOFA.

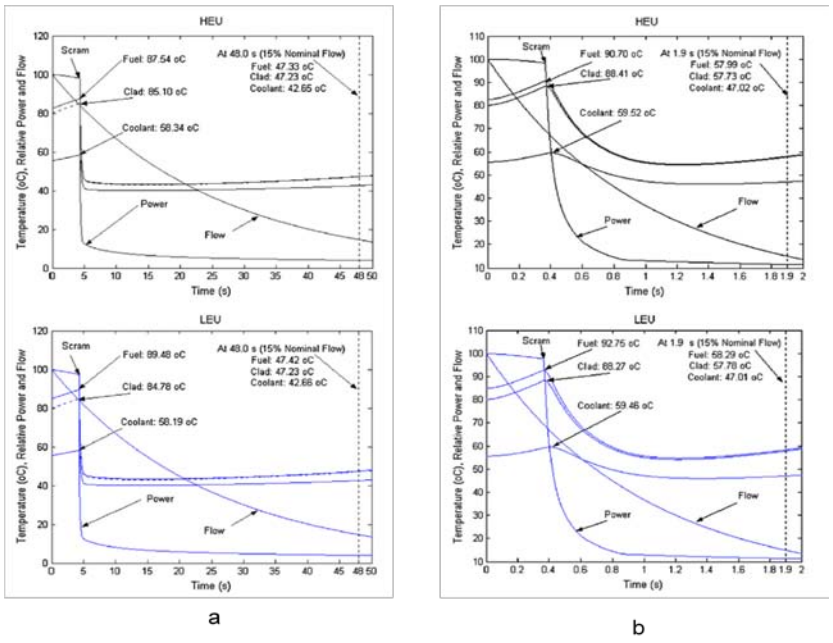

Figure 7-5 a: LOFA of HEU and LEU with time constant of 25 s;

b: LOFA of HEU and LEU with time constant of 1 s.

Table 21: LOFA results for HEU and LEU.

Main benchmark analysis results for loss of flow transients

Parameters	Core	CODE Institute						
		MODEL	RELAP 5/3.2 UPISA	RETRAC-PC LAS	PARET ANL	COSTAX-BOIL JEN	RELAP 4/5 JAERI	COBRA III-C Interatom
Slow loss of flow transient								
Power (MW) at scram	HEU	11.87	11.62	11.64	NA	11.8	NA	11.55
	LEU	11.69	11.56	11.62	NA	11.7	NA	11.46
Peak temperature (°C)								
Fuel center	HEU	87.54 (4.264)	NA	86.32 (4.237)	85.8 (4.29)	91.2 (4.27)	NA	87.4 (4.263)
	LEU	89.48 (4.264)	NA	87.31 (4.068)	86.8 (4.29)	91.9 (4.27)	NA	88.2 (4.263)
Clad surface	HEU	85.10 (4.265)	88.67 (4.305)	84.50 (4.239)	83.9 (4.29)	90.7 (4.27)	96.4 (4.20)	85.8 (4.263)
	LEU	84.78 (4.265)	88.41 (4.299)	84.44 (4.069)	83.7 (4.29)	90.3 (4.27)	96.1 (4.20)	85.5 (4.263)
Coolant outlet	HEU	58.34 (4.27)	58.78 (4.305)	58.68 (4.266)	58.9 (4.29)	58.3 (4.27)	57.7 (4.30)	55.6 (4.263)
	LEU	58.19 (4.27)	57.97 (4.300)	58.68 (4.088)	58.8 (4.29)	58.1 (4.27)	57.5 (4.30)	55.4 (4.263)
Temperature (°C) at 15% of flow								
Fuel center	HEU	47.33	NA	49.74	48.3	NA	NA	NA
	LEU	47.42	NA	NA	48.4	NA	NA	NA
Clad surface	HEU	47.23	49.34	49.66	48.2	NA	NA	NA
	LEU	47.23	49.38	NA	48.3	NA	NA	NA
Coolant outlet	HEU	42.65	43.47	42.18	43.3	NA	NA	NA
	LEU	42.66	43.50	NA	43.3	NA	NA	NA
Fast loss of flow transient								
Power (MW) at scram	HEU	11.8	11.87	11.75	NA	11.67	NA	11.5
	LEU	11.7	11.83	11.73	NA	11.67	NA	11.4
Peak temperature (°C)								
Fuel center	HEU	90.70 (0.37)	NA	90.50 (0.392)	89.2 (0.371)	94.5 (0.37)	NA	91.0 (0.363)
	LEU	92.75 (0.368)	NA	91.20 (0.391)	90.3 (0.371)	95.4 (0.37)	NA	91.9 (0.363)
Clad surface	HEU	88.41 (0.374)	91.28 (0.408)	88.56 (0.384)	87.5 (0.376)	94.0 (0.37)	98.4 (0.40)	89.5 (0.380)
	LEU	88.27 (0.374)	92.58 (0.400)	88.45 (0.394)	87.5 (0.371)	93.9 (0.37)	97.1 (0.40)	89.3 (0.363)
Coolant outlet	HEU	59.52 (0.41)	59.53 (0.503)	60.05 (0.474)	60.3 (0.451)	59.4 (0.43)	58.4 (0.48)	56.5 (0.460)
	LEU	59.46 (0.41)	59.50 (0.504)	60.05 (0.481)	60.3 (0.446)	59.3 (0.43)	58.1 (0.48)	56.4 (0.460)
Temperature (°C) at 15% of flow								
Fuel center	HEU	57.99	NA	NA	58.3	NA	NA	NA
	LEU	58.29	NA	NA	58.5	NA	NA	NA
Clad surface	HEU	57.73	NA	NA	58.1	NA	NA	NA
	LEU	57.78	NA	NA	58.2	NA	NA	NA
Coolant outlet	HEU	47.02	46.79	NA	46.6	NA	NA	NA
	LEU	47.01	46.70	NA	46.5	NA	NA	NA

Appendix C: Dynamic calculations of the IAEA safety MTR research reactor benchmark problem using RELAP5/3.2 code (Hamidouche et al., 2004)

Table 22 and Table 23 give the results of the LOFA that was simulated with the comparison between the various software codes for both HEU and LEU. Figure 7-6 and Figure 7-7 gives the graphs for cladding surface temperature of the LOFA.

Table 22: FLOFA of HEU and LEU

HEU and LEU – FLOFA results

Program name Laboratory		RELAP5/3.2 UPISA	PARET ANL	RETRAC-PC LAS	COSTAX-BOIL JEN	EUREKA-PT JAERI	COBRA III-C INTERATOM
Power core at scram (85% of nominal flow) (MW)	LEU	11.83 (0.190)	11.86 (0.295)	11.72 (0.185)	11.67	NA	11.4 (0.363)
	HEU	11.87 (0.200)	11.85 (0.295)	11.75 (0.192)	1167	NA	11.5 (0.363)
1st Peak cladding temperature (°C)	LEU	92.58 (0.400)	89.46 (0.505)	87.92 (0.400)	93.9 (0.37)	97.1 (0.40)	89.3 (0.363)
	HEU	91.28 (0.408)	89.43 (0.505)	91.74 (0.385)	94.0 (0.37)	98.4 (0.40)	89.5 (0.380)
1st Peak coolant temperature (°C)	LEU	59.50 (0.504)	60.84 (0.601)	59.92 (0.465)	59.3 (0.43)	58.1 (0.48)	56.4 (0.460)
	HEU	59.53 (0.503)	60.94(0.602)	60.04 (0.481)	59.4 (0.43)	58.4(0.48)	56.5 (0.460)
Flow inversion time (s)	LEU	7.40	4.415	7.36[a]	NA	NA	NA
	HEU	7.40	4.415	7.66[a]	NA	NA	NA
Coolant temperature at 15% of nominal flow	LEU	46.70	47.15	45.63	NA	NA	NA
	HEU	46.79	47.16	45.21	NA	NA	NA
2nd Peak cladding temperature (°C)	LEU	120.73 (10.00)	105.90 (8.51)	128.25 (7.36)[a]	NA	95.2 (10.0)	NA
	HEU	121.00 (10.20)	105.76 (8.91)	112.12 (7.36)[a]	NA	106.0 (10.0)	NA
2nd Peak cooling temperature (°C)	LEU	105.3 (11.90)	101.67 (9.14)	69.76[a]	NA	49.3 (10.0)	NA
	HEU	107.06 (11.10)	101.68 (9.13)	54.37[a]	NA	48.3 (10.0)	NA

Table 23: SLOFA for HEU and LEU

HEU and LEU – SLOFA results

Program name Laboratory		RELAP5/3.2 UPISA	PARET ANL	RETRAC-PC LAS	COSTAX-BOIL JEN	EUREKA-PT JAERI	COBRA III-C Interatom
Power core at scram (MW)	LEU	11.56 (4.102)	11.64 (3.87)	11.56 (4.050)	11.7 (4.06)	NA	11.46 (4.263)
	HEU	11.62 (4.098)	11.62 (3.915)	11.61 (4.047)	11.8 (4.06)	NA	11.55 (4.263)
1st Peak cladding temperature (°C)	LEU	88.41 (4.299)	84.56 (4.07)	84.63 4.240)	90.3 (4.27)	96.1 (4.20)	85.5 (4.263)
	HEU	88.67 (4.305)	84.51 (4.07)	84.69 (4.160)	90.7 (4.27)	96.4 (4.20)	85.8 (4.263)
1st Coolant peak temperature (°C)	LEU	57.97 (4.300)	58.83 (4.075)	58.82 (4.272)	58.1 (4.27)	57.5 (4.30)	55.4 (4.263)
	HEU	58.78 (4.305)	58.81 (4.075)	58.83 (4.16)	58.3 (4.27)	57.7 (4.30)	55.6 (4.263)
Clad temperature at 15% of flow (°C)	LEU	49.38 (47.50)	48.61 (43.58)	49.21 (47.19)	NA	41.1 (10.0)	NA
	HEU	49.34 (47.39)	48.61 (43.57)	49.56 (43.83)	NA	41.1 (10.0)	NA
Cool. temperature at 15 % of flow (°C)	LEU	43.50	43.43	42.42	NA	39.0 (10.0)	NA
	HEU	43.47	43.42	42.48	NA	39.0 (10.0)	NA
Flow inversion time (s)	LEU	57.40	62.84	57.26[a]		NA	NA
	HEU	57.40	61.82	57.26[a]		NA	NA
2nd Clad peak temperature (°C)	LEU	98.48 (61.58)	98.23 (70.74)	79.29 (57.26)[a]	43.9 (45.0)	NA	NA
	HEU	98.48 (61.58)	98.23 (70.74)	77.87 (57.26)[a]	43.9 (45.0)	NA	NA
2nd Coolant peak temperature (°C)	LEU	87.36 (64.20)	94.21 (70.74)	58.77 (57.26)[a]	44.0 (45.0)	NA	NA
	HEU	87.11 (64.19)	98.23 (70.74)	65.20 (57.26)[a]	43.9 (45.0)	NA	NA

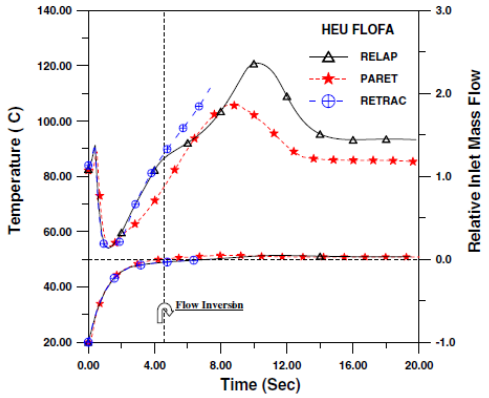

Figure 7-6: Cladding temperature and mass flow rate during FLOFA.

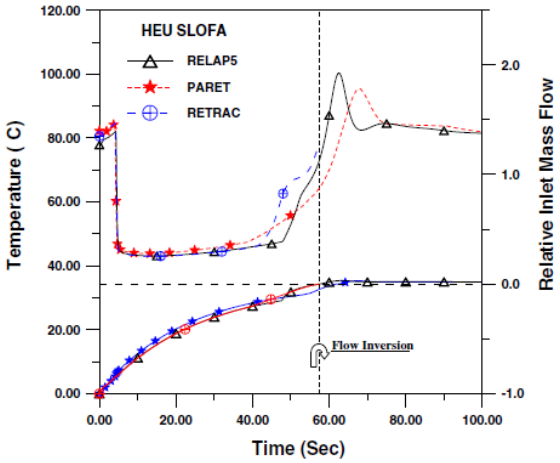

Figure 7-7: Cladding temperature and mass flow rate during SLOFA.endix D

Appendix D: Analysis of loss of coolant accidents in MTR pool type research reactor (Hamidouche & Si-Ahmed, 2010)

Figure 7-8 represents the inlet, outlet mass flow rates and the water level of the core during the accident. It can be seen how the level decreases over the time how the water drained from the pool.

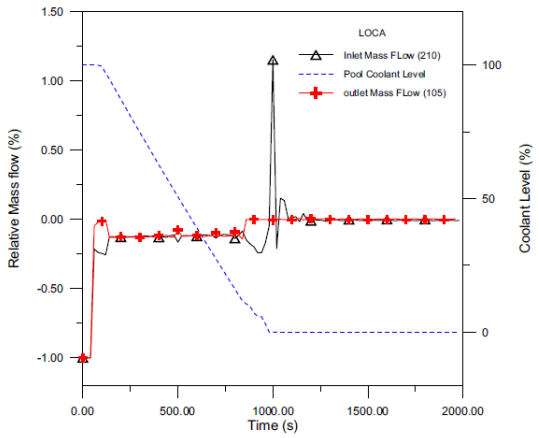

Figure 7-8: Mass flow and Water level (LOCA)

Figure 7-9 shows the cladding temperature evolution on the surface of the hottest channel in the core during the LOCA. During the beginning of the accident it can be seen that the water is still circulated through the core by the pumps. The heat was removed by natural convection. The cladding temperature is increasing as the water level decreases in the pool. Figure 7-9 shows the vapour that was produced on the fuel channel. After the core was drained, air is circulated between the plates that stop the increase of temperature by natural convection.

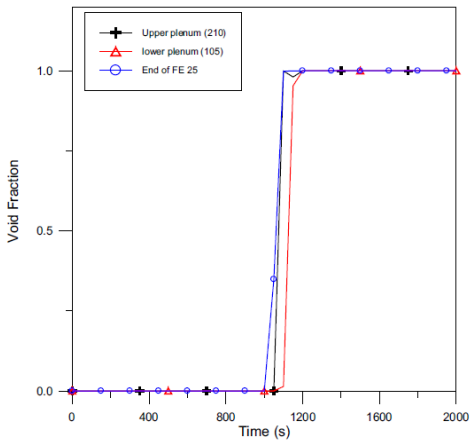

Figure 7-9: Evolution of void in fuel channel

Figure 7-10 represents the cladding surface temperature. It was found when the power level is lower than 4 MW, the cladding temperature stabilize at a certain time of the accident. The maximum cladding temperature was not exceeded for power levels lower than 4 MW. The maximum cladding temperature was below 500°C and the melting point of the aluminium is 600°C.

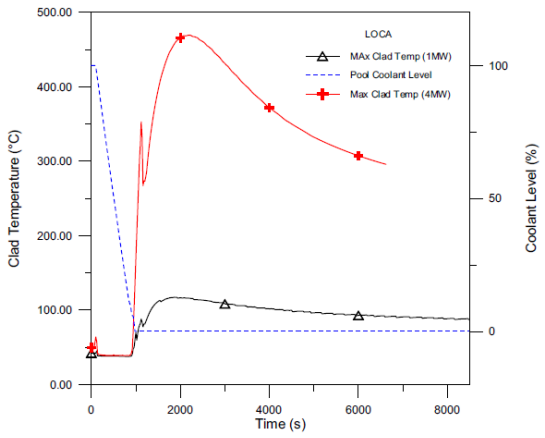

Figure 7-10: Cladding Surface Temperature during LOCA

Appendix E: Flow blockage analysis of a channel in a typical material test reactor core (Lu et al.*, 2009b)*

The results of the simulation compared to the results of the FLOFA in IAEA TECDOC 643 (1992) are given in Table 24.

Table 24: Code validation based on the FLOFA

	RELAP5/3.3/XJTU	/AEA[a]	RELAP5/3.2/UPISA[b]	RETRAC-PC/LAS[c]	PARET/ANL[c]	COSTAX-BOIL/JEN[c]	RELAP4/Mod5 /JAERI[c]	COBRA III-C /Interatom[c]
Peak temperature (°C)								
Fuel	95.35(0.37)	92.75(0.368)	NA	91.20(0.391)	90.3(0.371)	95.4(0.37)	NA	91.9(0.363)
Clad	92.52(0.37)	88.27(0.374)	92.58(0.400)	88.45(0.394)	87.5(0.371)	93.9(0.37)	97.1(0.40)	89.3(0.363)
Coolant	60.23(0.45)	59.46(0.41)	59.50(0.504)	60.05(0.481)	60.3(0.446)	59.3(0.43)	58.1(0.48)	56.4(0.460)
Temperature at 15% of flow (°C)								
Fuel	59.70(1.94)	58.29	NA	58.61(1.437)	58.5(1.9)	NA	NA	NA
Clad	59.36(1.94)	57.78	NA	58.33	58.2	NA	95.2(10.0)	NA
Coolant	46.82(1.94)	47.01	46.70	45.93	46.5	NA	49.3(10.0)	NA

Figure 7-1 and Figure 7-2 gives the temperature, power and flow rate transient parameter of the FLOFA simulation.

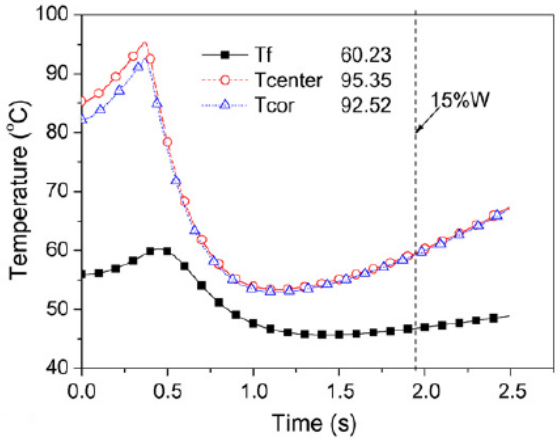

Figure 7-11: Temperatures parameters transient during FLOFA

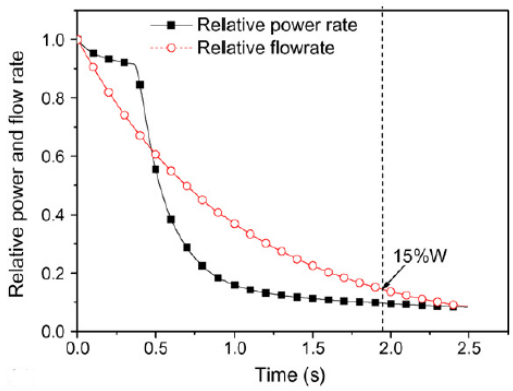

Figure 7-12: Relative power and flow rate parameters transient during FLOFA

For the partial blockage the mass flow in channel 3 was decreased to 5% of the nominal flow rate. In Figure 7-13 the mass flow in each of the 9 channels is given. It can be seen how the mass flow decreases in channel 3 because of the blockage and the mass flow in the other remaining channels increases.

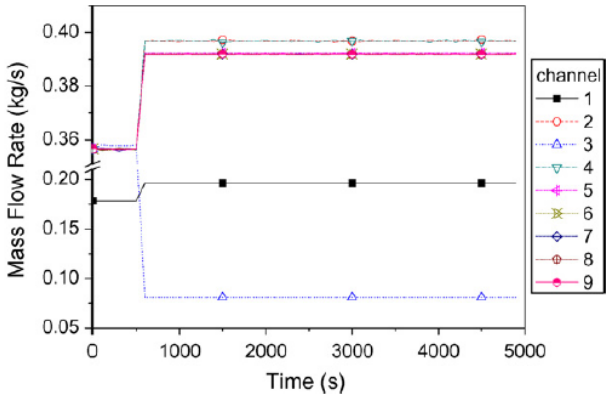

Figure 7-13: Mass flow rate in the different channels of the partial blockage simulation

Figure 7-14 gives the temperature variation of the coolant and fuel in channel 3

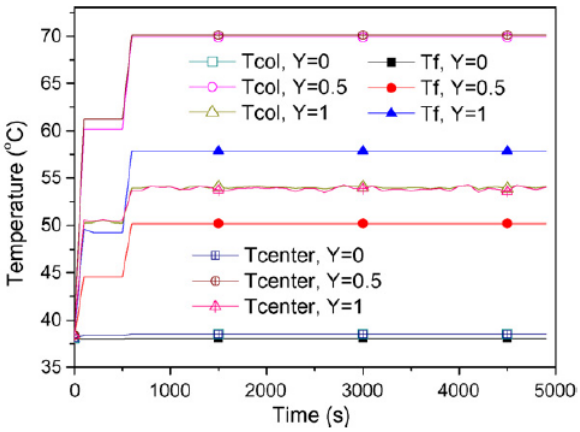

Figure 7-14: The temperature variation of the fuel and coolant in the partial obstructed channel.

In Figure 7-15 the mass flow in each of the 9 channels is given for the total flow channel blockage simulation. Figure 7-14 gives the temperature variation of the coolant and fuel in channel 3

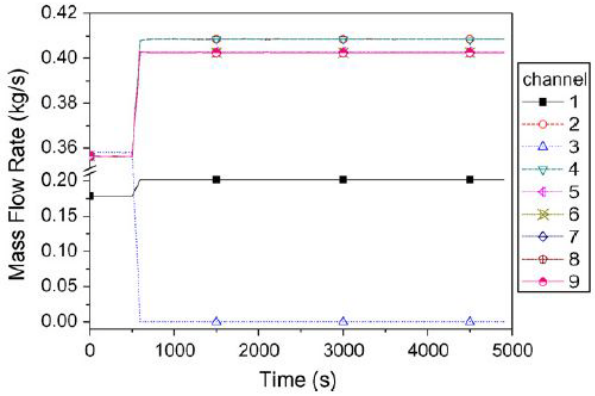

Figure 7-15: Mass flow rate of the different channels of the total blockage simulation

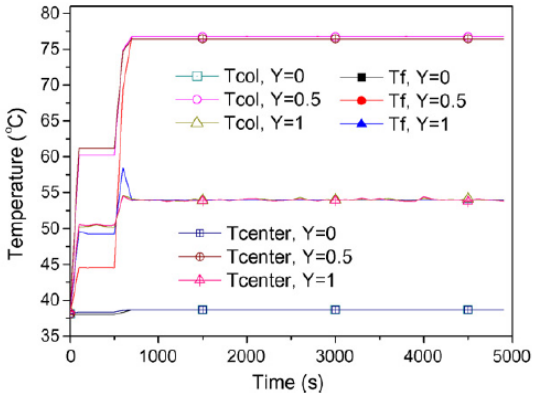

Figure 7-16: The temperature variation of the fuel and coolant in the total obstructed channel

Appendix F: Steady state calculation in EES of a single fuel assembly: Uniform power distribution

```
"Single Fuel Assembly with uniform power distribution calculations"

w_c=66.4/1000                          "Given in Table "
w_f=63/1000

n_1=23

L_f=w_f*n_1                            "Calculating the total fuel length with Eq (4.2)"
L_c=w_c*n_1                            "Calculating the total flow channel length with Eq (4.1)"

t_w=2.19/1000

A_flow=L_c*t_w                         "Calculating Total Flow area with Eq (4.3)"

L=0.6
Circum=(2*L_c+2*t_w)                   "Calculating Circumference with Eq (4.4)"

g=9.81
D_h=4*A_flow/Circum                    "Calculating the hydraulic diameter"

m_dot_t=1000 [m^3/hr]

num_assem=34

m_dot_f=1000*m_dot_t/3600

m_dot_a=m_dot_f/num_assem              "Calculating the mass flow through a single fuel assembly"

epsilon=1.5e-6
RR=epsilon/D_h

p_0i=170
T_0i=38

h_i=Enthalpy(Water,T=T_i,P=P_i)
rho_i=Density(Water,T=T_i,P=P_i)
Cp_i=Cp(Water,T=T_i,P=P_i)
V_i=m_dot_a/(rho_i*A_flow)

p_0i=p_i+0.5*rho_i*V_i^2/1000
T_0i=T_i+0.5*V_i^2/(Cp_i*1000)
h_0i=h_i+0.5*V_i^2/1000

"Initialize incremental loop"

m_dot_e[0]=m_dot_a
p_0e[0]=p_0i
p_e[0]=p_i
h_0e[0]=h_0i
h_e[0]=h_i
T_0e[0]=T_0i
T_e[0]=T_i
rho_e[0]=rho_i
V_e[0]=V_i
x_e[0]=L

n=10
Q_total=417.42

"Assembly increment loop"
```

```
DUPLICATE i=1,n

"Inlet properties"

m_dot_i[i]=m_dot_e[i-1]
p_0i[i]=p_0e[i-1]
p_i[i]=p_e[i-1]
h_0i[i]=h_0e[i-1]
h_i[i]=h_e[i-1]
T_0i[i]=T_0e[i-1]
T_i[i]=T_e[i-1]
rho_i[i]=rho_e[i-1]
V_i[i]=V_e[i-1]
x_i[i]=x_e[i-1]

"Outlet properties"

m_dot_e[i] - m_dot_i[i] = 0
p_0e[i] - p_0i[i] +DELTAp_vertical[i]  + DELTAp_0L[i] = 0
Q_[i] = m_dot[i]*(h_0e[i] - h_0i[i] + ((g*x_e[i]) - (g*x_i[i]))/1000)
p_0e[i]=p_e[i]+0.5*rho_e[i]*V_e[i]^2/1000
h_0e[i]=h_e[i]+0.5*V_e[i]^2/1000
T_e[i]=Temperature(Water,h=h_e[i],P=P_e[i])
T_0e[i]=T_e[i]+0.5*V_e[i]^2/(Cp_e[i]*1000)
Cp_e[i]=Cp(Water,T=T_e[i],P=P_e[i])
rho_e[i]=Density(Water,T=T_e[i],P=P_e[i])
V_e[i]=m_dot_e[i]/(rho_e[i]*A_flow)
x_e[i]=x_i[i]-L/n

"Average properties"

m_dot[i]=AVERAGE(m_dot_i[i],m_dot_e[i])
p_0[i]=AVERAGE(p_0i[i],p_0e[i])
h_0[i]=AVERAGE(h_0i[i],h_0e[i])

rho_[i]=Density(Water,T=T_[i],P=P_[i])
T_[i]=Temperature(Water,h=h_[i],P=P_[i])
Cp_[i]=Cp(Water,T=T_[i],P=P_[i])
V_[i]=m_dot[i]/(rho_[i]*A_flow)

p_0[i]=p_[i]+0.5*rho_[i]*V_[i]^2/1000
T_0[i]=T_[i]+0.5*V_[i]^2/(Cp_[i]*1000)
h_0[i]=h_[i]+0.5*V_[i]^2/1000

x_[i]=AVERAGE(x_i[i],x_e[i])


DELTAp_0L[i]=f[i]*L/(D_h*n)*0.5*rho_[i]*V_[i]^2/1000
DELTAp_vertical[i]=(rho_[i]*g*(x_e[i]-x_i[i]))/1000
f[i]=MoodyChart(Re[i], RR)
Q_[i]=Q_total/n

"Heat transfer calculations"

"Cladding"

D_c[i]=0.38/1000
A_c[i]=1.83264/n
```

```
k_c[i]=180
R_c[i]=D_c[i]/k_c[i]


"Uranium"

D_u[i]=0.255/1000
A_u[i]=1.7388/n
k_u[i]=50
R_u[i]=D_u[i]/(k_u[i]*A_u[i])

"Water"

mu_[i]=Viscosity(Water,T=T_[i],P=P_[i])
Re[i]=rho_[i]*V_[i]*D_h/mu_[i]
Pr[i]=Prandtl(Water,T=T_[i],P=P_[i])
NUSSELT[i]=0.023*Re[i]^0.8*Pr[i]^0.4
NUSSELT[i]=h_cw[i]*D_h/k_w[i]
k_w[i]=Conductivity(Water,T=T_[i],P=P_[i])

R_w[i]=1/(h_cw[i]*A_c[i])

1/UA[i]=R_w[i]+R_c[i]+R_u[i]


Q_dot_u[i]=Q_[i]*10^3/(D_u[i]*A_u[i])                    " [W/m^3]"

T_wall[i]=T_[i]+Q_dot_u[i]*D_u[i]/h_cw[i]

T_ci[i]=T_wall[i]

R_conv[i]=1/(h_cw[i])

T_co[i]=T_[i]+(R_c[i]+R_conv[i])*(Q_dot_u[i]*D_u[i])

T_ui[i]=T_co[i]

T_u[i]=Q_dot_u[i]*D_u[i]^2/(2*k_u[i])+T_co[i]

T_max[i]=T_u[i]

end
```

SOLUTION

Unit Settings: SI C kPa kJ mass deg

A_{flow} = 0.003345 [m^2]
C_{pl} = 4.182
ε = 0.0000015
h_{ol} = 159.3 [kJ/kgK]
L = 0.6 [m]
L_f = 1.449
$\dot{m}_f$ = 277.8 [kg/s]
n = 10
n_1 = 23
P_l = 167 [kPa]
ρ_l = 993 [kg/m^3]
T_{ol} = 38 [°C]
t_w = 0.00219
w_c = 0.0664

Circum = 3.059 [m]
D_h = 0.004374 [m]
g = 9.81
h_l = 159.3 [kJ/kgK]
L_c = 1.527
$\dot{m}_a$ = 8.17 [kg/s]
$\dot{m}_t$ = 1000 [m^3/hr]
num_{assem} = 34
p_{ol} = 170 [kPa]
Q_{total} = 417.4 [kW]
RR = 0.000343
T_l = 38 [°C]
V_l = 2.46 [m/s]
w_f = 0.063

159 potential unit problems were detected.

Arrays Table: Main

	$A_{o,l}$	$A_{u,l}$	$\overline{Cp_l}$	$Cp_{e,l}$	$\Delta p_{0L,l}$	$\Delta p_{vertical,l}$	$D_{o,l}$	$D_{u,l}$
0								
1	0.1833	0.1739	4.182	4.182	1.16	-0.5843	0.00038	0.000255
2	0.1833	0.1739	4.182	4.182	1.154	-0.5841	0.00038	0.000255
3	0.1833	0.1739	4.182	4.182	1.148	-0.5838	0.00038	0.000255
4	0.1833	0.1739	4.182	4.182	1.142	-0.5835	0.00038	0.000255
5	0.1833	0.1739	4.182	4.182	1.137	-0.5832	0.00038	0.000255
6	0.1833	0.1739	4.182	4.182	1.132	-0.5829	0.00038	0.000255
7	0.1833	0.1739	4.181	4.181	1.127	-0.5826	0.00038	0.000255
8	0.1833	0.1739	4.181	4.181	1.122	-0.5823	0.00038	0.000255
9	0.1833	0.1739	4.181	4.181	1.117	-0.582	0.00038	0.000255
10	0.1833	0.1739	4.181	4.181	1.112	-0.5817	0.00038	0.000255

Arrays Table: Main

	f_l	$\overline{h_l}$	$h_{0,l}$	$h_{0e,l}$	$h_{0l,l}$	$h_{ow,l}$	$h_{e,l}$	$h_{l,l}$	$k_{o,l}$	$k_{u,l}$	$k_{w,l}$
0				159.3			159.3				
1	0.02813	161.8	161.8	164.4	159.3	13662.369285	164.4	159.3	180	50	0.6159
2	0.02797	166.9	166.9	169.5	164.4	13812.174531	169.5	164.4	180	50	0.6176
3	0.02782	172.1	172.1	174.6	169.5	13961.259860	174.6	169.5	180	50	0.6193
4	0.02767	177.2	177.2	179.7	174.6	14109.623763	179.7	174.6	180	50	0.6209
5	0.02753	182.3	182.3	184.8	179.7	14257.265312	184.8	179.7	180	50	0.6225
6	0.02739	187.4	187.4	189.9	184.8	14404.183755	189.9	184.8	180	50	0.6241
7	0.02725	192.5	192.5	195	189.9	14550.378534	195	189.9	180	50	0.6256
8	0.02712	197.6	197.6	200.2	195	14695.849255	200.2	195	180	50	0.6271
9	0.02698	202.7	202.7	205.3	200.2	14840.595633	205.3	200.2	180	50	0.6286

Arrays Table: Main

	f_i	$\overline{h}_i$	$h_{0,i}$	$h_{0e,i}$	$h_{0l,i}$	$h_{ow,i}$	$h_{e,i}$	$h_{l,i}$	$k_{o,i}$	$k_{u,i}$	$k_{w,i}$
10	0.02686	207.8	207.8	210.4	205.3	14984.617459	210.4	205.3	180	50	0.63

Arrays Table: Main

	$\overline{\mu}_i$	$\dot{m}_i$	$\dot{m}_{ei}$	$\dot{m}_{li}$	$NUSSELT_i$	Pr_i	$\overline{P}_i$	$p_{0,i}$	$p_{0e,i}$
0			8.17						170
1	0.0006707	8.17	8.17	8.17	97.019673	4.554	166.707156	169.7	169.4
2	0.0006553	8.17	8.17	8.17	97.813262	4.438	166.133364	169.1	168.9
3	0.0006405	8.17	8.17	8.17	98.602626	4.326	165.565032	168.6	168.3
4	0.0006263	8.17	8.17	8.17	99.387923	4.218	165.001992	168	167.7
5	0.0006126	8.17	8.17	8.17	100.169304	4.115	164.444086	167.5	167.2
6	0.0005993	8.17	8.17	8.17	100.946914	4.015	163.891160	166.9	166.6
7	0.0005865	8.17	8.17	8.17	101.720892	3.92	163.343065	166.4	166.1
8	0.0005742	8.17	8.17	8.17	102.491370	3.828	162.799658	165.8	165.5
9	0.0005622	8.17	8.17	8.17	103.258473	3.74	162.260799	165.3	165
10	0.0005507	8.17	8.17	8.17	104.022319	3.655	161.726353	164.7	164.5

Arrays Table: Main

	$p_{0l,i}$	$p_{e,i}$	$p_{l,i}$	$\overline{Q}_i$	$\dot{Q}_{ul}$	Re_i	$\overline{\rho}_i$	$\rho_{e,i}$	$\rho_{l,i}$	$R_{o,i}$
0		167						993		
1	170	166.4	167	41.74	9.414E+08	15930	992.8	992.5	993	0.000002111
2	169.4	165.8	166.4	41.74	9.414E+08	16303	992.3	992.1	992.5	0.000002111
3	168.9	165.3	165.8	41.74	9.414E+08	16679	991.8	991.6	992.1	0.000002111
4	168.3	164.7	165.3	41.74	9.414E+08	17059	991.3	991.1	991.6	0.000002111
5	167.7	164.2	164.7	41.74	9.414E+08	17442	990.9	990.6	991.1	0.000002111
6	167.2	163.6	164.2	41.74	9.414E+08	17827	990.4	990.1	990.6	0.000002111
7	166.6	163.1	163.6	41.74	9.414E+08	18216	989.8	989.6	990.1	0.000002111
8	166.1	162.5	163.1	41.74	9.414E+08	18608	989.3	989	989.6	0.000002111
9	165.5	162	162.5	41.74	9.414E+08	19003	988.8	988.5	989	0.000002111
10	165	161.5	162	41.74	9.414E+08	19401	988.2	988	988.5	0.000002111

Arrays Table: Main

	$R_{oonv,i}$	$R_{u,i}$	$R_{w,i}$	$\overline{T}_i$	$T_{0,i}$	$T_{0e,i}$	$T_{0l,i}$	$T_{ol,i}$	$T_{oo,i}$
0						38			
1	0.00007319	0.00002933	0.0003994	38.610230	38.61	39.22	38	56.18	56.688073
2	0.0000724	0.00002933	0.0003951	39.832165	39.83	40.44	39.22	57.21	57.719435
3	0.00007163	0.00002933	0.0003908	41.054139	41.05	41.67	40.44	58.25	58.755811
4	0.00007087	0.00002933	0.0003867	42.276151	42.28	42.89	41.67	59.29	59.797017
5	0.00007014	0.00002933	0.0003827	43.498198	43.5	44.11	42.89	60.34	60.842875
6	0.00006942	0.00002933	0.0003788	44.720278	44.72	45.33	44.11	61.39	61.893213
7	0.00006873	0.00002933	0.000375	45.942386	45.94	46.55	45.33	62.44	62.947869
8	0.00006805	0.00002933	0.0003713	47.164519	47.17	47.78	46.55	63.5	64.006685
9	0.00006738	0.00002933	0.0003677	48.386668	48.39	49	47.78	64.56	65.069509
10	0.00006674	0.00002933	0.0003641	49.608828	49.61	50.22	49	65.63	66.136196

Arrays Table: Main

	$T_{e,i}$	$T_{l,i}$	$T_{max,i}$	$T_{u,i}$	$T_{ul,i}$	$T_{wall,i}$	UA_i	$\overline{V}_i$	$V_{e,i}$	$V_{l,i}$	$\overline{x}_i$
0	38								2.46		
1	39.22	38	57.300231	57.3	56.69	56.181275	2321	2.461	2.461	2.46	0.57
2	40.44	39.22	58.331593	58.33	57.72	57.212637	2345	2.462	2.462	2.461	0.51
3	41.67	40.44	59.367970	59.37	58.76	58.249014	2368	2.463	2.463	2.462	0.45
4	42.89	41.67	60.409176	60.41	59.8	59.290220	2391	2.464	2.465	2.463	0.39
5	44.11	42.89	61.455033	61.46	60.84	60.336077	2414	2.465	2.466	2.465	0.33

Arrays Table: Main

	$T_{e,l}$	$T_{i,l}$	$T_{max,l}$	$T_{u,l}$	$T_{ui,l}$	$T_{wall,l}$	UA_l	$\bar{V}_l$	$V_{e,l}$	$V_{i,l}$	$\bar{x}_l$
6	45.33	44.11	62.505372	62.51	61.89	61.386416	2437	2.467	2.467	2.466	0.27
7	46.55	45.33	63.560028	63.56	62.95	62.441071	2460	2.468	2.468	2.467	0.21
8	47.78	46.55	64.618843	64.62	64.01	63.499887	2483	2.469	2.47	2.468	0.15
9	49	47.78	65.681667	65.68	65.07	64.562711	2505	2.47	2.471	2.47	0.09
10	50.22	49	66.748354	66.75	66.14	65.629398	2528	2.472	2.473	2.471	0.03

Arrays Table: Main

	$x_{e,l}$	$x_{i,l}$
0	0.6	
1	0.54	0.6
2	0.48	0.54
3	0.42	0.48
4	0.36	0.42
5	0.3	0.36
6	0.24	0.3
7	0.18	0.24
8	0.12	0.18
9	0.06	0.12
10	0	0.06

Appendix G: Sinusoidal power distribution calculation in the axial direction of a single fuel assembly.

```
"Sinusiodal Power Distribution"

Power=417.422                                   "Total Power in Single Fuel Assembly"

x_1=-30                                         "Boundaries of the length in the axial direction"
x_2=30

Power/A=1/k_3*(sin(x_2*k_3)-sin(x_1*k_3))       "Using Eq (3.9) only for the z-direction to calculate A"

k_3=0.04985                                     "Caculated with Eq (3.10)"
                                                                              3
x[0]=-30

n=10                                            "Number of increments"

Duplicate i=1,n

increment[i]=i

x[i]=x[i-1]+6                                   "Calculated length per increment"

P_[i]/A=1/k_3*(sin(x[i]*k_3)-sin(x[i-1]*k_3))   "Using Eq (3.9) to determine the power at each increment"

end
```

SOLUTION

Unit Settings: SI C kPa kJ mass rad

A = 10.43
n = 10
x_1 = -30
k_3 = 0.04985
Power = 417.4
x_2 = 30

No unit problems were detected.

Arrays Table: Main

	x_i	$\bar{P}_i$	$Increment_i$
0	-30		
1	-24	13.906	1
2	-18	31.204	2
3	-12	45.731	3
4	-6	56.197	4
5	0	61.674	5
6	6	61.674	6
7	12	56.197	7
8	18	45.731	8
9	24	31.204	9
10	30	13.906	10

Appendix H: Steady state calculation in EES of a single fuel assembly: Sinusoidal power distribution

```
"Single Fuel Assembly with sinusiodal power distribution calculations"

w_c=66.4/1000                          "Given in Table "
w_f=63/1000

n_1=23

L_f=w_f*n_1                            "Calculating the total fuel length with Eq (4.2)"
L_c=w_c*n_1                            "Calculating the total flow channel length with Eq (4.1)"

t_w=2.19/1000

A_flow=L_c*t_w                         "Calculating Total Flow area with Eq (4.3)"

L=0.6
Circum=(2*L_c+2*t_w)                   "Calculating Circumference with Eq (4.4)"

g=9.81
D_h=4*A_flow/Circum                    "Calculating the hydraulic diameter"

m_dot_t=1000 [m^3/hr]

num_assem=34

m_dot_f=1000*m_dot_t/3600

m_dot_a=m_dot_f/num_assem              "Calculating the mass flow through a single fuel assembly"

epsilon=1.5e-6
RR=epsilon/D_h

p_0i=170
T_0i=38

h_i=Enthalpy(Water,T=T_i,P=P_i)
rho_i=Density(Water,T=T_i,P=P_i)
Cp_i=Cp(Water,T=T_i,P=P_i)
V_i=m_dot_a/(rho_i*A_flow)

p_0i=p_i+0.5*rho_i*V_i^2/1000
T_0i=T_i+0.5*V_i^2/(Cp_i*1000)
h_0i=h_i+0.5*V_i^2/1000

"Initialize incremental loop"

m_dot_e[0]=m_dot_a
p_0e[0]=p_0i
p_e[0]=p_i
h_0e[0]=h_0i
h_e[0]=h_i
T_0e[0]=T_0i
T_e[0]=T_i
rho_e[0]=rho_i
V_e[0]=V_i
x_e[0]=L

n=10

 Q_[1]=13.906                          "Sinusiodal Power distribution"
```

```
Q_[2]=31.204
Q_[3]=45.731
Q_[4]=56.197
Q_[5]=61.674
Q_[6]=61.674
Q_[7]=56.197
Q_[8]=45.731
Q_[9]=31.204
Q_[10]=13.906

Q_sum=sum(Q_[i],i=1,10)

"Assembly increment loop"

DUPLICATE i=1,n

"Inlet properties"

m_dot_i[i]=m_dot_e[i-1]
p_0i[i]=p_0e[i-1]
p_i[i]=p_e[i-1]
h_0i[i]=h_0e[i-1]
h_i[i]=h_e[i-1]
T_0i[i]=T_0e[i-1]
T_i[i]=T_e[i-1]
rho_i[i]=rho_e[i-1]
V_i[i]=V_e[i-1]
x_i[i]=x_e[i-1]

m_dot_e[i] - m_dot_i[i] = 0
p_0e[i] - p_0i[i] +DELTAp_vertical[i]  + DELTAp_0L[i] = 0
Q_[i] = m_dot[i]*(h_0e[i] - h_0i[i] + ((g*x_e[i]) - (g*x_i[i]))/1000)
p_0e[i]=p_e[i]+0.5*rho_e[i]*V_e[i]^2/1000
h_0e[i]=h_e[i]+0.5*V_e[i]^2/1000
T_e[i]=Temperature(Water,h=h_e[i],P=P_e[i])
T_0e[i]=T_e[i]+0.5*V_e[i]^2/(Cp_e[i]*1000)
Cp_e[i]=Cp(Water,T=T_e[i],P=P_e[i])
rho_e[i]=Density(Water,T=T_e[i],P=P_e[i])
V_e[i]=m_dot_e[i]/(rho_e[i]*A_flow)
x_e[i]=x_i[i]-L/n

"m_dot_e[i]=m_dot_i[i]
p_0e[i]=p_0i[i]
p_e[i]=p_i[i]
h_0e[i]=h_0i[i]
h_e[i]=h_i[i]
T_0e[i]=T_0i[i]
T_e[i]=T_i[i]
rho_e[i]=rho_i[i]
V_e[i]=V_i[i]
x_e[i]=x_i[i]+L/n"

"Average properties"

m_dot[i]=AVERAGE(m_dot_i[i],m_dot_e[i])
p_0[i]=AVERAGE(p_0i[i],p_0e[i])
h_0[i]=AVERAGE(h_0i[i],h_0e[i])

rho_[i]=Density(Water,T=T_[i],P=P_[i])
```

```
T_[i]=Temperature(Water,h=h_[i],P=P_[i])
Cp_[i]=Cp(Water,T=T_[i],P=P_[i])
V_[i]=m_dot[i]/(rho_[i]*A_flow)

p_0[i]=p_[i]+0.5*rho_[i]*V_[i]^2/1000
T_0[i]=T_[i]+0.5*V_[i]^2/(Cp_[i]*1000)
h_0[i]=h_[i]+0.5*V_[i]^2/1000

x_[i]=AVERAGE(x_i[i],x_e[i])


DELTAp_0L[i]=f[i]*L/(D_h*n)*0.5*rho_[i]*V_[i]^2/1000
DELTAp_vertical[i]=(rho_[i]*g*(x_e[i]-x_i[i]))/1000
f[i]=MoodyChart(Re[i], RR)


"Cladding"

D_c[i]=0.38/1000
A_c[i]=1.83264/n
k_c[i]=180
R_c[i]=D_c[i]/k_c[i]
R_conv[i]=1/h_cw[i]

"Uranium"

D_u[i]=0.255/1000
A_u[i]=1.7388/n
k_u[i]=50
R_u[i]=D_u[i]/(k_u[i]*A_u[i])

"Water"


mu_[i]=Viscosity(Water,T=T_[i],P=P_[i])
Re[i]=rho_[i]*V_[i]*D_h/mu_[i]
Pr[i]=Prandtl(Water,T=T_[i],P=P_[i])
NUSSELT[i]=0.023*Re[i]^0.8*Pr[i]^0.4
NUSSELT[i]=h_cw[i]*D_h/k_w[i]
k_w[i]=Conductivity(Water,T=T_[i],P=P_[i])

R_w[i]=1/(h_cw[i]*A_c[i])

1/UA[i]=R_w[i]+R_c[i]+R_u[i]


Q_dot_u[i]=Q_[i]*10^3/(D_u[i]*A_u[i])   "[W/m^3]"

T_wall[i]=T_[i]+Q_dot_u[i]*D_u[i]/h_cw[i]

T_ci[i]=T_wall[i]

T_co[i]=T_[i]+(R_c[i]+R_conv[i])*(Q_dot_u[i]*D_u[i])

T_ui[i]=T_co[i]

T_u[i]=Q_dot_u[i]*D_u[i]^2/(2*k_u[i])+T_co[i]

T_max[i]=T_u[i]
```

SOLUTION

Unit Settings: SI C kPa kJ mass deg

A_{flow} = 0.003345
C_{pl} = 4.182
ε = 0.0000015
h_{ol} = 159.3
L = 0.6
L_r = 1.449
$\dot{m}_r$ = 277.8
n = 10
n_1 = 23
P_l = 167
ρ_l = 993
T_{ol} = 38
t_w = 0.00219
w_c = 0.0664

Circum = 3.059
D_h = 0.004374
g = 9.81
h_l = 159.3
L_c = 1.527
$\dot{m}_a$ = 8.17
$\dot{m}_t$ = 1000 [m^3/hr]
num_{assem} = 34
p_{ol} = 170
Q_{sum} = 417.4
RR = 0.000343
T_l = 38
V_l = 2.46
w_r = 0.063

84 potential unit problems were detected.

Arrays Table: Main

	$A_{o,l}$	$A_{u,l}$	$\overline{Cp_l}$	$Cp_{e,l}$	$\Delta p_{0L,l}$	$\Delta p_{vertical,l}$	$D_{o,l}$	$D_{u,l}$
0								
1	0.1833	0.1739	4.182	4.182	1.162	-0.5844	0.00038	0.000255
2	0.1833	0.1739	4.182	4.182	1.158	-0.5843	0.00038	0.000255
3	0.1833	0.1739	4.182	4.182	1.153	-0.584	0.00038	0.000255
4	0.1833	0.1739	4.182	4.182	1.146	-0.5837	0.00038	0.000255
5	0.1833	0.1739	4.182	4.182	1.138	-0.5833	0.00038	0.000255
6	0.1833	0.1739	4.182	4.181	1.131	-0.5828	0.00038	0.000255
7	0.1833	0.1739	4.181	4.181	1.124	-0.5824	0.00038	0.000255
8	0.1833	0.1739	4.181	4.181	1.118	-0.582	0.00038	0.000255
9	0.1833	0.1739	4.181	4.181	1.113	-0.5817	0.00038	0.000255
10	0.1833	0.1739	4.181	4.181	1.111	-0.5816	0.00038	0.000255

Arrays Table: Main

	f_i	$\bar{h}_i$	$h_{0,i}$	$h_{0e,i}$	$h_{0l,i}$	$h_{ow,i}$	$h_{e,i}$	$h_{l,i}$	$k_{o,i}$	$k_{u,i}$	$k_{w,i}$
0				159.3			159.3				
1	0.02818	160.1	160.1	161	159.3	13612.270549	161	159.3	180	50	0.6153
2	0.02809	162.9	162.9	164.8	161	13693.449981	164.8	161	180	50	0.6163
3	0.02795	167.6	167.6	170.4	164.8	13831.394789	170.4	164.8	180	50	0.6178
4	0.02777	173.8	173.8	177.3	170.4	14013.199967	177.3	170.4	180	50	0.6199
5	0.02756	181.1	181.1	184.8	177.3	14222.095897	184.8	177.3	180	50	0.6221
6	0.02735	188.6	188.6	192.4	184.8	14439.154097	192.4	184.8	180	50	0.6245
7	0.02716	195.8	195.8	199.3	192.4	14645.099601	199.3	192.4	180	50	0.6266
8	0.027	202.1	202.1	204.9	199.3	14822.029455	204.9	199.3	180	50	0.6284
9	0.02688	206.8	206.8	208.7	204.9	14954.867632	208.7	204.9	180	50	0.6297
10	0.02681	209.5	209.5	210.4	208.7	15032.481605	210.4	208.7	180	50	0.6305

Arrays Table: Main

	$\bar{\mu}_i$	$\dot{m}_i$	$\dot{m}_{ei}$	$\dot{m}_{li}$	$NUSSELT_i$	Pr_i	$\bar{P}_i$	$p_{0,i}$	$p_{0e,i}$
0			8.17						170
1	0.0006759	8.17	8.17	8.17	96.75	4.594	166.706664	169.7	169.4
2	0.0006675	8.17	8.17	8.17	97.18	4.53	166.130372	169.1	168.8
3	0.0006534	8.17	8.17	8.17	97.92	4.423	165.557622	168.6	168.3
4	0.0006355	8.17	8.17	8.17	98.88	4.287	164.990241	168	167.7
5	0.0006158	8.17	8.17	8.17	100	4.139	164.429442	167.4	167.2
6	0.0005962	8.17	8.17	8.17	101.1	3.992	163.875763	166.9	166.6
7	0.0005784	8.17	8.17	8.17	102.2	3.86	163.329102	166.3	166.1
8	0.0005637	8.17	8.17	8.17	103.2	3.751	162.788802	165.8	165.5
9	0.000553	8.17	8.17	8.17	103.9	3.672	162.253758	165.3	165
10	0.0005469	8.17	8.17	8.17	104.3	3.627	161.722524	164.7	164.5

Arrays Table: Main

	$p_{0l,i}$	$p_{e,i}$	$p_{l,i}$	$\bar{Q}_i$	$\dot{Q}_{ui}$	Re_i	$\bar{\rho}_i$	$\rho_{e,i}$	$\rho_{l,i}$	$R_{o,i}$
0		167						993		
1	170	166.4	167	13.91	3.136E+08	15806	992.91535	992.8	993	0.000002111
2	169.4	165.8	166.4	31.2	7.038E+08	16007	992.66938	992.5	992.8	0.000002111
3	168.8	165.3	165.8	45.73	1.031E+09	16351	992.24265	992	992.5	0.000002111
4	168.3	164.7	165.3	56.2	1.267E+09	16812	991.66310	991.3	992	0.000002111
5	167.7	164.2	164.7	61.67	1.391E+09	17350	990.97302	990.6	991.3	0.000002111
6	167.2	163.6	164.2	61.67	1.391E+09	17920	990.22848	989.8	990.6	0.000002111
7	166.6	163.1	163.6	56.2	1.267E+09	18471	989.49605	989.1	989.8	0.000002111
8	166.1	162.5	163.1	45.73	1.031E+09	18952	988.84648	988.6	989.1	0.000002111
9	165.5	162	162.5	31.2	7.038E+08	19318	988.34633	988.1	988.6	0.000002111
10	165	161.5	162	13.91	3.136E+08	19534	988.04908	988	988.1	0.000002111

Arrays Table: Main

	$R_{oonv,l}$	$R_{u,l}$	$R_{w,l}$	$\overline{T}_l$	$T_{0,l}$	$T_{0e,l}$	$T_{0l,l}$	$T_{ol,l}$
0						38		
1	0.00007346	0.00002933	0.0004009	38.202897	38.203621	38.41	38	44.08
2	0.00007303	0.00002933	0.0003985	38.863271	38.863995	39.32	38.41	51.97
3	0.0000723	0.00002933	0.0003945	39.989376	39.990101	40.66	39.32	59
4	0.00007136	0.00002933	0.0003894	41.481272	41.481998	42.3	40.66	64.54
5	0.00007031	0.00002933	0.0003837	43.206551	43.207278	44.11	42.3	68.15
6	0.00006926	0.00002933	0.0003779	45.012057	45.012785	45.92	44.11	69.58
7	0.00006828	0.00002933	0.0003726	46.737463	46.738191	47.56	45.92	68.81
8	0.00006747	0.00002933	0.0003681	48.229560	48.230290	48.9	47.56	65.97
9	0.00006687	0.00002933	0.0003649	49.355865	49.356595	49.81	48.9	61.36
10	0.00006652	0.00002933	0.000363	50.016367	50.017098	50.22	49.81	55.34

Arrays Table: Main

	$T_{oo,l}$	$T_{e,l}$	$T_{i,l}$	$T_{max,l}$	$T_{u,l}$	$T_{ul,l}$	$T_{wall,l}$	UA_l	$\overline{V}_l$	$V_{e,l}$
0		38								2.46
1	44.246924	38.41	38	44.450860	44.45	44.25	44.078089	2313	2.46	2.46
2	52.347449	39.32	38.41	52.805064	52.81	52.35	51.968595	2326	2.461	2.461
3	59.559551	40.66	39.32	60.230209	60.23	59.56	59.004322	2348	2.462	2.462
4	65.227123	42.3	40.66	66.051268	66.05	65.23	64.544824	2376	2.463	2.464
5	68.894913	44.11	42.3	69.799380	69.8	68.89	68.146117	2409	2.465	2.466
6	70.325512	45.91	44.11	71.229979	71.23	70.33	69.576716	2443	2.467	2.468
7	69.488178	47.56	45.91	70.312323	70.31	69.49	68.805879	2475	2.469	2.47
8	66.528865	48.9	47.56	67.199523	67.2	66.53	65.973636	2503	2.47	2.471
9	61.734631	49.81	48.9	62.192246	62.19	61.73	61.355777	2523	2.472	2.472
10	55.505328	50.22	49.81	55.709264	55.71	55.51	55.336493	2535	2.472	2.473

Arrays Table: Main

	$V_{i,l}$	$\overline{x}_l$	$x_{e,l}$	$x_{i,l}$
0			0.6	
1	2.46	0.57	0.54	0.6
2	2.46	0.51	0.48	0.54
3	2.461	0.45	0.42	0.48
4	2.462	0.39	0.36	0.42
5	2.464	0.33	0.3	0.36
6	2.466	0.27	0.24	0.3
7	2.468	0.21	0.18	0.24
8	2.47	0.15	0.12	0.18
9	2.471	0.09	0.06	0.12
10	2.472	0.03	0	0.06

Appendix I: Reactor core power distribution calculation

"Power Distrubution Calculations for the core"

"Specify the boudary points on the axis"

x_1 = -24
x_2 = 24
y_1= -19
y_2 = 19
z_1 = -30
z_2 = 30

"The constant that was calculated for the x,y,z-directions"

k_1 = 0.05719
k_2 = 0.0722
k_3 = 0.04985

Power=1

"Determine the constant A with Eq (2.9)"

Power/A = (1/k_1*sin(x_2*k_1)-1/k_1*sin(x_1*k_1))*(1/k_2*sin(y_2*k_2)-1/k_2*sin(y_1*k_2))*(1/k_3*sin(z_2*k_3)-1/k_3*sin(z_1*k_3))

x_i =0
x_e = 4
y_i= 0
y_e = 3.8
z_i = -30
z_e = 30

P_i = A*1/(k_1*k_2*k_3)*(sin(x_e*k_1)-sin(x_i*k_1))*(sin(y_e*k_2)-sin(y_i*k_2))*(sin(z_e*k_3)-sin(z_i*k_3))

x_1i =4
x_1e = 8

x_2i =8
x_2e = 16

x_3i =16
x_3e = 24

y_4i= 3.8
y_4e = 11.4

x_4i =0
x_4e =8

y_7i= 11.4
y_7e = 19

x_8i =0
x_8e =4

"Converting the core with the assumtions that was made in section 3.6.1"

```
faktor_1=1.05072920                    "Taken the four courner flow channels into account"
faktor_2=1.07199                       "Taken the flow channel in the centre into account"
faktor_3=1.0522273                     "Taken the control fuek ellements into account"

faktor=faktor_1*faktor_2*faktor_3

n=10                                   "number of increments"

z_[0]=-30

Duplicate i=1,n

z_[i]=z_[i-1]+6

"Calculating the axial power distribution for each fuel assembly"

P_1[i]  = (A*1/(k_1*k_2*k_3)*(sin(x_4e*k_1)-sin(x_4i*k_1))*(sin(y_7e*k_2)-sin(y_7i*k_2))*(sin(z_[i]*k_3)-sin(z_[i-1]*k_3)))*10000
*faktor

P_2[i]/faktor  = (A*1/(k_1*k_2*k_3)*(sin(x_2e*k_1)-sin(x_2i*k_1))*(sin(y_7e*k_2)-sin(y_7i*k_2))*(sin(z_[i]*k_3)-sin(z_[i-1]*k_3)))
*10000

P_3[i]/faktor  = 0

P_4[i]/faktor  = 0

P_5[i]/faktor  = (A*1/(k_1*k_2*k_3)*(sin(x_4e*k_1)-sin(x_4i*k_1))*(sin(y_4e*k_2)-sin(y_4i*k_2))*(sin(z_[i]*k_3)-sin(z_[i-1]*k_3)))
*10000

P_6[i]/faktor  = (A*1/(k_1*k_2*k_3)*(sin(x_2e*k_1)-sin(x_2i*k_1))*(sin(y_4e*k_2)-sin(y_4i*k_2))*(sin(z_[i]*k_3)-sin(z_[i-1]*k_3)))
*10000*17/23

P_7[i]/faktor  = (A*1/(k_1*k_2*k_3)*(sin(x_3e*k_1)-sin(x_3i*k_1))*(sin(y_4e*k_2)-sin(y_4i*k_2))*(sin(z_[i]*k_3)-sin(z_[i-1]*k_3)))
*10000

P_8[i]/faktor =0

P_9[i]/faktor = (A*1/(k_1*k_2*k_3)*(sin(x_1e*k_1)-sin(x_1i*k_1))*(sin(y_e*k_2)-sin(y_i*k_2))*(sin(z_[i]*k_3)-sin(z_[i-1]*k_3)))*10000

P_10[i]/faktor  = (A*1/(k_1*k_2*k_3)*(sin(x_2e*k_1)-sin(x_2i*k_1))*(sin(y_e*k_2)-sin(y_i*k_2))*(sin(z_[i]*k_3)-sin(z_[i-1]*k_3)))
*10000

P_11[i]/faktor  = (A*1/(k_1*k_2*k_3)*(sin(x_3e*k_1)-sin(x_3i*k_1))*(sin(y_e*k_2)-sin(y_i*k_2))*(sin(z_[i]*k_3)-sin(z_[i-1]*k_3)))
*10000


end

"Calculating the total power per fuel assembly"

s1=sum(P_1[i],I=1,10)

s2=sum(P_2[i],I=1,10)

s3=sum(P_3[i],I=1,10)

s10=sum(P_10[i],I=1,10)

s5=sum(P_5[i],I=1,10)
```

```
s6=sum(P_6[i],I=1,10)

s7=sum(P_7[i],I=1,10)

s9=sum(P_9[i],I=1,10)

s11=sum(P_11[i],I=1,10)


s8=sum(P_8[i],I=1,10)

" Calculating the total power in a quarter core"

Power_total=s1+s2+s3+s10+s5+s6+s7+s11+s8+s9
```

SOLUTION

Unit Settings: SI C kPa kJ mass rad

A = 0.00002685	faktor = 1.185
$faktor_1$ = 1.051	$faktor_2$ = 1.072
$faktor_3$ = 1.052	k_1 = 0.05719
k_2 = 0.0722	k_3 = 0.04985
n = 10	Power = 1
$Power_{total}$ = 2500	P_i = 0.01598
s1 = 336.4	s10 = 293.1
s11 = 156.9	s2 = 267.2
s3 = 0	s5 = 629.6
s6 = 369.6	s7 = 267.7
s8 = 0	s9 = 179.5
x_1 = -24	x_{1e} = 8
x_{1i} = 4	x_2 = 24
x_{2e} = 16	x_{2i} = 8
x_{3e} = 24	x_{3i} = 16
x_{4e} = 8	x_{4i} = 0
x_{8e} = 4	x_{8i} = 0
x_e = 4	x_i = 0
y_1 = -19	y_2 = 19
y_{4e} = 11.4	y_{4i} = 3.8
y_{7e} = 19	y_{7i} = 11.4
y_e = 3.8	y_i = 0
z_1 = -30	z_2 = 30
z_e = 30	z_i = -30

No unit problems were detected.

Arrays Table: Main

	$\bar{z}_i$	$P_{1,i}$	$P_{2,i}$	$P_{3,i}$	$P_{5,i}$	$P_{6,i}$	$P_{7,i}$	$P_{8,i}$	$P_{9,i}$	$P_{10,i}$	$P_{11,i}$
0	-30										
1	-24	11.207	8.902	0	20.974	12.314	8.919	0	5.981	9.763	5.227
2	-18	25.147	19.975	0	47.065	27.631	20.013	0	13.422	21.908	11.728
3	-12	36.855	29.274	0	68.976	40.495	29.330	0	19.671	32.107	17.188
4	-6	45.290	35.974	0	84.763	49.763	36.042	0	24.173	39.456	21.122
5	0	49.704	39.480	0	93.023	54.613	39.555	0	26.528	43.301	23.180
6	6	49.704	39.480	0	93.023	54.613	39.555	0	26.528	43.301	23.180
7	12	45.290	35.974	0	84.763	49.763	36.042	0	24.173	39.456	21.122
8	18	36.855	29.274	0	68.976	40.495	29.330	0	19.671	32.107	17.188
9	24	25.147	19.975	0	47.065	27.631	20.013	0	13.422	21.908	11.728
10	30	11.207	8.902	0	20.974	12.314	8.919	0	5.981	9.763	5.227

Arrays Table: Main

	$P_{4,i}$
0	
1	0
2	0
3	0
4	0
5	0
6	0
7	0
8	0
9	0
10	0